1954

Determination of stress-strain characteristics of materials subjected to dynamic loading

Richard C. Dove
Iowa State College

INFORMATION TO USERS

This manuscript has been reproduced from the microfilm master. UMI films the text directly from the original or copy submitted. Thus, some thesis and dissertation copies are in typewriter face, while others may be from any type of computer printer.

The quality of this reproduction is dependent upon the quality of the copy submitted. Broken or indistinct print, colored or poor quality illustrations and photographs, print bleedthrough, substandard margins, and improper alignment can adversely affect reproduction.

In the unlikely event that the author did not send UMI a complete manuscript and there are missing pages, these will be noted. Also, if unauthorized copyright material had to be removed, a note will indicate the deletion.

Oversize materials (e.g., maps, drawings, charts) are reproduced by sectioning the original, beginning at the upper left-hand corner and continuing from left to right in equal sections with small overlaps.

ProQuest Information and Learning
300 North Zeeb Road, Ann Arbor, MI 48106-1346 USA
800-521-0600

DETERMINATION OF STRESS-STRAIN CHARACTERISTICS OF MATERIALS SUBJECTED TO DYNAMIC LOADING

by

Richard C. Dove

A Dissertation Submitted to the
Graduate Faculty in Partial Fulfillment of
The Requirements for the Degree of
DOCTOR OF PHILOSOPHY

Major Subject: Theoretical and Applied Mechanics

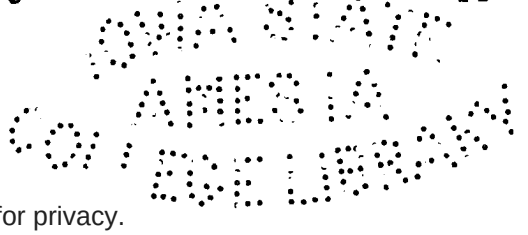

Approved:

Signature was redacted for privacy.

In Charge of Major Work

Signature was redacted for privacy.

Head of Major Department

Signature was redacted for privacy.

Dean of Graduate College

Iowa State College
1954

TABLE OF CONTENTS

	Page
LIST OF SYMBOLS	iv
INTRODUCTION	1
REVIEW OF LITERATURE	3
THEORETICAL INVESTIGATION	13
Theoretical Basis for a Stress-Strain-Time Relationship	14
The Proposed Stress-Strain-Time Relationship	19
Application of the Relationship to Constant Rate of Strain	21
Application of the Relationship to Constant Rate Strain Cycling	24
Application of the Relationship to Sinusoidal Straining	27
Application of the Relationship to Sinusoidal Strain Cycling	29
Application of the Relationship for the Evaluation of Hysteresis Losses	32
EXPERIMENTAL INVESTIGATION	33
Description of Relaxation Test Equipment	34
Evaluation and Calibration of Relaxation Test Equipment	38
Description of Wave Propagation Test Equipment	49
Material Tested	53
Preliminary Investigations	53
RESULTS	64
Evaluation of Material Constants	64
Comparison of Theoretical and Experimental Results	71
Constant rate of strain tests	71
Wave propagation tests	86
SUMMARY AND CONCLUSIONS	95
RECOMMENDATIONS FOR FURTHER INVESTIGATIONS	97

Page

LITERATURE CITED 99

ACKNOWLEDGMENTS 106

APPENDICES 107

Appendix A: Records and Data from Evaluation and Calibration Tests 107

Appendix B: Data from Preliminary Tests 112

Appendix C: Records and Data from Tests Made to Evaluate Material Constants . . 121

Appendix D: Tabular Forms Used for the Computation of Results 125

LIST OF SYMBOLS

b	rate of strain
c	velocity of propagation of strain waves
c_o	approximate value of c; $c_o = \sqrt{\frac{E}{\rho}}$
c_s	velocity of Rayleigh surface waves; $c_o \simeq 0.9\sqrt{\frac{G}{\rho}}$
d	diameter
e	base of the natural logarithm
f	function
$f_u(\epsilon)$	$f_u(\epsilon) = \frac{d\sigma_u}{d\epsilon}$, if $f_u(\epsilon)$ is a constant it may be replaced by E_u
$f_r(\epsilon)$	$f_r(\epsilon) = \frac{d\sigma_r}{d\epsilon}$, if $f_r(\epsilon)$ is a constant it may be replaced by E_r
h	wave length of a sinusoidal strain pulse
m	slope of a curve
n	any number
p	constant used as an exponent in the relaxed stress-strain relationship
q	constant used as an exponent in the unrelaxed stress-strain relationship
r	used as a subscript, refers to the condition of relaxed stress
s	creep or growth in the direction of applied load
t	time

u	used as a subscript, refers to the condition of unrelaxed stress
x	used for an integration substitution
z	used for an integration substitution
A	cross sectional area
B	constant appearing in Equation (6)
C	constant appearing in Equation (6)
E	Young's modulus (modulus of elasticity)
E_u	Young's modulus associated with the unrelaxed stress-strain curve
E_r	Young's modulus associated with the relaxed stress-strain curve
F	applied force
G	shear modulus
K_n	constants
L	length
M	constant used as a coefficient in the relaxed stress-strain relationship
N	constant used as a coefficient in the unrelaxed stress-strain relationship
P	period of sinusoidal strain pulse
R	ratio $\frac{N - M}{N}$ if p = q
T	time interval during which strain remains constant
W	energy loss during a straining-unstraining cycle

α	reciprical stress, used as a limiting value of stress
Δ	used to indicate a small increment
γ	viscosity
ϵ	normal strain
ϵ_i	particular value of normal strain
ϵ_m	maximum value of normal strain obtained
μ	Poisson's ratio
π	3.14159 etc.
ρ	density
σ	normal stress
σ_b	normal stress existing across crystal, molecular or grain boundaries
τ	relaxation coefficient
τ'	$\tau \frac{Eu}{Er}$
ω	angular frequency of sinusoidal strain waves
$\dot{\epsilon}$	the dot represents differentiation with respect to time

INTRODUCTION

Research to find new materials and new designs which will permit use of existing materials is handicaped by a lack of understanding of just how materials do behave when they are subjected to dynamic loads. This problem is not new and a large amount of work, both experimental and theoretical, has been done by previous investigators. However, the great amount of work that has been done in the past several years in this area and the amount that is currently in progress offer the best evidence that the problem remains unsolved and also that the solution is becoming increasingly important.

The special aspect of material behavior considered in this investigation is the material's stress-strain characteristics. When a dynamic load is involved the stress-strain characteristics are affected by the time element in two distinct ways. First, the stress-strain characteristics appear to be dependent upon the rate, time duration, and rate of repetition of the loading. Secondly, when a load is applied rapidly the effects of that load are not felt at all points throughout the loaded material at the same time. That is, effects of an applied load such as elastic normal strain, elastic shear strain, and plastic

flow propagate from the point of load application throughout the material with a finite velocity. The purpose of this investigation was to develop a method for determining or predicting a material's stress-strain characteristics which takes both of these important aspects of the time element into account. The investigation has been confined to the determination of stress-strain characteristics in those cases for which the dynamic loading produces either simple tension or simple compression.

REVIEW OF LITERATURE

Since the theory of elasticity was established elasticians have related the various properties of elastic solids (Young's modulus (E), Poisson's ratio (μ) shear modulus (G), etc.) to the velocity with which various disturbances are propagated through such solids.

The most widely used expression for the velocity of propagation of a longitudinal (tensile or compressive) strain wave through an elastic solid is

$$c = \sqrt{\frac{E}{\rho}} \qquad (1)$$

in which c = velocity of strain wave propagation,

E = Young's modulus of elasticity,

ρ = density of the material.

This equation results from the application of Newton's second law and it is developed and discussed in many texts in the fields of vibrations, dynamics, theory of sound, and elasticity (1, 2, 3, 4, 5, 6, 7)[1]. Several authors (5, 7) have pointed out that this expression is exact, even for an elastic material, only when the dimensions of the material perpendicular to the direction of wave propagation are

---

[1]Numerals in parentheses refer to corresponding items listed under the heading, "LITERATURE CITED".

infinitely small. That is, this expression is developed for the plane stress case or, in terms of work and energy, the energy required to overcome lateral inertia is considered to be zero. Both Lord Rayleigh (5) and Love (7) present methods for making an approximate correction for the effect of lateral inertia on the velocity of longitudinal wave propagation.

An expression for the velocity of longitudinal wave propagation in an elastic solid of infinite extent has also been developed (6, 7). It is

$$c = \sqrt{\frac{E}{\rho} \frac{(1 - \mu)}{(1 + \mu)(1 - 2\mu)}} \qquad (2)$$

in which μ = Poisson's ratio. Equation (2) results when the wave equation written from Newton's second law is solved for the plane strain case.

The velocity of longitudinal strain propagation through an elastic material of finite size is not expressed by either equation (1) or (2). Actually, the theory for the solution of this problem was developed independently and presented by both Pochhammer (8) and Chree (9). The Pochhammer-Chree theory was little used however until in 1941 when Bancroft (10) used it to show that in a circular rod the velocity of propagation of a longitudinal strain wave is

$$c = \sqrt{\frac{E}{\rho}} \times f(d, h, \mu) \qquad (3)$$

in which d = rod diameter,

h = wave length of the propagating wave.

Bancroft shows how to evaluate the function $f(d, h, \mu)$ and points out that, as would be expected, when $\frac{d}{h} = 0$ (i.e., an infinitely small rod or an infinitely large wave length)

$$c = \sqrt{\frac{E}{\rho}} = c_o .$$

For all values of $\frac{d}{h}$ greater than zero the value of c is less than c_o, and as

$$\frac{d}{h} \rightarrow \infty$$

the value of c approaches the velocity of propagation of Rayleigh surface waves.

$$c_{\left(\frac{d}{h} = \infty\right)} = c_s \simeq 0.9 \sqrt{\frac{G}{\rho}} . \qquad (4)$$

in which G = modulus of elasticity in shear.

Davies (11) has extended the Pochhammer-Chree theory to cover propagation of non-sinusoidal strain pulses by replacing the original pulse by a Fourier series and then working with the wave lengths of the components. Davies also has used the Pochhammer-Chree theory to show how longitudinal strain waves are dispersed and distorted during their propagation through an elastic material.

Using the approximation $c = \sqrt{\frac{E}{\rho}}$ Donnell (12) has discussed longitudinal strain waves produced by

1. variable forces
2. forces applied at intermediate points along the length of a bar
3. moving forces
4. and the effect of change in bar cross section on longitudinal waves.

Using the same approximation, De Juhasz (13) has presented a very complete graphical method to be used in studying the division between potential and kinetic energy associated with longitudinal strain waves and also for analysing the effects of reflection of strain waves from various types of ends. Cole (14) has effectively reduced De Juhasz's graphical analysis of wave reflection down to a system of equations suitable for use in design work. In addition, Cole has studied longitudinal wave transmission through systems of pinned end rods.

The foregoing indicates that the mechanism of longitudinal wave propagation has been studied in considerable detail for an elastic material. However, the possibility of the material's properties being dependent upon rate of straining, time duration of strain, or rate of repetition of strain has not been considered in these studies.

The mechanism of longitudinal wave propagation when the

strain is large enough to produce plastic action was first studied by von Kármán (15) and Taylor (16). The von Kármán-Taylor theory gives the velocity of propagation as

$$c = \sqrt{\frac{\partial\sigma/\partial\epsilon}{\rho}} \qquad (5)$$

in which $\partial\sigma/\partial\epsilon$ = tangent modulus of elasticity at the value of strain of interest. This theory predicts that for a material having a tangent modulus in the plastic range less than the elastic modulus the velocity of propagation of plastic strains will be less than for elastic strains.

In general, the theory of plastic wave propagation has not been extended and refined as has the theory of elastic wave propagation[1]. However, in proposing the theory von Kármán stated that in the plastic range a material's properties were almost certainly affected by the rate of straining, and therefore the tangent modulus ($\partial\sigma/\partial\epsilon$) to be used in equation (5) should not be taken from the stress-strain diagram obtained from the usual static test. The results of recent experimental work by Sternglass and Stuart (21) confirm this statement.

---

[1]Additional theoretical work on plastic wave propagation has been done in some rather special areas, however. White (17) has discussed the effect of a yield point on plastic wave propagation and White and Griffis (18) have postulated that internally reflected secondary stress waves are originated by all plastic wave disturbances. Wood (19) and Weibull (20) both point out that with large plastic strains the velocity of wave propagation may be appreciably affected by the change in the material's density.

Malvern (22) has proposed that in the plastic region the stress may be expressed as

$$\sigma = f(\epsilon) + B \ln(1 + C\dot{\epsilon}'') \qquad (6)$$

in which $f(\epsilon)$ = static stress-strain relationship,

$\dot{\epsilon}'' = \frac{\partial}{\partial t}$ of the plastic component of strain,

B = constant,

and C = constant.

Using equation (6) Malvern has extended the von Kármán-Taylor theory to take the rate of straining in the plastic region into account.

Investigators working with rubber and rubber-like materials have always been concerned with the time dependence of material behavior. The term "visco-elastic" is applied to such materials because it has been common practice to explain their behavior in terms of models which are made up of combinations of viscous and elastic elements (dash pots and springs).[1]

A coefficient of viscosity (γ) has long been considered a property of such materials and it is used to explain observed creep and relaxation phenomena. Recently, expressions for the velocity of longitudinal wave propagation

---

[1]The two basic models are (a) spring and dash pot in series - Maxwell solid, (b) spring and dash pot in parallel-Voigt solid. These two basic models may be combined in a number of ways.

in terms of material constants have been worked out for various types of these visco-elastic solids. Kolsky (23) gives the velocity of longitudinal wave propagation in a Voigt solid in terms of the usual E and ρ in addition to the coefficient of viscosity (γ) of the dash pot element and the frequency (ω) of the propagating sinusoidal waves. Hillier (24) gives the velocity of longitudinal wave propagation in a Maxwell solid in terms of E and ρ, in addition to a relaxation constant defined as $\frac{\gamma}{E}$ and the frequency (ω) of the propagating sinusoidal waves. For a combination Voigt-Maxwell solid, Hillier gives the velocity of longitudinal wave propagation in terms of two elastic constants (E_1 and E_2), ρ, the relaxation constant ($\frac{\gamma}{E}$), and ω. Theoretical work on the velocity of wave propagation in various types of visco-elastic solids has been conducted under a United States Government contract by the Division of Applied Mathematics, Brown University. The series of published reports on this work (25, 26, 27) offers a good source for the mathematical details involved in this type of analysis. Lethersich and Pelzer (28) have deduced an expression for the velocity of longitudinal wave propagation in a combination Voigt-Maxwell solid which includes a correction for lateral inertia. In all of these equations c is expressed in terms of ω, the frequency of sinusoidal waves. This means that c has been taken as being dependent

on rate of repetition of strain rather than upon rate of strain. Furthermore, in the development of all of these equations the elastic (E) and viscous (η) coefficients have been taken as constants. Nolle (29) has shown that at least for several rubber-like materials both E and η are frequency dependent.

The results of many experimental studies on dynamic loading are questionable because inertia forces were not accounted for or because the finite velocity of strain wave propagation was disregarded. However, within the past ten years, dynamic loading tests, the results of which appear to be reliable, have been conducted on a variety of materials. The fact that most material properties are in some way affected by the rate of straining has been adequately demonstrated. Nolle's work on the frequency dependence of the elastic and viscous properties of rubber-like materials has already been mentioned. Kolsky (30) has shown that the stress-strain curves for copper, lead, several plastics, and natural rubber are greatly affected by the rate of straining. Clark and Duwez (31) have shown that at high rates of straining the tensile properties of steel are considerably altered. Johnson, Wood, and Clark (32) have shown that the compression stress-strain curve for 2S aluminum is influenced by the rate of straining. Hsiao and Sauer (33) have demonstrated that the elastic

modulus (E) of polystyrene is dependent upon the rate of strain to a measurable extent even at moderate strain rates. Fine (34) has pointed out that the difference between isothermal properties which might be associated with low strain rates and adiabatic properties which might be associated with high strain rates is not sufficient to explain the observed difference in behavior between static and dynamic loading.

The significance of the work previously done in this field may be briefly summarized as follows.

The mechanism by which strain waves, produced by dynamic loading, are propagated in an elastic solid has been worked out in considerable detail. However, it has been assumed that material properties are not dependent on rate of strain and hence are not affected by dynamic loading.

The mechanism of propagation of plastic strain waves, produced by dynamic loading, is not understood as well as the mechanism of elastic wave propagation; but the difference between static and dynamic behavior in the plastic region has been recognized and the effect of strain rate is being considered.

Visco-elastic solids show a very marked difference in their behavior under the action of static as compared to dynamic loads. However, the theoretical work on these solids has been largely based on models which are known to

be inadequate for the explanation even of static behavior. Furthermore, the theoretical work has, for the most part, related stress to strain and rate of repetition of strain (i.e., frequency of strain cycling). This makes the theory difficult to apply to transient dynamic loads.

Recent experimental studies show that for many materials the stress-strain characteristics are apparently affected by the rate of straining, even in the normal elastic range.

THEORETICAL INVESTIGATION

The results of the experimental studies referred to in the previous section which have shown a material's stress-strain characteristics to be different under conditions of dynamic and static loading have increased interest in finding a suitable method of accounting for this difference.

The method of approach which has received by far the most attention is based upon the revaluation of material properties using impact tests rather than the standard static tests.[1] If then, a material's behavior under dynamic loading conditions is to be investigated the numerical values of the properties (E, μ, G, etc.) established by impact tests are substituted into the appropriate theoretical equations (elastic or plastic theory). This method requires a distinct division between dynamic loading and non-dynamic loading. The existence of such a distinct division is not borne out by the experimental studies. Rather, a material's stress-strain characteristics change progressively as the rate of straining changes. A more reasonable point of view appears to be that virtually all loading conditions are dynamic, the difference being only a matter of degree. The ideal relationship to be sought is

---

[1]Campbell (35) has suggested using a wave propagation technique for establishing a "dynamic" stress-strain curve.

one in which the stress is expressed as a function of strain and time and which allows the strain to be obtained by following any strain-time path whatsoever.

Theoretical Basis for a Stress-Strain-Time Relationship

In discussing Eyring's Rate theory, Fredrickson and Eyring (36) offer a molecular explanation of how a material's stress-strain characteristics depend on the time of loading. This theory has been applied by Hogan (37) to explain creep rate at constant stress and it appears to the writer that it can also be used as a starting point for the development of the stress-strain characteristics of a material subjected to dynamic loading.

According to this theory the time rate of creep or growth of a material in the direction of a steady, normal force may be expressed as a hyperbolic sine function, thus

$$\dot{s} = K \sinh(\alpha \sigma_b) \qquad (7)$$

in which $\dot{s}$ is the creep or growth rate, (T^{-1}),

K is a constant having dimensions of reciprocal time (T^{-1}),

α is an inverse stress level parameter having dimensions of length squared divided by force (L^2/F), and

σ_b is the stress across the bond.

Zener (38) has shown how this equation for rate of creep can be reduced to an equation for rate of stress relaxation, under conditions of constant strain, by considering slip band phenomenon. However, in Zener's method for reducing this creep rate equation to a stress relaxation equation, the introduction of the slip band concept is not essential. According to Zener (38) the strain associated with a load applied in zero time may be expressed as:

$$\epsilon = \frac{\sigma}{E_u} + K_1 s \qquad (8)$$

in which σ is the suddenly applied normal stress,

E_u is the unrelaxed elastic modulus (i.e., the slope of the stress-strain curve that would result if the stress is applied in zero time),

K_1 is a proportionality factor, and

s is the creep.

This indicates that the increase in strain which will occur is proportional to the creep.

Furthermore, according to Zener (38), if the applied stress (σ) remains constant the stress existing across the bonds within the material may be expressed as:

$$\sigma_b = \sigma - K_2 s \qquad (9)$$

in which K_2 is a proportionality factor. This indicates that the decrease in bond stress is also proportional to

the creep.

Substituting equation (9) into equation (7) gives

$$\frac{d}{dt}\left(\frac{\sigma - \sigma_b}{K_2}\right) = K \sinh \alpha \sigma_b$$

or

$$\frac{d\sigma_b}{dt} = \frac{d\sigma}{dt} - K_2 K \sinh \alpha \sigma_b \ , \qquad (10)$$

and from (8) and (9)

$$\epsilon = \frac{\sigma}{E_u} + K_1 \frac{\sigma - \sigma_b}{K_2}$$

or

$$\epsilon = \sigma\left(\frac{1}{E_u} + \frac{K_1}{K_2}\right) - \frac{K_1}{K_2}\sigma_b \quad . \qquad (11)$$

Zener defines a relaxed elastic modulus (E_r) as

$$\frac{1}{E_r} = \frac{1}{E_u} + \frac{K_1}{K_2} \quad .$$

From which

$$\frac{K_1}{K_2} = \frac{E_u - E_r}{E_u E_r} \quad .$$

He also defines a relaxation time τ' as

$$\tau' = \frac{1}{\alpha K K_2} \quad .$$

If these are substituted into equations (10) and (11) the results are

$$\frac{d\sigma_b}{dt} = \frac{d\sigma}{dt} - \frac{1}{\alpha\tau'} \sinh \alpha\sigma_b \qquad (12)$$

and

$$\epsilon = \frac{\sigma}{E_r} - \frac{E_u - E_r}{E_u E_r} \sigma_b \qquad (13)$$

respectively. These two equations are referred to by Zener as the "governing equations" derivable from the Eyring theory.

To apply these equations for the solution of relaxation of stress under a condition of constant strain Zener assumes that at some time the stress and the strain are both identically zero and the strain is then instantly increased to a value ϵ_c at time equal zero and held constant. By substituting ϵ_c for ϵ in equation (13) and taking the derivative with respect to time the following result is obtained if E_r and E_u are treated as constants.

$$0 = \frac{d\sigma}{dt} - \frac{E_u - E_r}{E_u} \frac{d\sigma_b}{dt}$$

or

$$\frac{d\sigma}{dt} = \frac{E_u - E_r}{E_u} \frac{d\sigma_b}{dt} \quad . \qquad (14)$$

Substituting equation (14) into equation (12) gives

$$\frac{d\sigma_b}{dt}\left(1 - \frac{E_u - E_r}{E_u}\right) = -\frac{1}{\alpha\tau'} \sinh \alpha\sigma_b$$

or

$$\frac{d\sigma_b}{dt} = - \frac{1}{\alpha \gamma' \frac{E_r}{E_u}} \sinh \alpha \sigma_b \quad . \tag{15}$$

By defining a new relaxation time

$$\gamma = \gamma' \frac{E_r}{E_u}$$

equation (15) reduces to

$$\frac{d\sigma_b}{dt} = - \frac{1}{\alpha \gamma} \sinh \alpha \sigma_b \quad . \tag{16}$$

Before any slip occurs (the unrelaxed state) the stress across the bonds (σ_{bu}) is equal to the stress applied (σ_u) and hence equation (14) can be integrated to

$$\sigma = \frac{E_u - E_r}{E_u} \sigma_b + \frac{E_r}{E_u} \sigma_u$$

or

$$\sigma = \sigma_u \left(\frac{E_r}{E_u} + \frac{E_u - E_r}{E_u} \frac{\sigma_b}{\sigma_u} \right) . \tag{17}$$

If now, equation (16) is solved for the bond stress at any time (σ_b) and this value substituted into (17) the final result is the desired expression for the applied stress at any time in terms of the unrelaxed stress, or stress at zero time, (σ_u); and the material constants E_u, E_r and γ .

The Proposed Stress-Strain-Time Relationship

The stress (σ) at any time (t) following straining to a given value of (ϵ) in zero time can be investigated by applying equations (16) and (17). The stress-strain-time relationship is developed here for the particular case in which the stress level parameter ($\frac{1}{\alpha}$) is considered to be much greater than the bond stress (σ_b).[1]

For this case equation (16) gives

$$\ln \sigma_b = - \frac{t}{\tau} + C ,$$

and since $\sigma_b = \sigma_u$ when $t = 0$

$$\frac{\sigma_b}{\sigma_u} = e^{-\frac{t}{\tau}} . \qquad (18)$$

---

[1]The general case could be handled mathematically but as yet α is not an established material property. If stress relaxation is found to be exponential, this is taken as evidence that σ_b is much less than ($1/\alpha$). If, on the other hand, stress relaxation is found to be logarithmic this is taken as evidence that σ_b must be much greater than ($1/\alpha$), since for this case $\sinh \alpha \sigma_b$ may be replaced by

$\frac{1}{2} e^{\alpha \sigma_b}$. Then equation (16) gives

$$\sigma_b = \sigma_u - \frac{1}{\alpha} \ln \left[e^{\alpha \sigma_u} \left(\frac{t}{2\tau} \right) + 1 \right] .$$

and substituting this into (17) gives

$$\sigma = \sigma_u - 3 \frac{E_u - E_r}{E_u} \frac{1}{\alpha} \ln \left[e^{\alpha \sigma_u} \left(\frac{t}{2\tau} \right) + 1 \right] .$$

Substitution of (18) into (17) gives

$$\sigma = \sigma_u \left(\frac{E_r}{E_u} + \frac{E_u - E_r}{E_u} \; e^{-\frac{t}{\tau}} \right)$$

or

$$\sigma = E_u \epsilon - \epsilon (E_u - E_r)(1 - e^{-\frac{t}{\tau}}) \qquad (19)$$

or

$$\sigma = E_r \epsilon + \epsilon (E_u - E_r) \, e^{-\frac{t}{\tau}} \qquad (19a)$$

in which the unrelaxed stress (σ_u) has been replaced by the product of the unrelaxed elastic modulus (E_u) and the strain (ϵ).

The interpretation of equations (19) and (19a) is as follows. The stress at any time (t) can be expressed either as the stress that results from the application of a given strain in zero time ($E_u \epsilon$, the unrelaxed stress) minus the amount of relaxation that has occurred between time equal to zero and time equal to t (equation (19)), or as the stress that results from the application of a given strain in infinite time ($E_r \epsilon$, the completely relaxed stress) plus the amount of relaxation which has not yet occurred when time equals t (equation (19a)). Equation (19) or (19a) is the equation for the σ- t curve at any given value of ϵ, this value of strain being obtained in zero time. This last condition clearly indicates that in this integrated form equation (19) is not suitable for determining the stress

strain curve associated with any actual rate of straining; therefore a differential equation having the same form as equation (19) is introduced.

$$d\sigma = f_u(\epsilon)d\epsilon - d\epsilon\left[f_u(\epsilon) - f_r(\epsilon)\right]\left[1 - e^{-\frac{t}{\tau}}\right] \qquad (20)$$

in which E_u and E_r have been replaced by $f_u(\epsilon)$ and $f_r(\epsilon)$ respectively to indicate that the stress-strain curve need not be a straight line even in the relaxed or unrelaxed states.

In equation (20) the term

$$d\epsilon\left[f_u(\epsilon) - f_r(\epsilon)\right]$$

represents the amount a given $d\sigma$ produced by $d\epsilon$ will relax in infinite time. This term can be replaced by

$$R\, f_u(\epsilon)\, d\epsilon$$

in which R is the fraction of $d\sigma$, at time equal to zero, which can be relaxed in infinite time. Then

$$d\sigma = f_u(\epsilon)d\epsilon - Rf_u(\epsilon)\left[1 - e^{-\frac{t}{\tau}}\right]d\epsilon. \qquad (20a)$$

Application of the Relationship to Constant Rate of Strain

When the strain is increasing at a constant rate ($\dot{\epsilon} = b$) up to some value of ϵ' the relaxation time associated with each $d\sigma$ can be expressed as

$$t = \int_{\epsilon}^{\epsilon'} \frac{d\epsilon}{\dot{\epsilon}} = \frac{\epsilon' - \epsilon}{b}$$

and if the obtained value of strain (ϵ') is held constant for a time 'T' then the total relaxation time associated with each $d\sigma$ is

$$t = \frac{\epsilon' - \epsilon}{b} + T \tag{21}$$

Substituting equation (21) for t in equation (20a) and integrating gives

$$\sigma = \int_{0}^{\epsilon'} f_u(\epsilon)d\epsilon - Rf_u(\epsilon)d\epsilon \left[1 - e^{+\frac{\epsilon}{b\tau} - \frac{\epsilon'}{b\tau} - \frac{T}{\tau}} \right]$$

or

$$\sigma = \int_{0}^{\epsilon'} f_r(\epsilon)d\epsilon + \int_{0}^{\epsilon'} R\, e^{+\frac{\epsilon}{b\tau} - \frac{1}{\tau}\left(\frac{\epsilon'}{b} + T\right)} f_u(\epsilon)d\epsilon. \tag{22}$$

The form of the integrated expression will of course depend upon the form of $f_r(\epsilon)$, R, τ , and $f_u(\epsilon)$. The development which follows assumes the following forms:

R = constant

τ = constant

$f_r(\epsilon) = M\epsilon^p$

$f_u(\epsilon) = N\epsilon^q$

in which M, N, p, and q are constant, and by the definition of R if

R = constant then

p = q .

This particular selection was made on the basis of results

obtained in some of the preliminary experimental work which will be described in a later section.

Integration of equation (22) subject to the preceding condition gives

$$\sigma = \frac{M\epsilon^p}{p+1} + RNe^{-\frac{1}{\tau}\left(\frac{\epsilon}{b} + T\right)} \int_0^{\epsilon} e^{+\frac{\epsilon}{b\tau}} \epsilon^p \, d\epsilon \ .$$

The last term can be integrated by parts to a finite series of $(p + 1)$ terms when p is zero or a positive integer. When p is not a whole number the last term is integrated by parts to form an infinite series.

$$\int_0^{\epsilon} e^{+\frac{\epsilon}{b\tau}} \epsilon^p d\epsilon = e^{\frac{\epsilon}{b\tau}} \epsilon^{p+1} \left[\frac{1}{p+1} - \frac{(\epsilon/b\tau)}{(p+1)(p+2)} + \frac{(\epsilon/b\tau)^2}{(p+1)(p+2)(p+3)} \right.$$

$$\left. - \ldots\ldots \frac{(-1)^{n+1}(\epsilon/b\tau)^{n-1}}{(p+1)(p+2)\ldots\ldots(p+n)} \ldots\ldots \right.$$

The final result is

$$\sigma = \frac{M\epsilon^{p+1}}{p+1} + RNe^{-\frac{T}{\tau}} \epsilon^{p+1} \left[\epsilon, \text{ Series}\right] \qquad (23)$$

in which

$$\left[\epsilon, \text{ Series}\right] = \left[\frac{1}{p+1} - \frac{(\epsilon/b\tau)}{(p+1)(p+2)} + \ldots \right.$$

$$\left. \frac{(-1)^{n+1}(\epsilon/b\tau)^{n-1}}{(p+1)(p+2)\ldots(p+n)} \ldots \right.$$

This series can be shown to be convergent for all finite values of $(\epsilon/b\tau)$ by the ratio test, and since it is an alternating series the error committed by summing only n terms is known to be less than the value of the (n+1)th term.

The interpretation of equation (23) is as follows. The stress (σ) associated with any given value of strain (ϵ), produced by straining at a constant rate (b), may be expressed as the value of stress associated with that strain when the straining takes place at an infinitely slow rate $(\frac{M\epsilon^{p+1}}{p+1}$ - the relaxed stress) plus the unrelaxed stress still existing. If ϵ is held constant the amount of unrelaxed stress decreases exponentially.

Application of the Relationship to Constant Rate Strain Cycling

For the strain-time cycle shown in Figure 1 the stress-strain relation can be developed as follows. For $0 \leq t_1 \leq \frac{\epsilon_m}{b}$ equation (23) applies.

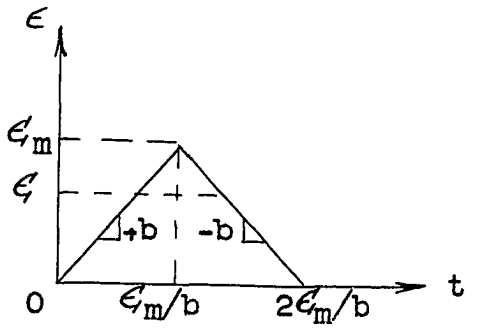

Figure 1. ϵ - t diagram.

For $\frac{\epsilon_m}{b} \leq t_1 \leq \frac{2\epsilon_m}{b}$ the stress corresponding to any strain (ϵ) can be expressed by evaluating the relaxation that takes place during the time when the strain is less than ϵ' and, in addition, the relaxation that occurs during the time when the strain is greater than ϵ' .

The time of relaxation associated with values of stress (σ) corresponding to values of strain (ϵ) less than ϵ' is

$$t = \frac{\epsilon' - \epsilon}{b} + \frac{2}{b}\left[\epsilon_m - \epsilon'\right] \qquad (24)$$

in which

$$\frac{2}{b}\left[\epsilon_m - \epsilon'\right]$$

may be considered as the time during which a value of strain equal to ϵ' is held constant, and hence this term can be used to replace T in equations (21) thru (23). A given value of stress developed during the increase in strain from ϵ' to ϵ_m is subject to relaxation for the entire time during which that value of stress exists, therefore the relaxation that occurs as strain goes from ϵ' to ϵ_m and back to ϵ' is

$$2\int_{\epsilon'}^{\epsilon_m} R\left(1 - e^{-\frac{\epsilon_m - \epsilon}{b\gamma}}\right) f_u(\epsilon)\, d\epsilon \quad . \qquad (25)$$

Hence, the value of stress associated with any value of strain (ϵ') occurring during the unloading portion of the strain cycle is

$$\sigma = \frac{M\epsilon^{p+1}}{p+1} + RN\epsilon^{p+1}\left[\epsilon, \text{ Series}\right] e^{-\frac{2}{b\tau}\left[\epsilon_m-\epsilon\right]}$$

$$- 2R\int_{\epsilon}^{\epsilon_m} \left(1 - e^{-\frac{\epsilon_m-\epsilon}{b\tau}}\right) f_u(\epsilon)d\epsilon \quad . \tag{26}$$

The last term in this equation can be written as

$$- 2R\left[N\int_{\epsilon}^{\epsilon_m} \epsilon^p d\epsilon - e^{-\frac{\epsilon_m}{b\tau}} N\int_{\epsilon}^{\epsilon_m} e^{+\frac{\epsilon}{b\tau}} \epsilon^p \, d\epsilon\right] \quad .$$

These terms can be integrated as before and equation (26) can then be written as

$$\sigma = \frac{M\epsilon^{p+1}}{p+1} + RN\epsilon^{p+1}\left[\epsilon, \text{ Series}\right]\left[e^{-\frac{2}{b\tau}(\epsilon_m-\epsilon)} - 2e^{-\frac{1}{b\tau}(\epsilon_m-\epsilon)}\right] - \frac{2RN(\epsilon_m^{p+1} - \epsilon^{p+1})}{p+1}$$

$$+ 2RN\epsilon_m^{p+1}\left[\epsilon_m, \text{ Series}\right] \quad . \tag{26a}$$

Equation (26a) gives the value of stress associated with a given value of strain (ϵ), produced by straining at a constant rate (b) to some strain (ϵ_m) greater than (ϵ) and then unstraining at the same rate (b) from (ϵ_m) back to (ϵ). Since the lowest value of stress which can exist with a given value of strain is a point on the relaxed stress strain curve the application of equation (26a) must be

restricted so that

$$\sigma \geq \frac{M\epsilon^{p+1}}{p+1} \quad .$$

This restriction is discussed further in the section titled RESULTS.

Application of the Relationship to Sinusoidal Straining

For the case in which the magnitude of strain increases sinusoidally with time, Figure 2, the relaxation time associated with each $d\sigma$ is

$$t = \int_{\epsilon}^{\epsilon'} \frac{d\epsilon}{\dot{\epsilon}} = \int_{\epsilon}^{\epsilon'} \frac{d\epsilon}{\epsilon_m \omega \cos \omega t_1}$$

$$t = \int_{\epsilon}^{\epsilon'} \frac{d\epsilon}{\epsilon_m \omega \cos(\sin^{-1} \frac{\epsilon}{\epsilon_m})}$$

$$t = \frac{1}{\omega}(\sin^{-1} \frac{\epsilon'}{\epsilon_m} - \sin^{-1} \frac{\epsilon}{\epsilon_m}) \quad . \tag{27}$$

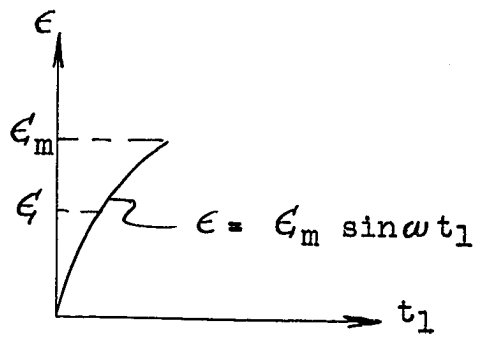

Figure 2. ϵ - t diagram.

Substitution of this relaxation time into equation (20a) and integrating gives

$$\sigma = \frac{M\epsilon^{p+1}}{p+1} + RNe^{-\frac{1}{\omega\tau}\sin^{-1}\frac{\epsilon}{\epsilon_m}} \int_0^{\epsilon} e^{+\frac{1}{\omega\tau}\sin^{-1}\frac{\epsilon}{\epsilon_m}} \epsilon^p \, d\epsilon. \tag{28}$$

With the value of p undefined (as a fraction, odd integer, or even integer) the integration of the last term in this equation is unnecessarily complicated; therefore it seems desirable from the practical point of view to leave this integration until the value of $f_u(\epsilon)$ (or $f_r(\epsilon)$) is established for a particular material.

The form of the $\sigma - \epsilon$ relationship for sinusoidally increasing strain can be illustrated by taking a particular case. With p = 0 (i.e., unrelaxed and relaxed stress-strain curves are straight lines), $f_r(\epsilon) = M$ and $f_u(\epsilon) = N$ then

$$\sigma = M\epsilon + RNe^{-\frac{1}{\omega\tau}\sin^{-1}\frac{\epsilon}{\epsilon_m}} \int_0^{\sin^{-1}\frac{\epsilon}{\epsilon_m}} e^{+\frac{x}{\omega\tau}} \epsilon_m \cos x \, dx$$

in which

$$x = \sin^{-1}\frac{\epsilon}{\epsilon_m}$$

or

$$\sigma = M\epsilon + \frac{RN\omega^2\tau^2}{1+\omega^2\tau^2}\left[\epsilon + \frac{1}{\omega\tau}\left(\sqrt{\epsilon_m^2 - \epsilon^2} - \epsilon_m e^{-\frac{1}{\omega\tau}\sin^{-1}\frac{\epsilon}{\epsilon_m}}\right)\right]. \tag{29}$$

Application of the Relationship to Sinusoidal Strain Cycling

For the case illustrated in Figure 3 a method similar to that applied in the constant rate strain cycling problem can be used to develop the complete σ - ϵ relationship.

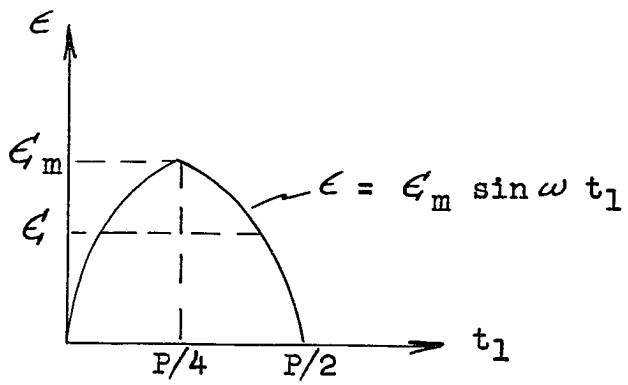

Figure 3. ϵ - t diagram.

Again for the case in which p = 0, then for $0 \leq t_1 \leq \frac{P}{4}$ equation (28) or (29) applies. For $\frac{P}{4} \leq t_1 \leq \frac{P}{2}$ the time of relaxation associated with values of stress (σ) corresponding to values of strain (ϵ) less than ϵ' is

$$t = \frac{1}{\omega}\left(\sin^{-1}\frac{\epsilon'}{\epsilon_m} - \sin^{-1}\frac{\epsilon}{\epsilon_m}\right) + \frac{2}{\omega}\left(\frac{\pi}{2} - \sin^{-1}\frac{\epsilon'}{\epsilon_m}\right) \quad (30)$$

in which

$$\frac{2}{\omega}\left(\frac{\pi}{2} \sin^{-1} \frac{\epsilon'}{\epsilon_m}\right)$$

may be considered as the time during which a value of strain equal to ϵ' is held constant.

The additional relaxation that occurs as the strain goes from ϵ' to ϵ_m and back to ϵ' is

$$2\int_{\epsilon'}^{\epsilon_m} R\left(1 - e^{-\frac{1}{\omega\tau}\left(\frac{\pi}{2} - \sin^{-1}\frac{\epsilon}{\epsilon_m}\right)}\right) f_u(\epsilon)\, d\epsilon \quad . \qquad (31)$$

Hence, the value of stress associated with any value of strain (ϵ') occurring during the unloading portion of the strain cycle is

$$\sigma = M\epsilon + \frac{RN\omega^2\tau^2}{1+\omega^2\tau^2} e^{-\frac{2}{\omega\tau}\left[\frac{\pi}{2} - \sin^{-1}\frac{\epsilon'}{\epsilon_m}\right]} \times \left[\epsilon' + \frac{1}{\omega\tau}\left(\sqrt{\epsilon_m^2 - \epsilon'^2} - \epsilon_m e^{-\frac{1}{\omega\tau}\sin^{-1}\frac{\epsilon'}{\epsilon_m}}\right)\right]$$

$$- 2\int_{\epsilon'}^{\epsilon_m} R\left(1 - e^{-\frac{1}{\omega\tau}\left(\frac{\pi}{2} - \sin^{-1}\frac{\epsilon}{\epsilon_m}\right)}\right) f_u(\epsilon)\, d\epsilon \quad . \qquad (32)$$

The last term in this equation can be written as

$$- 2\,RN\left[(\epsilon_m - \epsilon) - e^{-\frac{\pi}{2\omega\tau}} \int_{\epsilon}^{\epsilon_m} e^{+\frac{1}{\omega\tau}\sin^{-1}\frac{\epsilon}{\epsilon_m}}\, d\epsilon\right]$$

which integrates to

$$- 2\,RN\left\{(\epsilon_m - \epsilon) - \frac{\omega^2\tau^2}{1+\omega^2\tau^2}\left[\epsilon_m - e^{-\frac{1}{\omega\tau}\left(\frac{\pi}{2} - \sin^{-1}\frac{\epsilon}{\epsilon_m}\right)}\left(\frac{\sqrt{\epsilon_m^2 - \epsilon^2}}{\omega\tau} + \epsilon\right)\right]\right\},$$

and equation (32) can then be written as

$$\sigma = M\epsilon + \frac{RN\omega^2\tau^2}{1+\omega^2\tau^2}\, e^{-\frac{2}{\omega\tau}\left[\frac{\pi}{2} - \sin^{-1}\frac{\epsilon}{\epsilon_m}\right]}$$

$$\times\left[\epsilon + \frac{1}{\omega\tau}\left(\sqrt{\epsilon_m^2 - \epsilon^2} - \epsilon_m\, e^{-\frac{1}{\omega\tau}\sin^{-1}\frac{\epsilon}{\epsilon_m}}\right)\right]$$

$$- 2RN\left\{(\epsilon_m - \epsilon) - \frac{\omega^2\tau^2}{1+\omega^2\tau^2}\left[\epsilon_m - e^{-\frac{1}{\omega\tau}\left(\frac{\pi}{2} - \sin^{-1}\frac{\epsilon}{\epsilon_m}\right)}\right.\right.$$

$$\left.\left.\left(\frac{\sqrt{\epsilon_m^2 - \epsilon^2}}{\omega\tau} + \epsilon\right)\right]\right\}. \qquad (32a)$$

Application of the Relationship for the Evaluation of Hysteresis Losses

The energy loss, per unit volume of material, associated with constant rate, or sinusoidal strain cycling can be evaluated by integration of equations (23) and (26a), or (29) and (32a). The stress-strain curve for a single loading-unloading cycle will be similar to that represented in Figure 4.

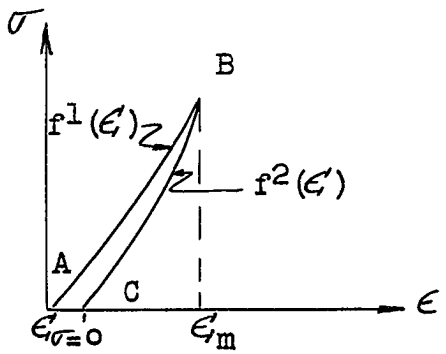

Figure 4. $\sigma - \epsilon$ diagram.

For the curve A-B; $f^1(\epsilon)$ can be taken as equation (23) if the loading occurs at constant strain rate, or as equation (29) if the increase in strain is sinusoidal. For the curve B-C; $f^2(\epsilon)$ can be taken as equation (26a) if the unloading occurs at constant strain rate, or as equation (32a) if the decrease in strain is sinusoidal. Then

$$W = \int_0^{\epsilon_m} f^1(\epsilon)\, d\epsilon - \int_{\epsilon_{\sigma=0}}^{\epsilon_m} f^2(\epsilon)\, d\epsilon \quad . \tag{33}$$

EXPERIMENTAL INVESTIGATION

The experimental investigation consisted of several rather distinct phases. Test equipment which could be used to evaluate material constants involved in $f_u(\epsilon)$, $f_r(\epsilon)$, and τ was designed and constructed (this is referred to as relaxation test equipment). In addition, since the reaction of the test equipment itself to dynamic loading has a very important effect on any results which may be obtained by using that equipment it was felt that a complete evaluation and calibration of this relaxation test equipment was necessary. Following this evaluation and calibration, the relaxation test equipment was used for certain preliminary tests. These tests were performed for the purpose of providing information which could be used to check assumptions and to guide in the selection of functions which were used in the theoretical investigation. Equipment (referred to as wave propagation test equipment) which could be used to study strain wave propagation in the same material as was to be tested in the relaxation test equipment was set up. This was done in order to provide for a completely independent method of checking results.

Therefore, the experimental investigation is discussed under the following subheadings.

1. Description of Relaxation Test Equipment
2. Evaluation and Calibration of Relaxation Test Equipment
3. Description of Wave Propagation Test Equipment
4. Material Tested
5. Preliminary Investigations

The actual evaluation of the material constants associated with $f_u(\epsilon)$, $f_r(\epsilon)$ and τ and the comparison between theoretical and experimental results are discussed in the section titled RESULTS.

Description of Relaxation Test Equipment

The test equipment shown in Figure 5 was designed and constructed for the purpose of straining a specimen at various rates to a specified value and then holding the strain constant.

The top and bottom supports (Parts Numbers (2) and (7) in Figure 5) were securely bolted to a 4 in. by 9.5 lb. Std. I Beam which was in turn bolted to a vertical 2 in. by 8 in. timber. The specimen to be tested, (5), rests on (2) and supports the steel plate (4). The specimen (5) is compressed between (4) and (2) when (4) is drawn vertically downward by a force exerted on the pull bar (3). This force may be exerted in either of two ways; a weight may be dropped on the stop plate (9) or the loading nut (8) may be

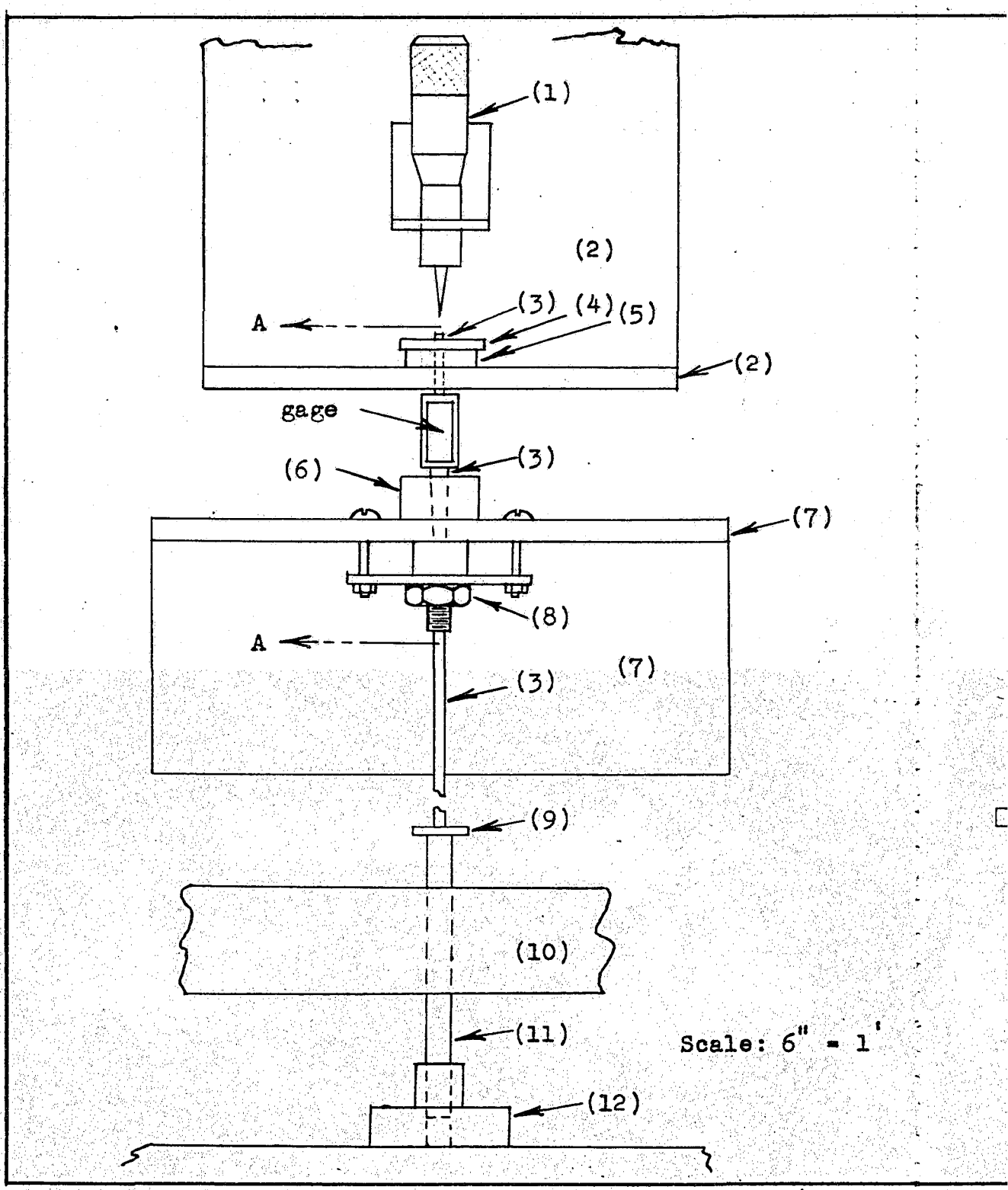

Figure 5. Stress relaxation test e

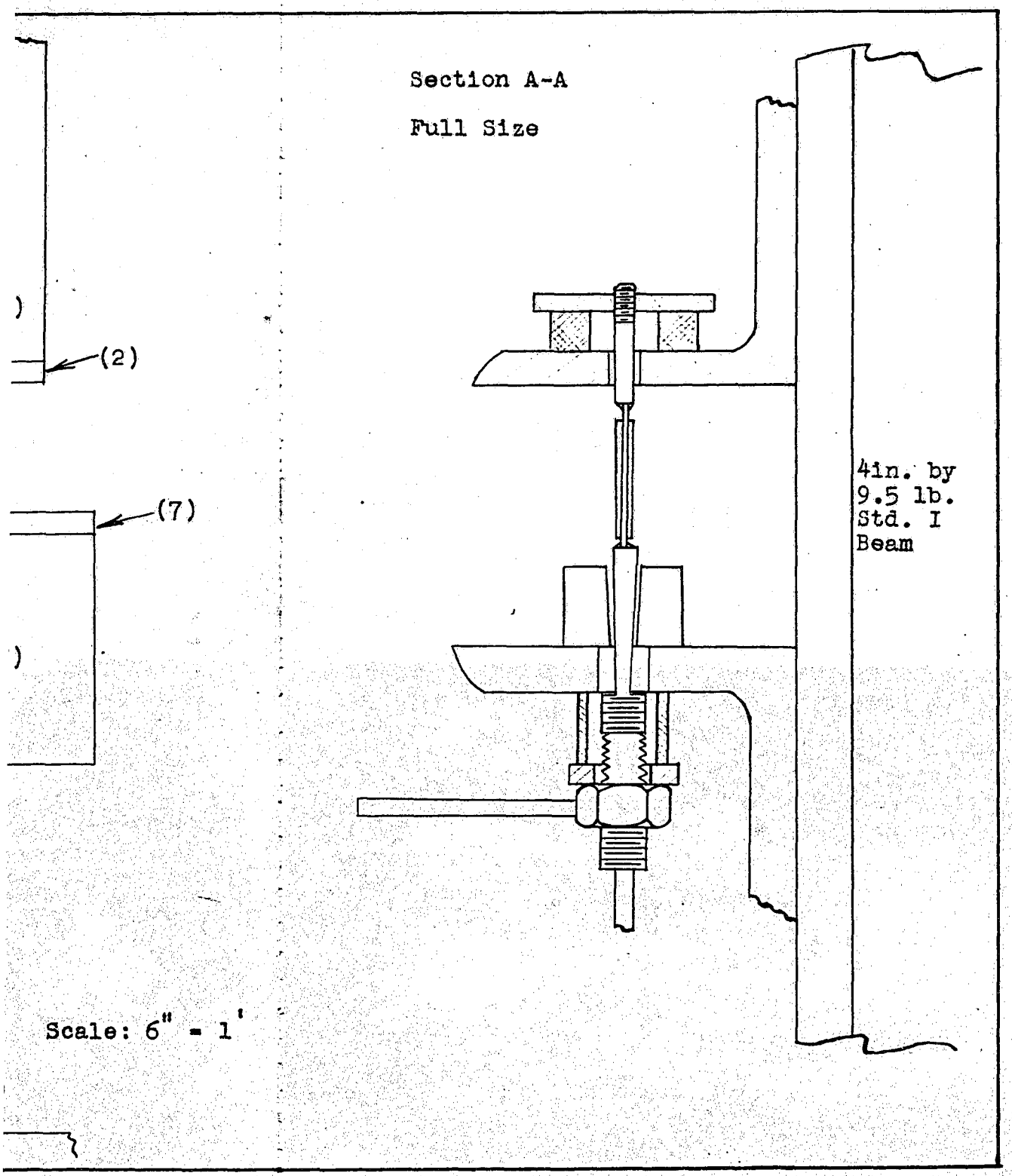

Stress relaxation test equipment.

turned. When the compressive force is exerted by means of a falling weight, the tapered portion of (3) is passed through a soft lead block (6) containing a mating tapered hole. This block (6) is fastened to (7), and the wedging of the taper on (3) in (6) permits the maximum value of compressive strain produced to be maintained. (This block (6) is removed when the compressive load is applied by means of the loading nut (8).)

The flat portion of the pull bar (3), which is marked "Gage" in Figure 5, consists of a piece of 0.004 in. thick brass shim stock on which two SR-4 strain gages are cemented back to back. These gages measure the strain produced by the total resistance offered to the downward motion of the pull bar (3). The total resistance includes not only the resistance to compression offered by the specimen but also the forces necessary to accelerate all of the masses moving with (3) above the gages. The electrical components used with these gages will be described later in this section and the evaluation of accelerating forces will be discussed in the section titled "Evaluation and Calibration of Relaxation Test Equipment".

The pull bar (3) is connected to an extension rod (11) which extends into the induction coil (12). This extension rod is guided by the wooden bearing block (10) and any motion of (3) changes the position of the extension rod in

the induction coil. The electrical effect produced by this change in position provides the means for measuring the compression of the specimen.

The micrometer (1) mounted above the specimen was used for the calibration of the electrical signal produced by the induction coil. The method of calibration and the effects of any lost motion which may occur are discussed in the section titled "Evaluation and Calibration of Relaxation Equipment".

The two SR-4 strain gages mounted back to back on the pull bar were type A-5 gages for which the gage resistance equals 120.2 ± .2 ohms, and the gage factor equals 2.00. These gages were connected as opposite arms in a Wheatstone bridge circuit. The remaining two arms of the bridge consisted of two additional gages of the same lot number (#126) as the active gages, mounted on the same material as the active gages, but in an unstrained condition. This arrangement provides for temperature compensation, elimination of signal due to flexural strain, and for doubling of the signal due to tensile strain.

The induction coil used to measure the motion of the pull bar had an impedance of approximately 500 ohms at 2000 cps. This coil was connected as one arm in a Wheatstone bridge circuit, and the remaining three arms consisted of three nearly identical coils. Two of the three inactive

coils were uncored while the third contained a moveable core for obtaining initial balance of the bridge.

These two bridges were connected for recording as shown in Figure 6. For the complete electrical details of recording instruments see (39) "Literature Cited".

Evaluation and Calibration of Relaxation Test Equipment

In designing the test equipment (Figure 5) to be used in the experimental investigation, the effect of the finite velocity of wave propagation on the results of studies made at high strain rates was given first consideration. During any period when a specimen is being strained by the displacement of one of its ends, the magnitude of strain will not be uniform throughout the specimen length. When the time required for the strain wave to propagate a distance equal to the specimen length is relatively large compared to the time during which the end displacement is applied, the average strain over the specimen length differs from the strain at the displaced end by a considerable amount. A bar fixed at one end and being strained by constant velocity displacement of the opposite end can be used as an example (Figure 7a). If the velocity of end displacement is taken as v, and the velocity of longitudinal wave

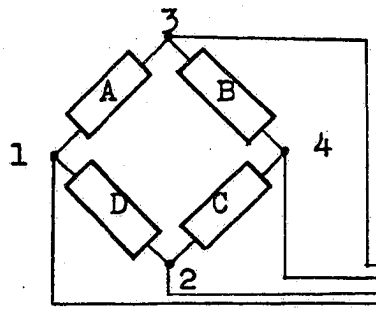

Gages "A" and "C" mounted back to back on pull bar. Gages "B" and "D" mounted back to back on unstrained strip.

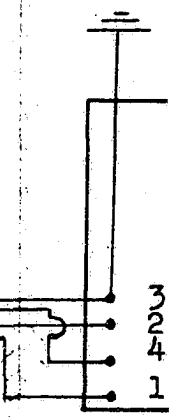

Type A-5, SR-4 Gages for measuring pull bar load.

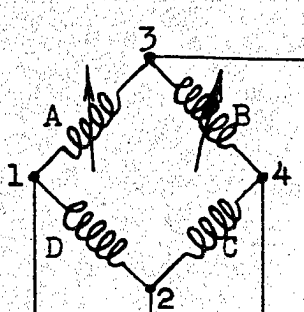

Core in coil "A" connected to pull bar.
Core in coil "B" adjustable for initial balancing.

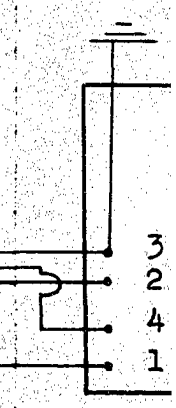

Induction coils for measuring displacement of pull bar.

Figure 6. Bridge circuits for measuring force and

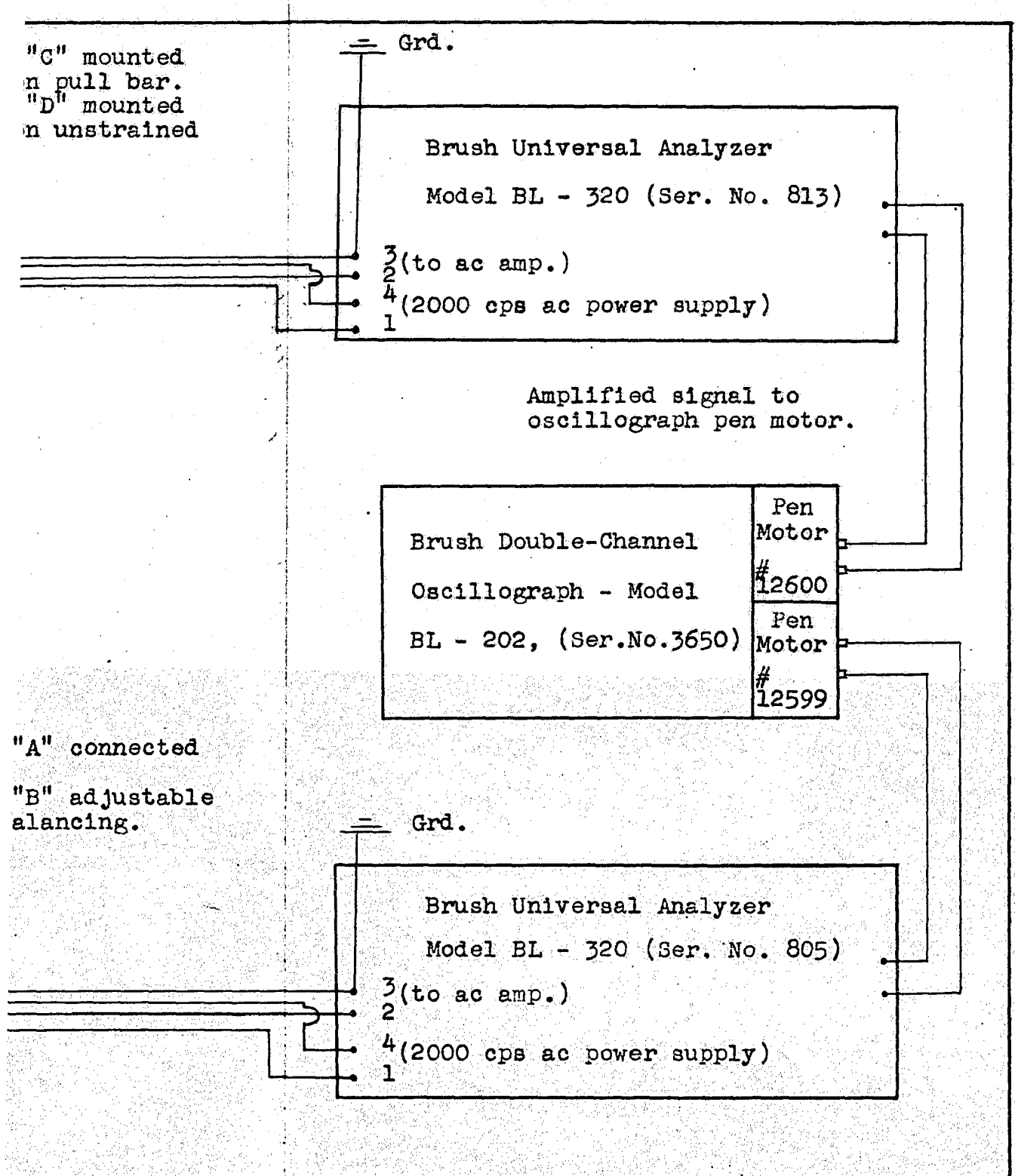

uits for measuring force and displacement.

propagation as c, then the strain produced is $\frac{v}{c}$.[1] At a time t the length of the bar which is strained will be equal to ct. The strain-length-time diagram (Figure 7b) shows the strain at any point along the length of the bar, at any time after the displacement begins (t = 0) and before the strain wave reaches the fixed end (t = L/c). If the end displacement is continued for a time sufficiently long for end reflections to occur, the strain at any point along the length of the specimen, at any time during the straining period can be represented on the strain-length-time diagram (Figure 7c). In order to insure that the maximum strain at any point along the length of the specimen will differ from the average strain by only a small amount the length must be kept to such a value that numerous reflections of the strain wave will have occurred during the time interval of interest. The number of steps in the strain-time plane of the ϵ - L - t diagram (Figure 7c) is given by

$$n \text{ steps} = t \frac{c}{2L} . \qquad (34)$$

Since $\sqrt{\frac{E}{\rho}}$ may be taken as a reasonable approximation for c,

---

[1] In a time dt the displacement of the end will equal v dt. This displacement is the total elongation of that length of material affected in time dt, which is c dt. The strain is $\frac{v\ dt}{c\ dt}$ or $\frac{v}{c}$. Timoshenko (40) points out that Sir Thomas Young saw this ratio as strain and discussed its significance in 1807.

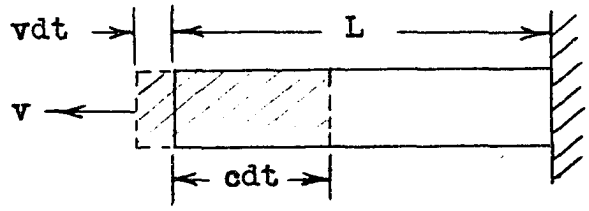

(a) Bar fixed at one end, opposite end displaced with velocity = c.

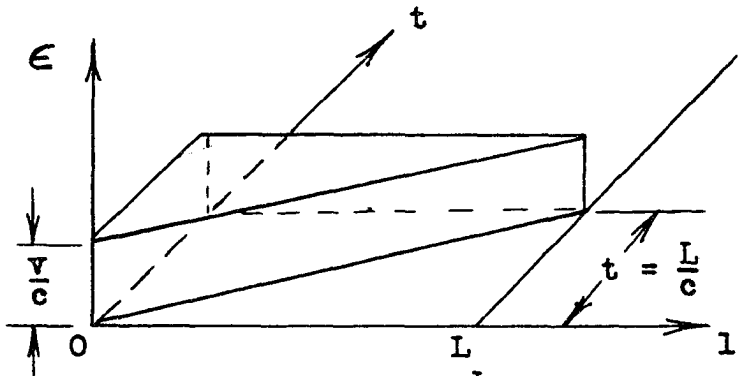

(b) ϵ-l-t diagram for $0 \leq t \leq \frac{L}{c}$, before reflection from fixed end.

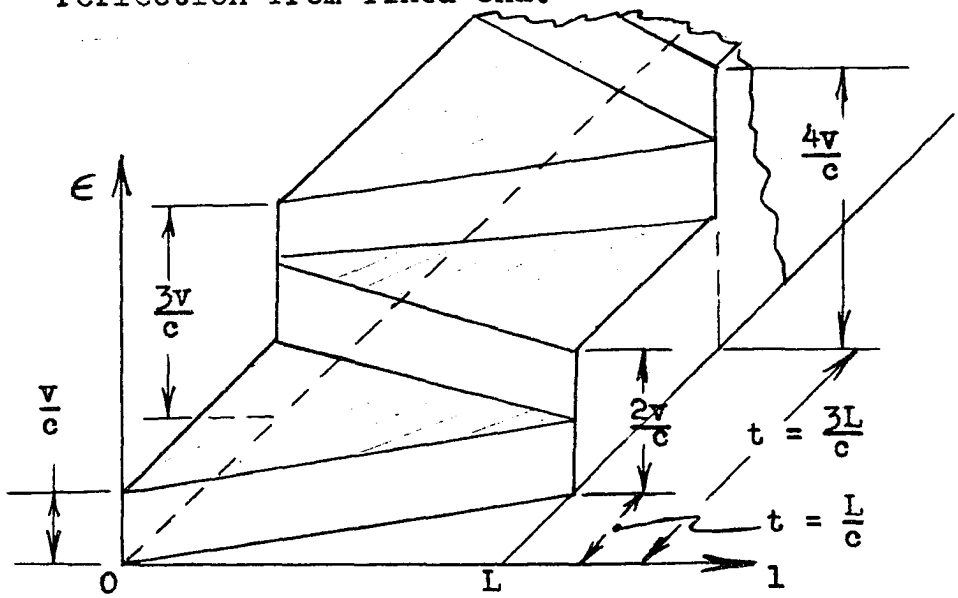

(c) ϵ-l-t diagram for $t > \frac{L}{c}$, effect of end reflections.

Figure 7. Strain-length-time diagram.

the length of specimen necessary to enable the average strain to be used for the strain at the displaced end with any prescribed degree accuracy can be determined. For the rubber on which tests were made:

$E = 1800$ psi (Static Test Value at Room Temperature, furnished by the Manufacturer.)

sp. wt. $= 72.9$ lb./ft^3 (From Volume and Weight Measurements.)

$$c = \sqrt{\frac{E}{\rho}} = \frac{1800 \times 1728 \times 386}{72.9} = 4{,}050 \text{ in/sec}$$

$$\text{n steps} = t \frac{c}{2L} = 2{,}025 \frac{t}{L}$$

If $L = 0.25$ in. then for a time interval as small as 0.01 second

$$\text{n steps} = 81 .$$

Therefore, at the end of the first 0.01 second interval the average strain can be used for the strain at the displaced end of the specimen and the error involved will be equal to, or less than, 1 part in 81; provided that the values used in the above computation apply. Readings of average strain taken at times greater than 0.01 second after the beginning of straining will of course be even better approximations for the strain at the displaced end. Since, with the recording system to be used, the strain readings could not

be evaluated for times less than 0.01 second the test equipment was designed for a specimen of 0.25 inch length.

Since the test equipment was to hold the test specimen at a constant value of strain for any period of time following the application of the strain, the effect of strain and any creep which might occur in the pull bar between the specimen and the point of load application were given special consideration. The distance between the point of load application and the specimen was made as short as possible. The cross-section of the pull bar below the point at which the strain gages were applied was selected only on a basis of desired rigidity; however the pull bar cross-section at the gage location had to be reduced to a value that would strain sufficiently under load to produce a measurable signal. A maximum applied load of 20 pounds was assumed, then a cross sectional area of 0.002 square inches (0.004 in. by 0.5 in.) was selected for the region where the gages were to be applied. This gave an expected stress of

$$\sigma = \frac{F}{A} = \frac{20}{0.002} = 10{,}000 \text{ psi} .$$

The material selected was cold rolled brass, and hence the strain expected at the gages was

$$\epsilon = \frac{\sigma}{E} = \frac{10{,}000}{15 \times 10^6} = 667 \ \mu\text{in/in.}$$

With a load of 20 pounds the total elongation of the pull bar was computed as 0.000,78 inches. Thus, even for 100% stress relaxation within the test specimen (i.e., after being strained to a given amount the stress required to hold the specimen in that strained state drops to zero) the release of the load on the pull bar will produce, in a 0.25 inch specimen, an increase in strain of only 0.3%.

Any creep which might occur in the pull bar during the period in which the strain is to be held constant would act to reduce the strain and thus give a false (too large) value for the amount of stress relaxation. Any creep in the strain gage bond would not affect the amount of specimen strain, but bond creep too would produce an apparent value of stress relaxation greater than the true value. The magnitude of stress relaxation error due to these two types of creep is very difficult to estimate and therefore tests were conducted on the completed equipment to evaluate this error. A specimen made of steel was used in place of the usual rubber specimen; the load was applied at various rates and to magnitudes of stress at least as great as those which would be encountered in later tests. Since the steel specimen was strained only a very small amount; any apparent stress relaxation could, under the circumstances of these tests, be attributed to creep in the pull bar or in the gage bond. A reproduction of the oscillograph record taken during one of these tests is presented in Appendix A. A study of

this record indicates that gage bond creep does not occur to a measurable extent (i.e., the gage signal returns to the original zero upon removal of the load). The gradual decrease in the gage signal does indicate that the pull bar creeps with time. This relief of load due to a given amount of pull bar creep will be much less than it is in these tests when the rubber specimen is in place due to the lower modulus of the rubber; therefore the error in measuring stress relaxation should be very small.

The total resistive load measured by the pull bar gages consists of two parts; the resistance offered by the test specimen to strain, and the accelerating forces. Since the mass of material which must be accelerated could not be reduced to zero, it was necessary to determine the magnitude of these accelerating forces. The tests conducted for this purpose consisted of assembling the test equipment without any test specimen in place. The load nut was then turned to produce magnitudes of acceleration at least as great as those that would be produced in later tests. A reproduction of the oscillograph record taken during one of these tests is presented in Appendix A. This record indicates that the accelerating forces are not of sufficient magnitude to produce a measurable stress.

The effect of inertia on the pen of the recording oscillograph was also considered, since any overshoot of

the recording pen will produce records in which the apparent stress relaxation is greater than the actual stress relaxation. Tests made with a steel test specimen in place indicated that for loading times of less than 0.04 second pen overshoot makes the records questionable. Reproductions of these records are presented in Appendix A.

The SR-4 strain gages mounted on the pull bar for the purpose of measuring the applied force were calibrated in conjunction with the associated recording equipment. The lead block ((6) Figure 5) was removed and the extension rod ((11) Figure 5) disconnected from the pull bar ((3) Figure 5). With a specimen in place, a load calibration curve was taken by stacking scale weights on the stop plate (9). The amplification setting of the recording equipment was adjusted and set so as to produce approximately 25 mm. of pen displacement with an applied load of 20 pounds. In order to insure that the amplification factor could be reproduced in all subsequent tests the pen displacement produced by a standard calibration resistor (390,000 ohms) connected in parallel with gage 'A' (Figure 6) was recorded. In all subsequent tests the amplification was set so as to produce the required pen displacement when the same calibration resistor was connected in parallel with gage 'A'. The applied force calibration curve which was used in the analysis of the experimental data is given as Figure 8a.

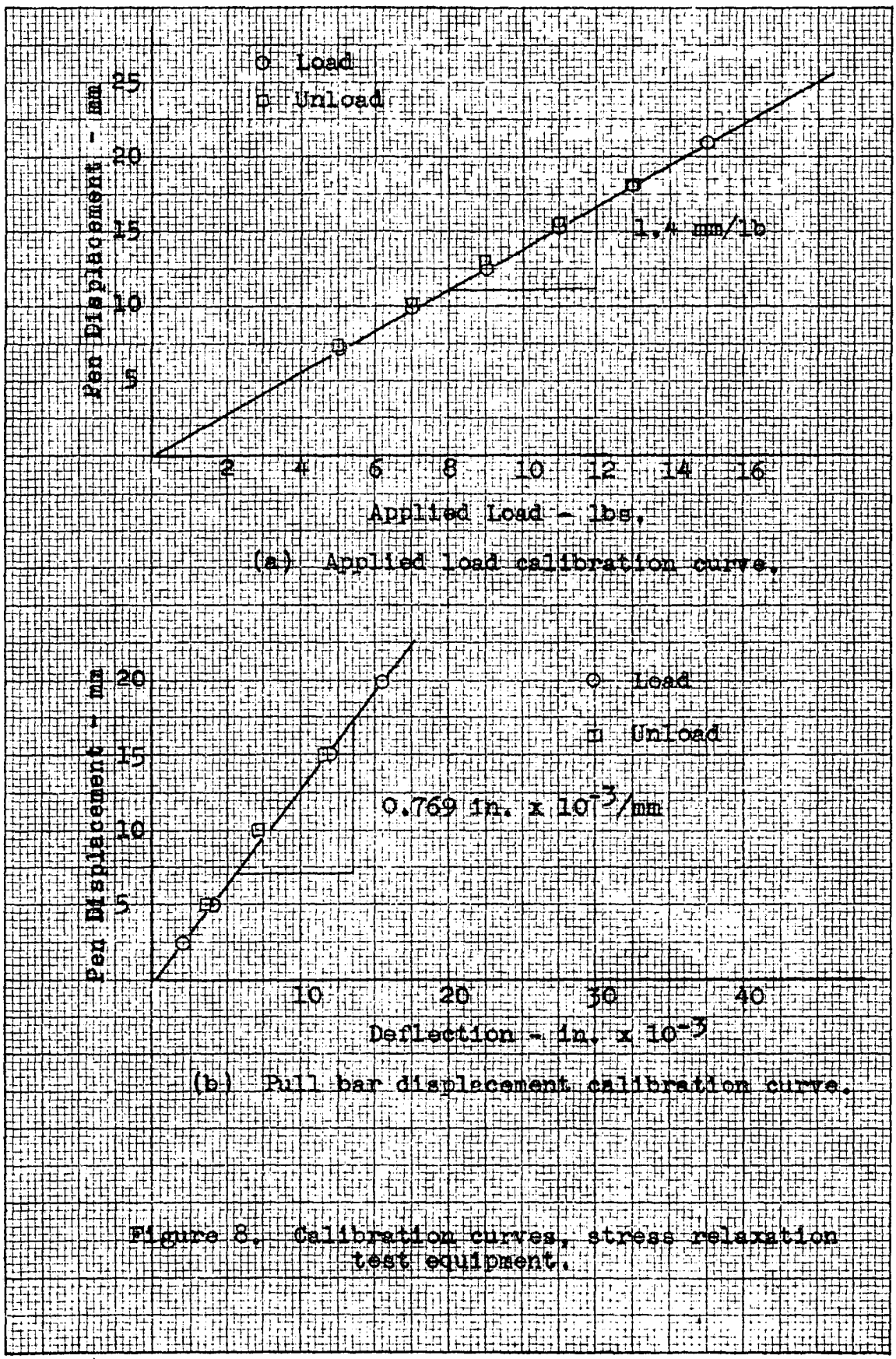

(a) Applied load calibration curve.

(b) Pull bar displacement calibration curve.

Figure 8. Calibration curves, stress relaxation test equipment.

The tabulated data from which this curve was constructed are presented in Appendix A.

The induction coils ((12) Figure 5) used to measure pull bar displacement were calibrated in conjunction with the associated recording equipment. With the test equipment completely assembled (except for the lead block (6)) the specimen was compressed by turning the loading nut. Displacement of the upper end of the pull bar was measured by means of the depth micrometer, and these measured values of displacement were recorded together with the corresponding pen displacement produced by the unbalance of the induction coil bridge. The amplification setting of the recording equipment was adjusted and set to produce approximately 20 mm. of pen displacement when the pull bar displacement measured 0.015 inch. A standard calibration resistor was used as previously described to insure reproducability of the amplification setting. It will be noted that by measuring the pull bar displacement at the upper end the extension of the pull bar was eliminated in the calibration. Any lost motion between the plate (4) and the test specimen and/or in any of the threaded connections would, of course, cause the displacement of the pull bar to be greater than the amount by which the test specimen is compressed. There are no restoring forces associated with the lost motion however, and therefore lost motion is

indicated by zero shift on the displacement-time record. It was discovered that lost motion could be reduced to a negligible amount if some time after assembling the test equipment and before running the actual test the specimen was loaded to a small value of compression and released. This procedure was followed during the entire experimental program. The pull bar displacement calibration curve which was used in the analysis of the experimental data is given as Figure 8b. The tabulated data from which this curve was constructed are presented as Appendix A.

Description of Wave Propagation Test Equipment

The test equipment shown in Figure 9 was set up for the purpose of studying the nature of longitudinal wave propagation in rods. This equipment was used to study wave propagation in the same material as was tested in the relaxation test equipment.

The rubber rod used in these tests was hung from the ceiling. The lower end of the test rod was attached to a loudspeaker voice coil which was energized by a sinusoidal signal. The Hewlett-Packard audio-oscillator used as a signal source made a wide range of frequencies available. A microswitch (SW_1 in Figure 9) was inserted between the signal amplifier and the loudspeaker to that the loudspeaker could be energized with signals of small time duration.

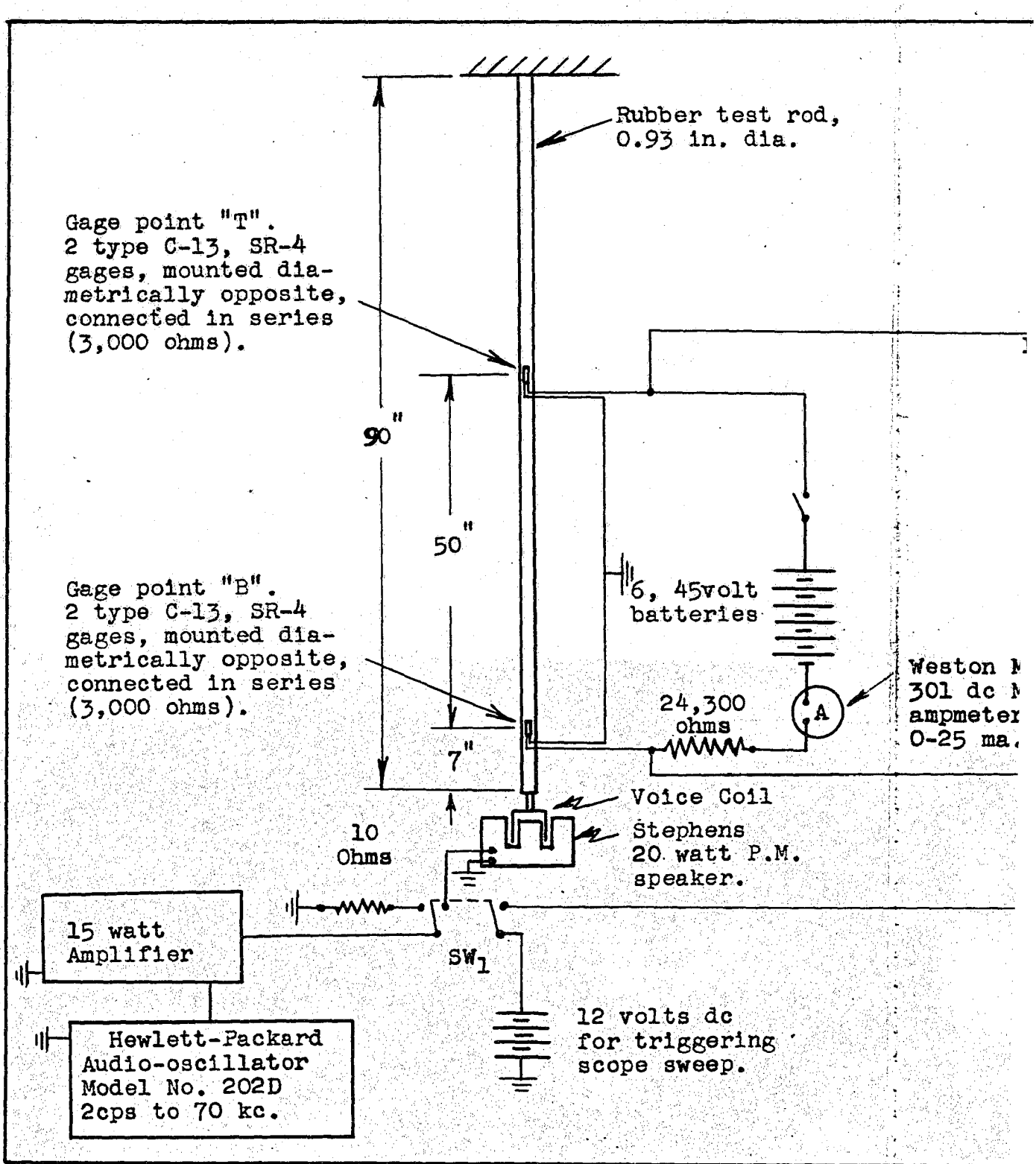

Figure 9. Wave propagation test eq

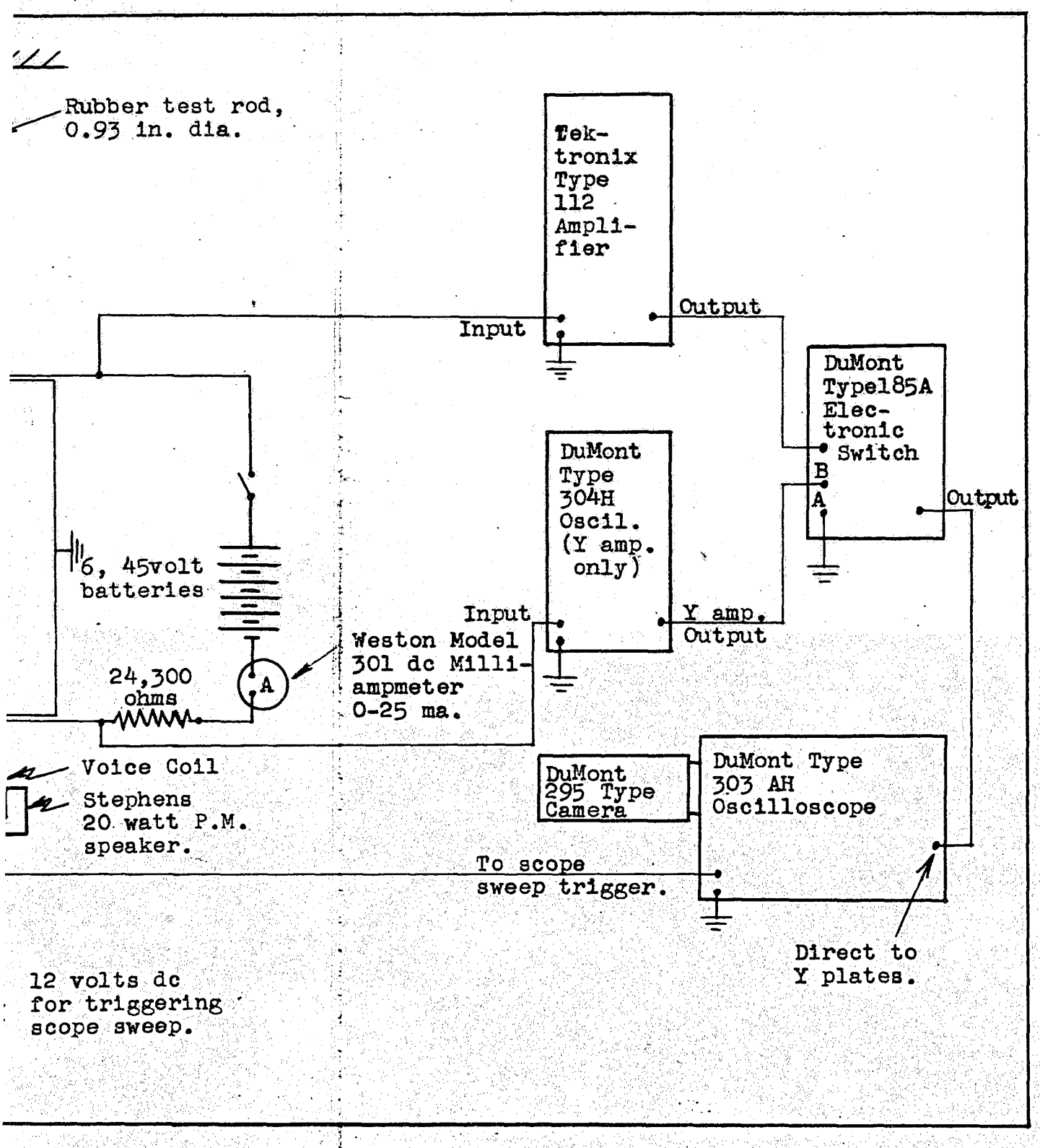

ıre 9. Wave propagation test equipment.

The sinusoidal displacement of the lower end of the rod produces sinusoidal strain waves which are propagated through the rod from bottom to top. Type SR-4 strain gages[1] were mounted on diametrically opposite sides of the test rod at a point approximately seven inches above the lower end and at a second point 50 inches above the first. The two diametrically opposite gages at each location were connected in series to eliminate signals due to flexural strain. The theory of strain measurements using resistance type gages in a potentiometer circuit is available in several papers and texts (41, 42, 43) and will not be repeated here.

A change in longitudinal strain at either gage point (B or T in Figure 9) causes a change in gage resistance and this in turn causes a change in potential across the gage point. Potential changes across the two gage points were picked up and amplified separately. After amplification the signals from the two gage points were introduced into the Du Mont electronic switch. This switch permitted simultaneous observation of the signals from the two gage points (T and B) by alternately switching to the vertical deflection plates of the Du Mont 303 AH oscilloscope first one signal and then the other. The sweep (or time base)

---

[1]The gages were type C-13 which have a resistance of 1500 ± 5 ohms and a gage factor of 3.18.

on the Du Mont 303 AH oscilloscope was set so as to trigger at the same instant that the loudspeaker was energized (i.e., when the switch SW_1 is closed).

During a test the sequence of events was as follows.

1. The Hewlett-Packard audio-oscillator was set to produce the frequency desired for the strain pulses.
2. The microswitch (SW_1) was depressed causing a train of sinusoidal strain pulses to be originated at the lower end of the test rod and at the same time causing the 303 AH oscilloscope to begin its sweep. Due to the action of the electronic switch two separate traces appear on the oscilloscope screen.
3. When the first strain pulse reaches the first gage point (B on Figure 9) the gage signal causes displacement of one of the traces on the oscilloscope screen.
4. When that same first strain pulse reaches the second gage point (T on Figure 9) the signal from this gage point causes displacement of the other trace.

The Du Mont oscilloscope record camera was used to record the traces just described. The time required for a strain pulse to travel from gage point B to gage point T is available from this type of record. In addition, any change in the shape of the strain pulse which may occur as it

travels from B to T can also be observed.

Material Tested

The material tested was supplied in the form of a rubber rod by the Chemical and Physical Research Laboratories of The Firestone Tire and Rubber Company. The rod was fabricated by an extrusion process followed by vulcanization, and had a diameter of 0.93 inches and a length of approximately 100 inches.

Individual relaxation specimens were produced by cutting slices approximately 0.25 inches thick from one end. The cutting was done on a power saw or in a miter box, and the rod was held steady during this cutting operation by means of 1 in. by 1 in. wood splints taped on opposite sides of the rod. A 0.50-in. diameter, centrally located hole was then removed from each slice with a standard $\frac{1}{2}$-in. gasket cutter. The parallel surfaces of each specimen were finished by hand on 00 sandpaper.

The 90-in. length of rod remaining after these relaxation specimens were removed was used for the wave propagation test.

Preliminary Investigations

The first set of tests was conducted on the relaxation test equipment for the purpose of determining, (1) the general shape of the compressive stress-strain curve with a

constant strain rate, (2) the effect of the strain rate on the stress-strain curve, (3) the general shape of the stress-time curve with strain held constant; and (4) the effect the rate of straining and the value of strain obtained on the stress-time curve.

In this first set of tests Specimen No. 1 was strained at various rates up to values of strain of approximately 5 percent, and this maximum value of strain was then held constant. The values recorded were the applied force vs time and the total deformation vs time. From measured values of the original cross-section and height these recorded values were converted to stress vs time and strain vs time. Figure 10 shows the stress-time and the strain-time curves for the tests of this first set. The stress-strain curves taken from these stress-time, strain-time curves are shown on Figure 11. From these figures the following general, but important facts are apparent: The effect of the strain rate on the value of stress required to produce a given strain is easily measured with this equipment, except for values of strain less than two percent where experimental errors tend to obscure the effect of strain rate. The decrease in stress with time (stress relaxation) when the strain is held constant is readily available when the strain value is as high as five percent. The stress-strain diagram is not characterized by a straight

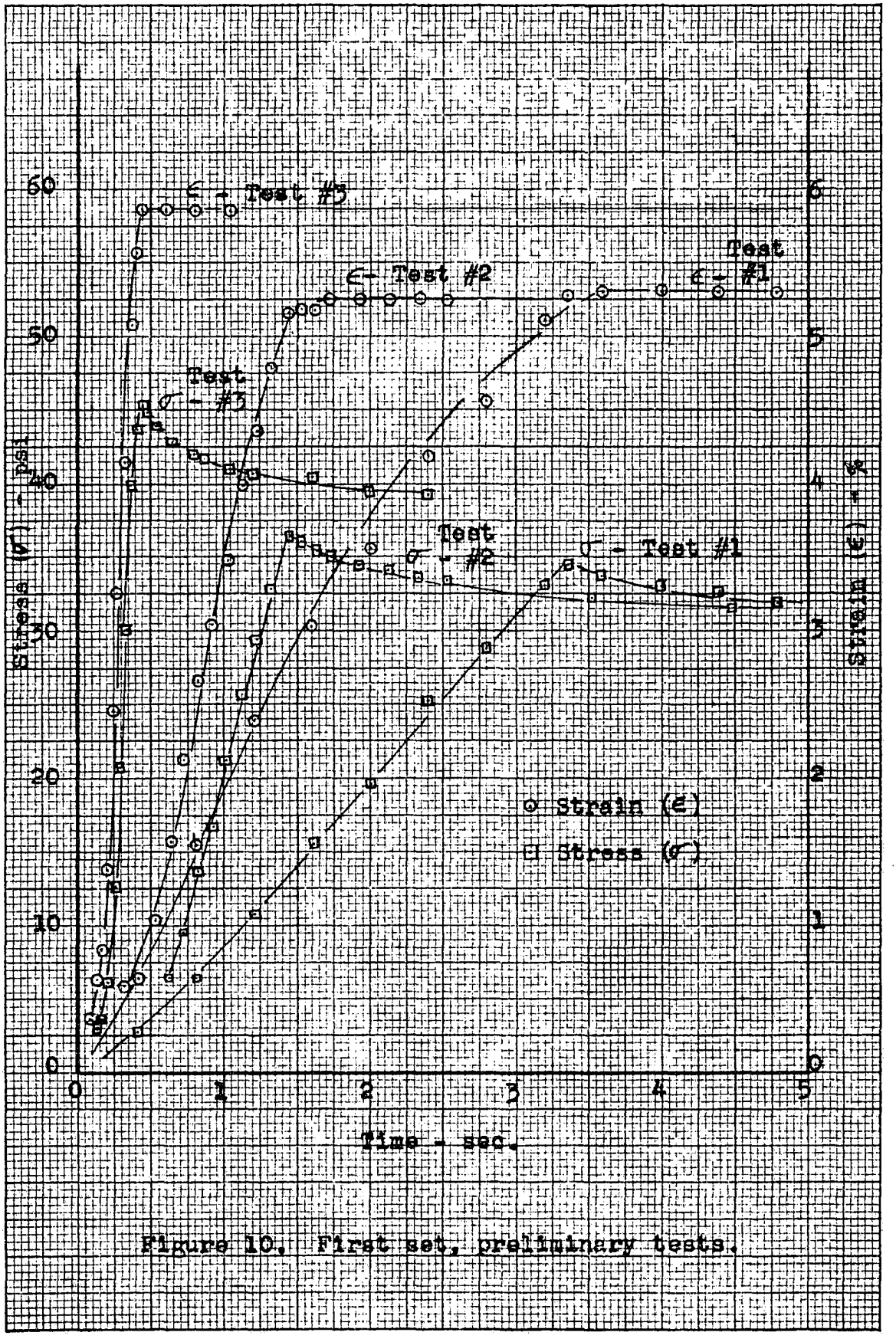

Figure 10. First set, preliminary tests.

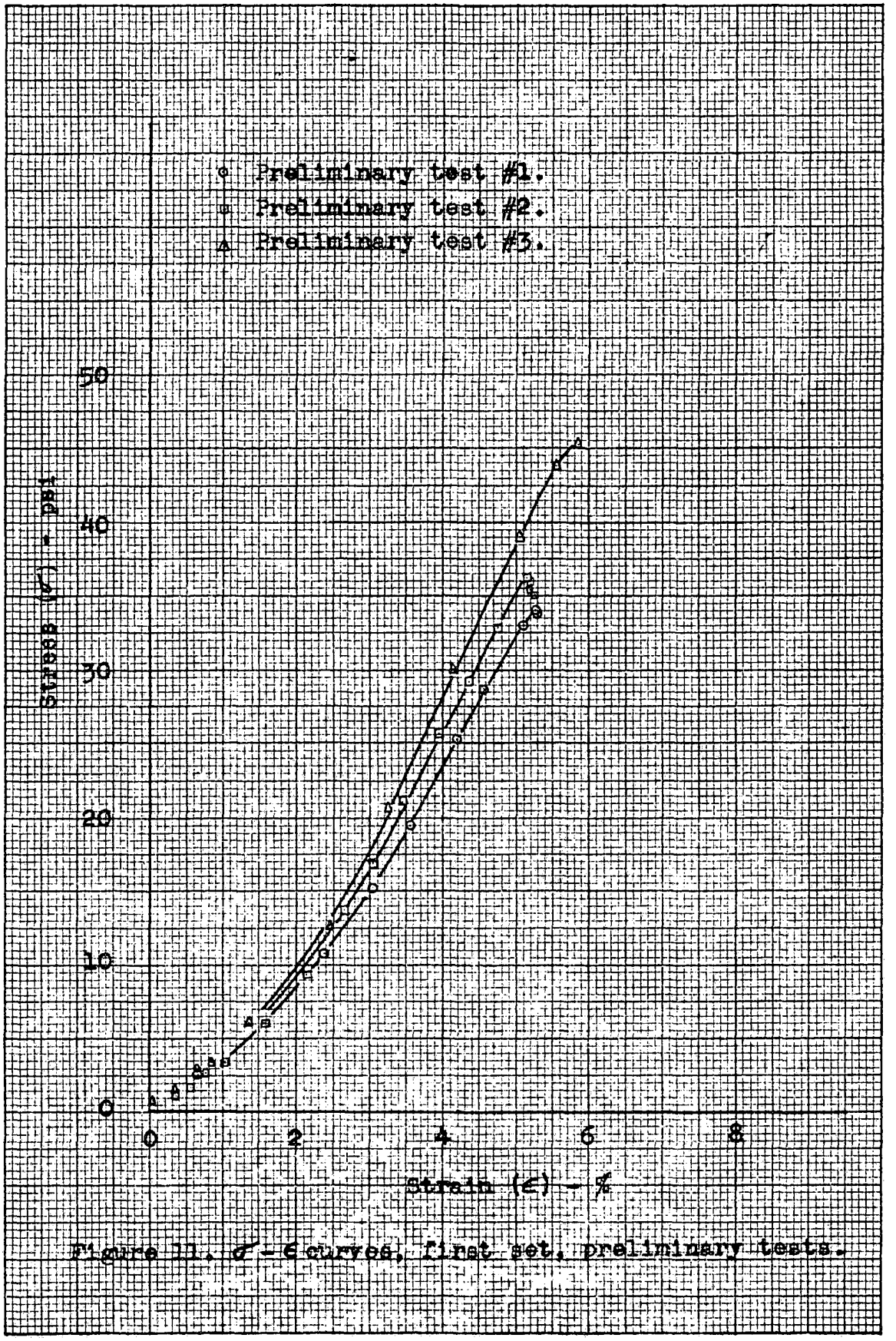

Figure 11. $\sigma - \epsilon$ curves, first set, preliminary tests.

line at any of the rates tested. Tabulated data from which Figure 10 was constructed are presented in Appendix B.

A second set of tests was conducted to find the form of $f_u(\epsilon)$, and $f_r(\epsilon)$ and also to determine whether or not R and τ could be assumed to be independent of the magnitude of strain. A direct experimental evaluation of $f_u(\epsilon)$ is of course impossible since by definition of $f_u(\epsilon)$ the time of loading must be equal to zero. To overcome this difficulty instead of loading Specimen No. 2 continuously from a value of zero strain to a value of maximum strain, the total strain was applied in six nearly equal increments. After each increment of strain (and hence stress) was applied, sufficient time was allowed for a large part of the stress relaxation to occur. The stress increments associated with the six strain increments were added. The result was a stress-strain curve for which the relaxation is limited to the sum of the amounts by which each individual stress increment can relax during its time of application. The step curve showing the incremental increases in stress and strain, and the stress-strain curve constructed from this by the addition of the stress increments are shown on Figure 12. The lower stress-strain curve shown on Figure 12 was obtained from a second test on Specimen No. 2 in which the strain was produced as slowly as possible with intermediate stops of sufficient length to allow nearly complete

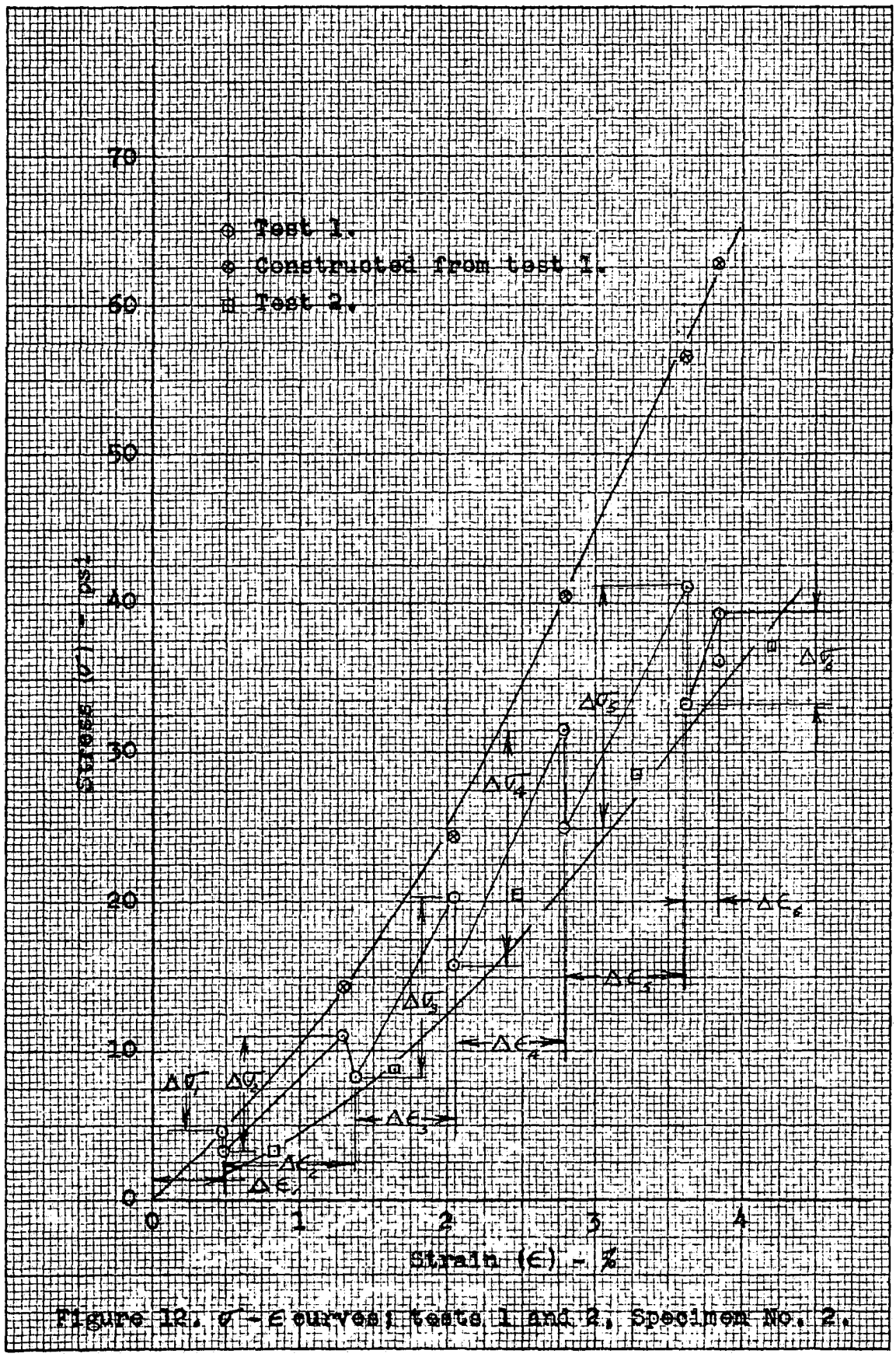

Figure 12. σ - ε curves; tests 1 and 2, Specimen No. 2.

relaxation of stress. This lower curve will be taken as the relaxed stress-strain diagram, while the upper curve will be interpreted as an experimental approach to the unrelaxed stress-strain diagram. These same two curves plotted on logarithmic coordinates are shown on Figure 13. These curves indicate that a reasonable form for $f_r(\epsilon)$ is $M\epsilon^p$, and also that a reasonable form for $f_u(\epsilon)$ is $N\epsilon^q$ provided that the true unrelaxed curve is not too far different from this experimental unrelaxed curve. Further, these curves indicate that p = q and hence R is a constant within this range of strain.

The data on stress relaxation following each incremental addition of stress in the first test of this set were used to investigate the influence of strain level on the exponential relaxation constant (τ). From equation (19) or (20) τ can be defined by means of the expression:

Relaxation of $\Delta\sigma$ in time (t) $= \Delta\sigma_{t=0} - \Delta\sigma_{t=t}$

$$= \Delta\epsilon\left[f_u(\epsilon) - f_r(\epsilon)\right]\left(1 - e^{-\frac{t}{\tau}}\right)$$

$$= R\Delta\epsilon f_u(\epsilon)\left(1 - e^{-\frac{t}{\tau}}\right)$$

$$= R\Delta\sigma_{t=0}\left(1 - e^{-\frac{t}{\tau}}\right),$$

or

$$R\Delta\sigma_{t=0} - \left(\Delta\sigma_{t=0} - \Delta\sigma_{t=t}\right) = R\Delta\sigma_{t=0}\, e^{-\frac{t}{\tau}},$$

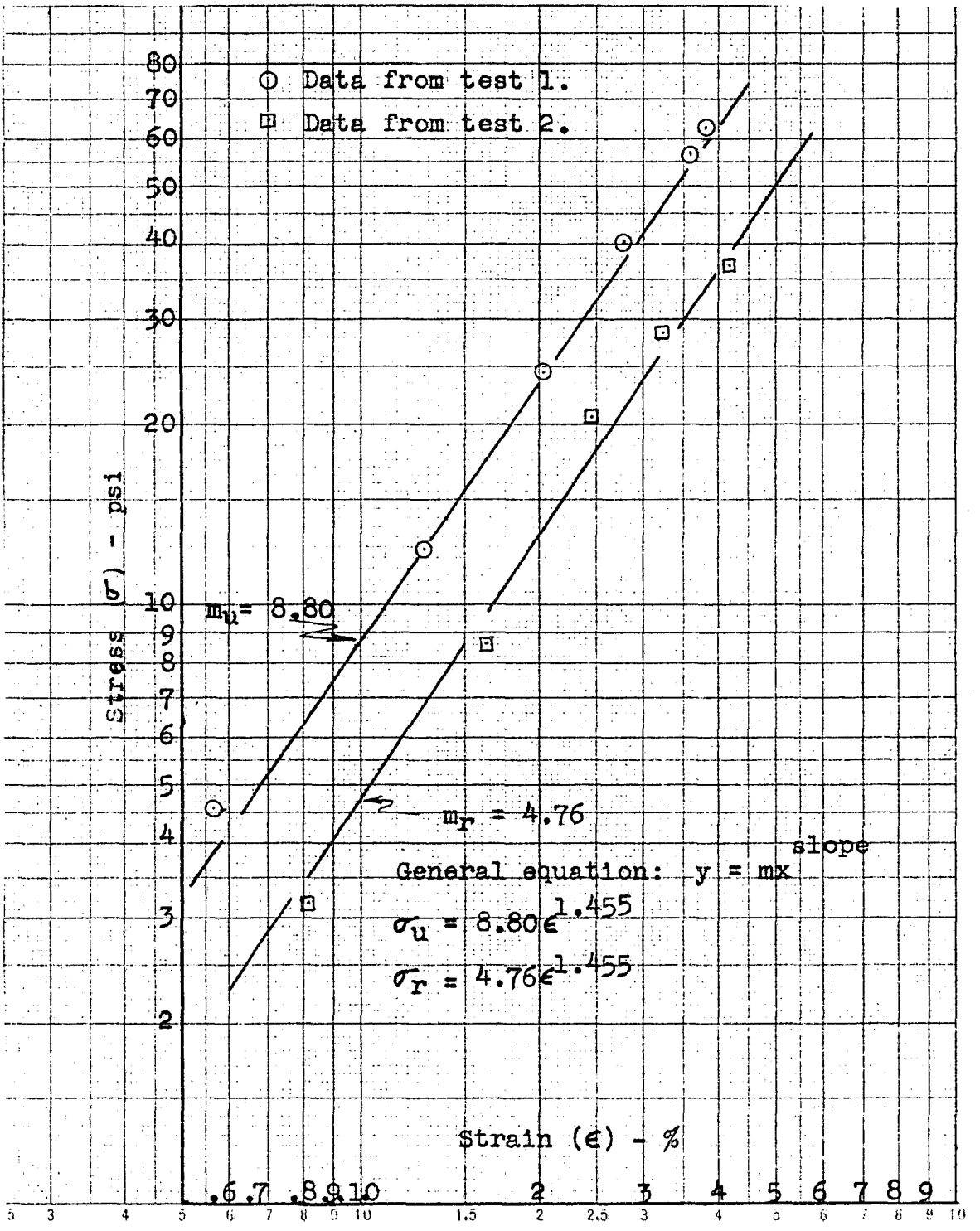

Figure 13. Log-log σ - ϵ curves, Specimen No. 2.

in which

$$R = \frac{f_u(\epsilon) - f_r(\epsilon)}{f_u(\epsilon)} \quad .$$

Values of $f_u(\epsilon)$ and $f_r(\epsilon)$ were taken from the logarithmic plot, Figure 13 as

$$f_u(\epsilon) = + (8.8)(1.455)\, \epsilon^{+ 0.455}$$

and

$$f_r(\epsilon) = + (4.76)(1.455)\, \epsilon^{+ 0.455}$$

which gives a value for R of

$$R = + 0.455 \ .$$

Using this value for R and the stress vs time data recorded following each incremental addition of strain (and stress) values of $\left[R\Delta\sigma_{t=0} - (\Delta\sigma_{t=0} - \Delta\sigma_{t=t}) \right]$ were plotted against t for the first five increments of strain ($\Delta\epsilon$). (The time at which the peak value of strain was obtained in the sixth increment of strain addition was not clearly defined and hence no reliable relaxation data could be obtained from this portion of the test.) The value of time used in this particular analysis was the elapsed time from the obtainment of the peak value of the increment of strain to the time of interest, i.e., the time required to apply a given $\Delta\epsilon$ was not included in the relaxation time (t). The curves thus

obtained are shown on Figure 14. On this semi-logarithmic plot the value of τ can be taken as proportional to the reciprical of the slope. From this plot it appears that the magnitude of τ remains nearly constant for values of strain between 1 and 4 percent. At a strain level of 0.57 percent the value of τ appears to be less than at higher strains, but as previously pointed out there is considerable experimental error involved when the strain level is less than 1 percent. Values for $f_u(\epsilon)$ and τ were not taken from the data obtained during these preliminary tests; their numerical evaluation is covered in the following section. Tabulated data from which Figures 12, 13, and 14 were constructed are presented in Appendix B.

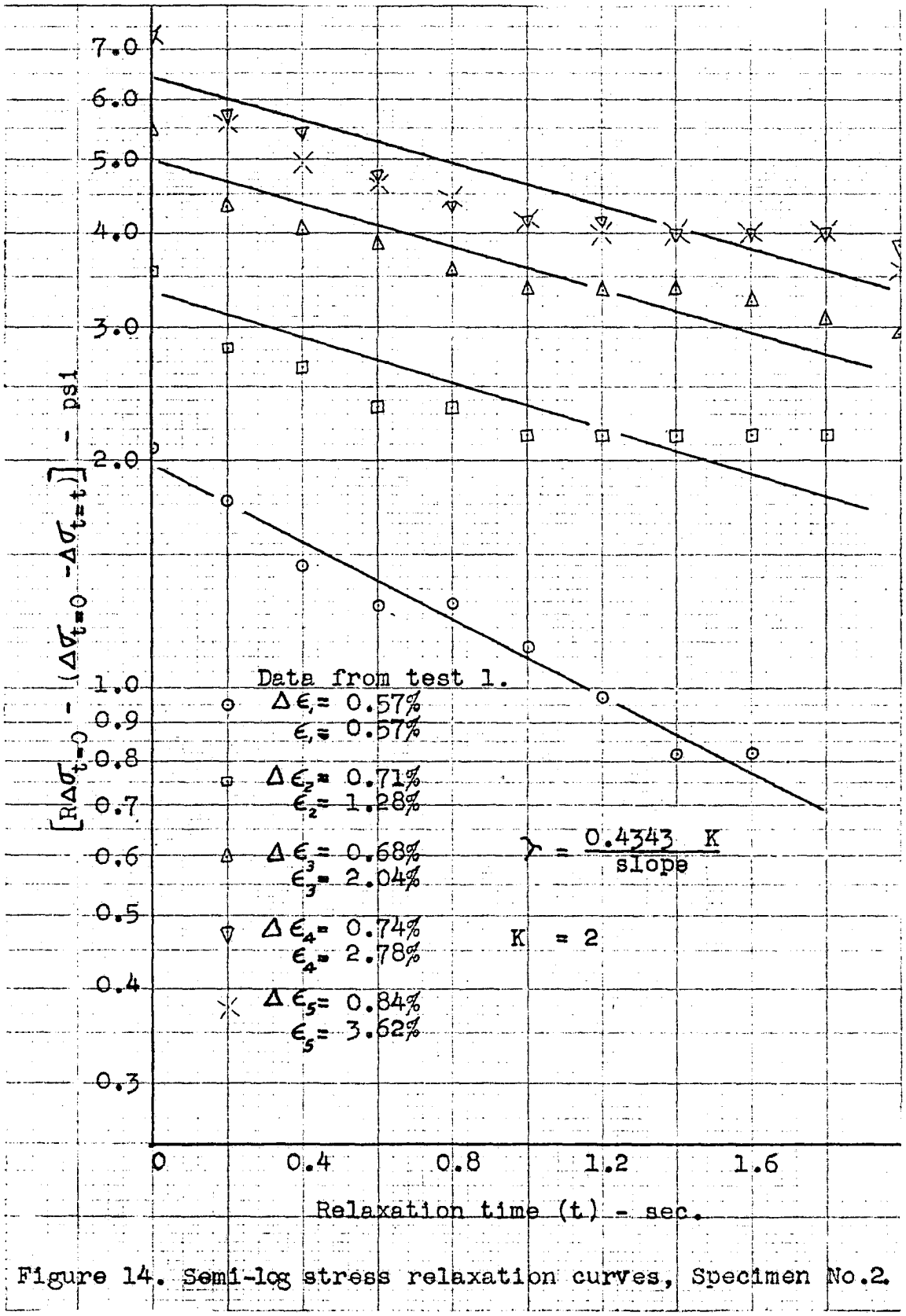

Figure 14. Semi-log stress relaxation curves, Specimen No.2.

RESULTS

Evaluation of Material Constants

Before the theoretical expressions previously developed can be applied the material constants $f_u(\epsilon)$, $f_r(\epsilon)$, and τ must be evaluated. Several methods for evaluating these constants are discussed below. As previously pointed out $f_u(\epsilon)$ can not be evaluated directly by a single constant rate of strain test which requires a finite loading time. However, if a test can be conducted for which the loading time is small compared to the value of τ the value of $f_u(\epsilon)$ thus determined should be adequate to predict the effect of straining at rates for which the loading time is comparable to, or greater than, τ . For this purpose a third test was performed on Specimen No. 2 in which the total strain was applied in five nearly equal increments and the stress was allowed to relax between each increment. The rate of application of each of these increments of strain was made as great as possible (the limitation of the test equipment and the recorder previously discussed were taken into account). The step curve showing the incremental increases in stress and strain, and the stress-strain curve constructed from this by the addition of the stress

increments are shown on Figure 15. The lower curve on Figure 15 is a reproduction of the lower curve on Figure 12 since it was constructed using the data from the same preliminary test. These two curves (unrelaxed and relaxed stress-strain diagrams) are replotted on logarithmic coordinates in Figure 16 and from this plot the values of $f_u(\epsilon)$ and $f_r(\epsilon)$ are taken as

$$f_u(\epsilon) = (10.8)(1.455)\epsilon^{0.455} = + 15.71\,\epsilon^{+0.455}$$

$$f_r(\epsilon) = (4.76)(1.455)\epsilon^{0.455} = + 6.94\,\epsilon^{+0.455}$$

The data on stress relaxation following each incremental increase in strain (and hence stress) were used to evaluate the relaxation constant τ in the following manner.

Equation (23) may be rewritten as

$$\left(\sigma_{\epsilon,T} - \frac{M\epsilon^{p+1}}{p+1}\right) e^{+\frac{T}{\tau}} = RN\epsilon^{p+1}\left[\epsilon, \text{Series}\right],$$

and

$$RN\epsilon^{p+1}\left[\epsilon, \text{Series}\right] = \text{constant}$$

for any given test.

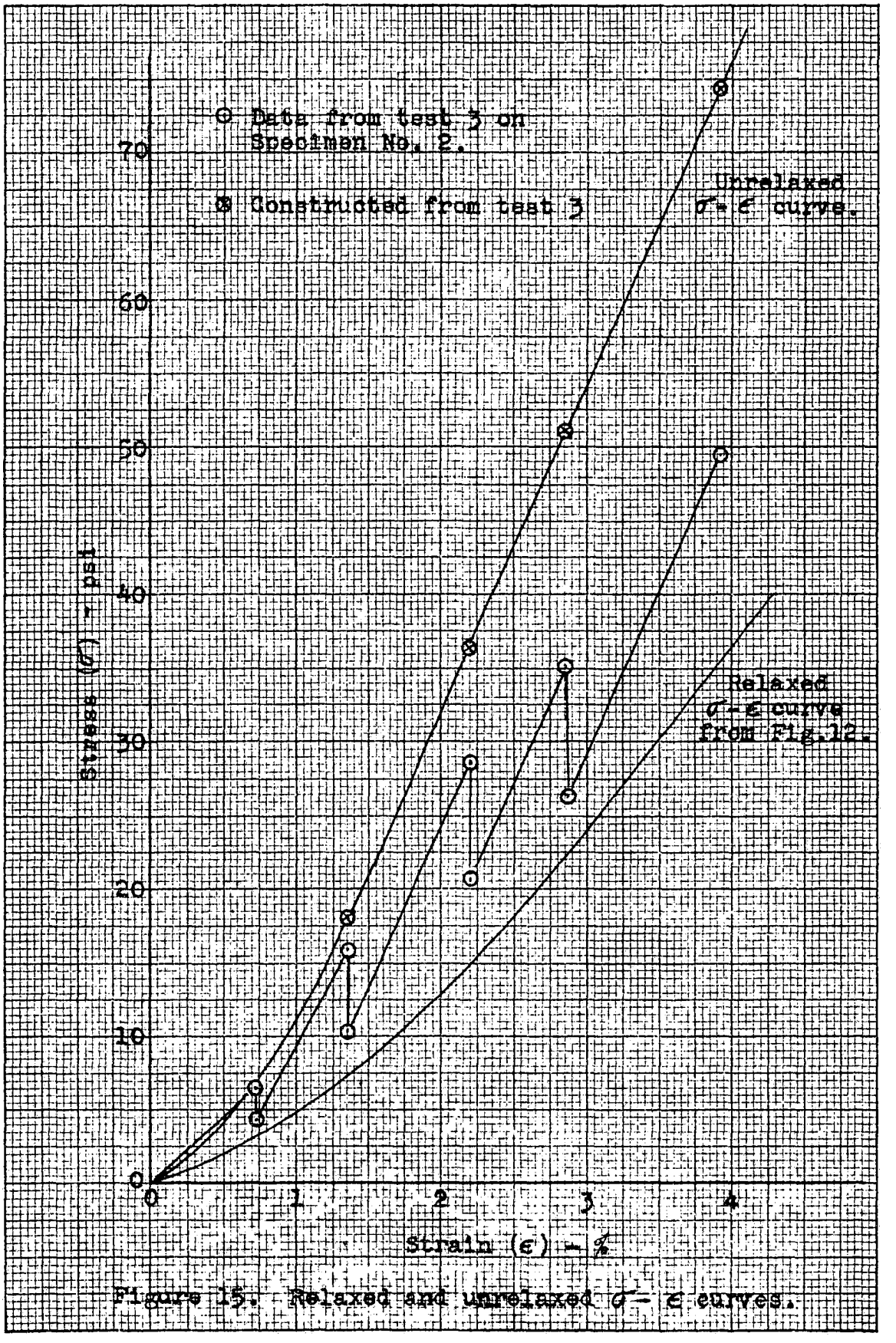

Figure 15. Relaxed and unrelaxed $\sigma - \varepsilon$ curves.

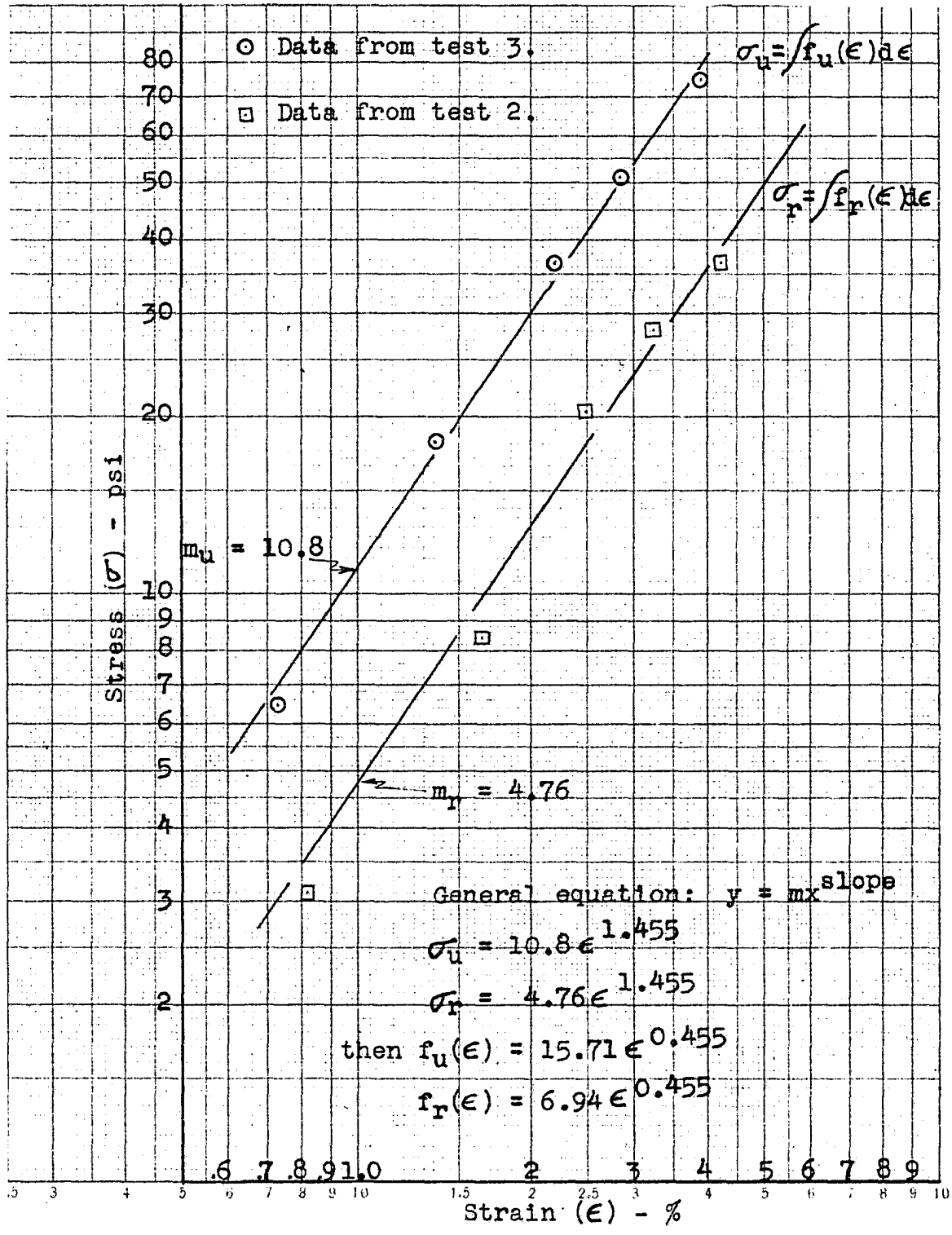

Figure 16. Log-log plot of relaxed and unrelaxed curves.

Therefore, the stresses at various values of T (the time lapse during which ϵ is held constant) are related by

$$(\sigma_{\epsilon,T_1} - \frac{M\epsilon^{p+1}}{p+1}) e^{\frac{1}{\tau}(T_1-T_2)} = (\sigma_{\epsilon,T_2} - \frac{M\epsilon^{p+1}}{p+1}) .$$

If then, T_1 is taken as zero and $(\sigma_{\epsilon,T_2} - \frac{M\epsilon^{p+1}}{p+1})$ is plotted vs T_2 on semi-logarithmic coordinates the value of τ may be taken as proportional to the reciprocal of the slope. Figure 17 is such a plot, the data being taken from the relaxation period following the second, third and fourth incremental strain increases during the third test on Specimen No. 2. From Figure 17 the value of τ is taken as

$$\tau = + 0.69 \text{ seconds.}$$

Reproductions of the records and tabulated data from which Figure 15, 16, and 17 were constructed are presented in Appendix C.

As previously mentioned the preliminary test in which the unrelaxed stress-strain curve was approached indicated that $f_u(\epsilon)$ is of the same form as $f_r(\epsilon)$ and also that R is equal to a constant. Using this information ($f_u(\epsilon) = N\epsilon^q$ and R = constant so that p = q) both $f_u(\epsilon)$ and τ could also be evaluated from one or more additional constant rate of strain tests with the aid of equation (23).

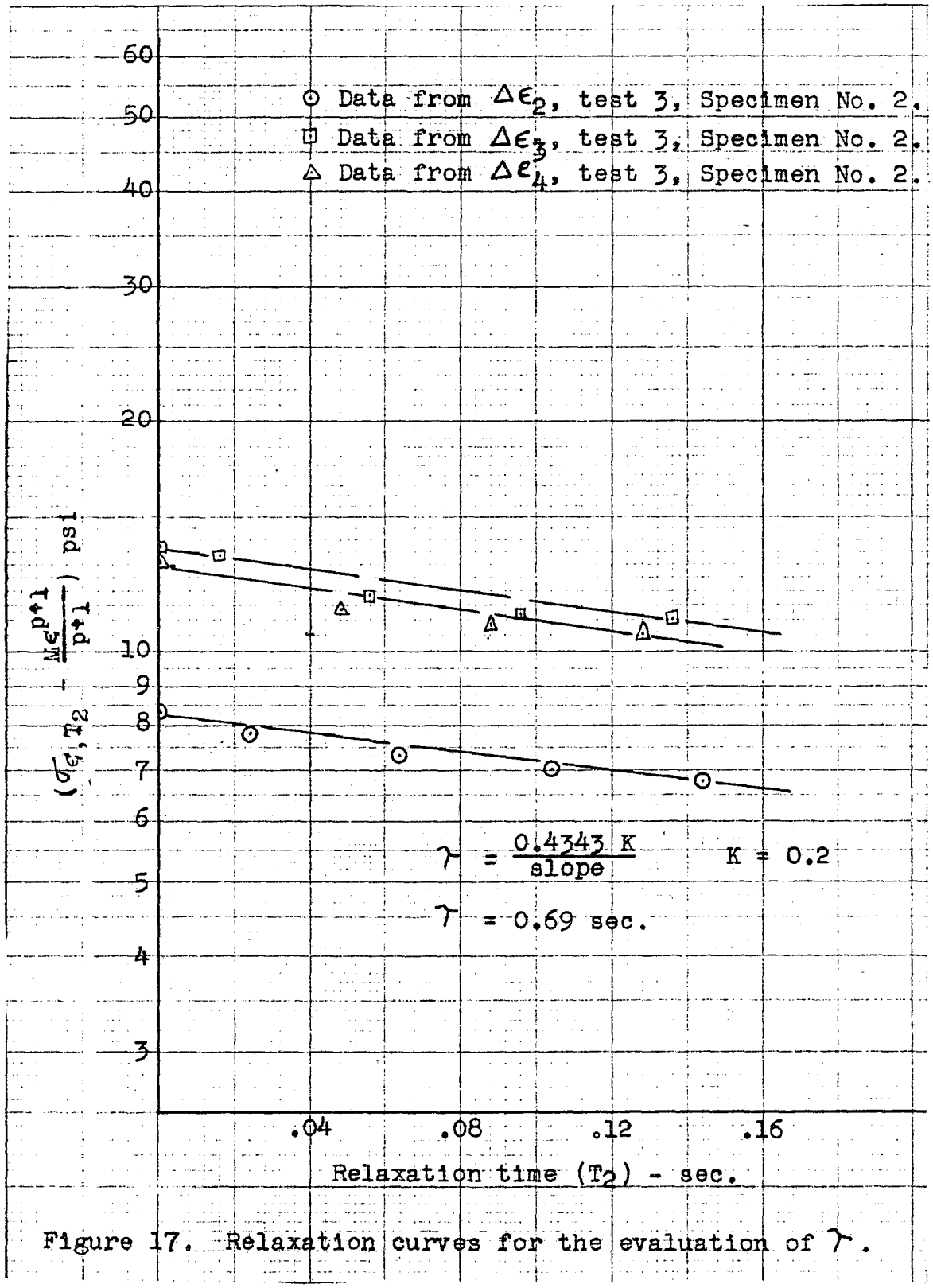

Figure 17. Relaxation curves for the evaluation of γ.

Rewriting equation (23) as before,

$$RN = \frac{\sigma_{\dot{\epsilon},T} - \frac{M\dot{\epsilon}^{p+1}}{p+1}}{e^{-\frac{T}{\tau}}\,\dot{\epsilon}^{p+1}\left[\dot{\epsilon}, \text{ Series}\right]} \quad .$$

The left hand side of this equation is equal to a single unknown constant RN.

From this it appears that τ (and then N) could be evaluated from a single additional constant rate of strain test by substitution of observed values of σ for given values of $\dot{\epsilon}$ with T equal to zero. This method is difficult to apply, however, because the solution for τ will depend upon measurements of such accuracy that the relaxation which occurs during the straining period can be observed. It also appears from this that τ (and then N) could be evaluated from two additional constant rate of strain tests by substituting observed values of σ with $b = b_1$, and again with $b = b_2$ for $\dot{\epsilon}$ = constant and T = 0. This method appears to be experimentally practical, but it involves a trial and error type of solution for each set of rates (b_1 and b_2) that it is desired to use.

Comparison of Theoretical and Experimental Results

The theory and the adequacy of the method of evaluating the material constants were tested by comparing the observed behavior to the predicted behavior of the material under various conditions of loading.

Constant rate of strain tests

To predict the shape of the $\sigma - \epsilon$ curve produced by various constant rates of strain, equation (23) is used with T set equal to zero. For predicting the shape of the $\sigma - t$ curve after a given value of strain has been obtained by straining at any constant rate equation (23) is again used but with $T \neq 0$.

Using the values for $f_u(\epsilon)$, $f_r(\epsilon)$, and γ given in the preceding section,

$$RN = \left(\frac{N - M}{N}\right) N = N - M = 15.71 - 6.94 = 8.77$$

so equation (23) may be written as

$$\sigma = 4.76\, \epsilon^{1.455} + 8.77\, \epsilon^{1.455}\, e^{-\frac{T}{0.69}} \qquad \left[\epsilon, \text{Series}\right] . \qquad (35)$$

This expression has been solved for various values of b, ϵ ,

and T using the tabular form presented in Appendix D. The stress-strain curves predicted for the various constant straining rates are shown as solid lines on Figure 18. The stress-time (relaxation) curves predicted for the constant strain period following the development of that strain at a given rate are shown as solid lines on Figure 19.

Test numbers 4, 5, and 6 were conducted on the relaxation test equipment to permit comparison between the predicted and observed stress-strain and relaxation curves. The measured values of $\sigma - \epsilon - t$ from test numbers 4, 5, and 6 are superimposed on Figures 18 and 19. The comparison between the predicted and observed $\sigma - \epsilon$ curves is complicated by the fact that test numbers 4, 5, and 6 were not true constant rate of strain tests. How much these tests depart from constant rate tests is indicated by the strain-time curves for these tests shown on Figure 20. In Figure 18 the theoretical curves have been plotted for strain rates equal to the average strain rates obtained in tests 4, 5, and 6. The pronounced reduction in maximum stress which is apparently associated with the gradual decrease in strain rate during the last portion of the loading cycle is of particular interest. The theoretical stress-time curves shown on Figure 19 have also been plotted for strain rates equal to the average strain rates obtained in tests 4, 5, and 6. The difference between the predicted and

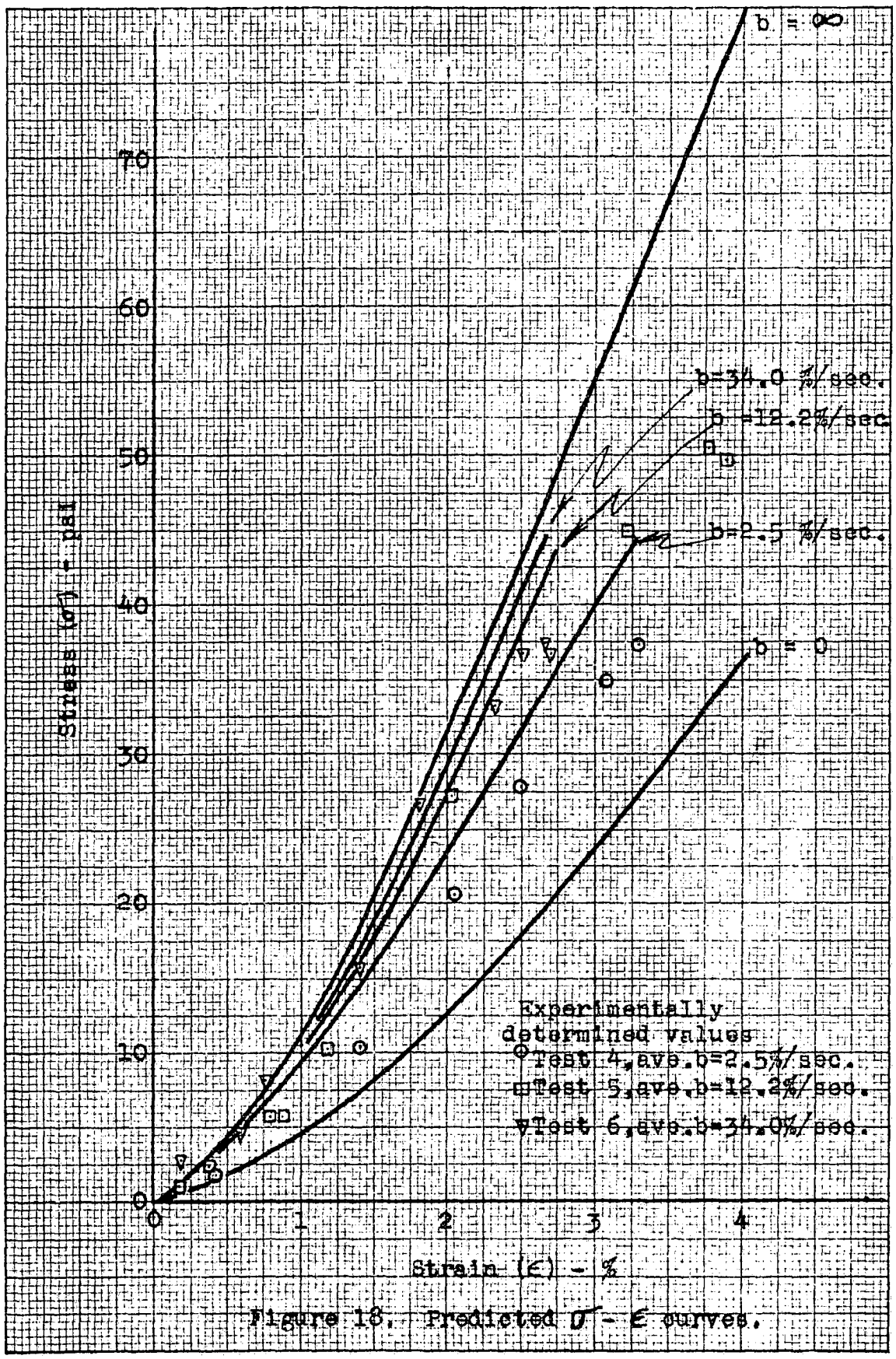

Figure 18. Predicted σ - ϵ curves.

Form E-5

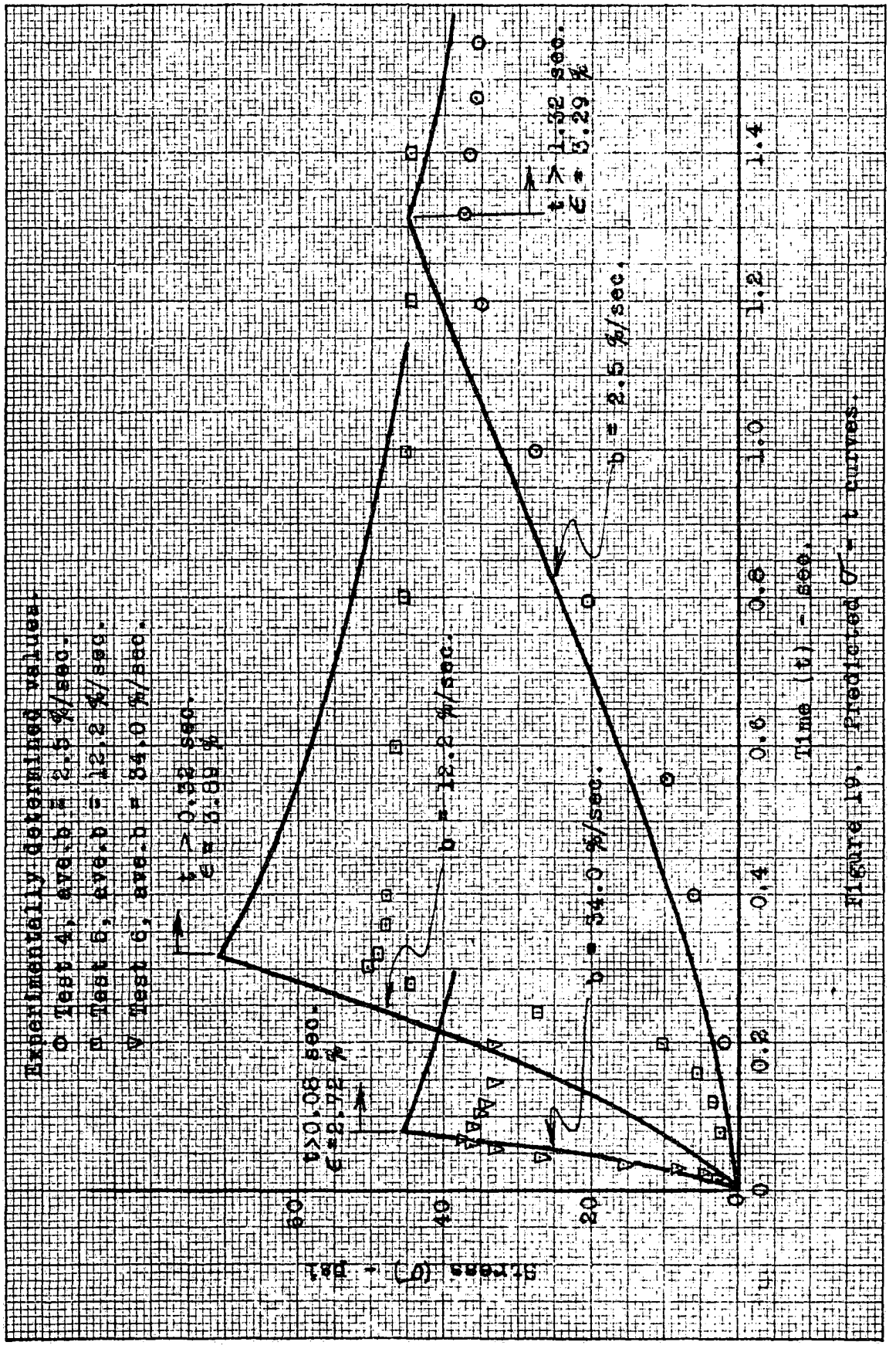
Experimentally determined values
o Test 4, ave.b = 2.5 %/sec.
□ Test 6, ave.b = 12.2 %/sec.
Δ Test 6, ave.b = 34.0 %/sec.
ε = 3.88 %
t = 0.52 sec.
b = 12.2 %/sec.
b = 34.0 %/sec.
b = 2.5 %/sec.
ε = 5.29 %
t = 1.22 sec.
Stress (σ) - psi
Time (t) - sec.
Figure 19. Predicted σ - ε curves.

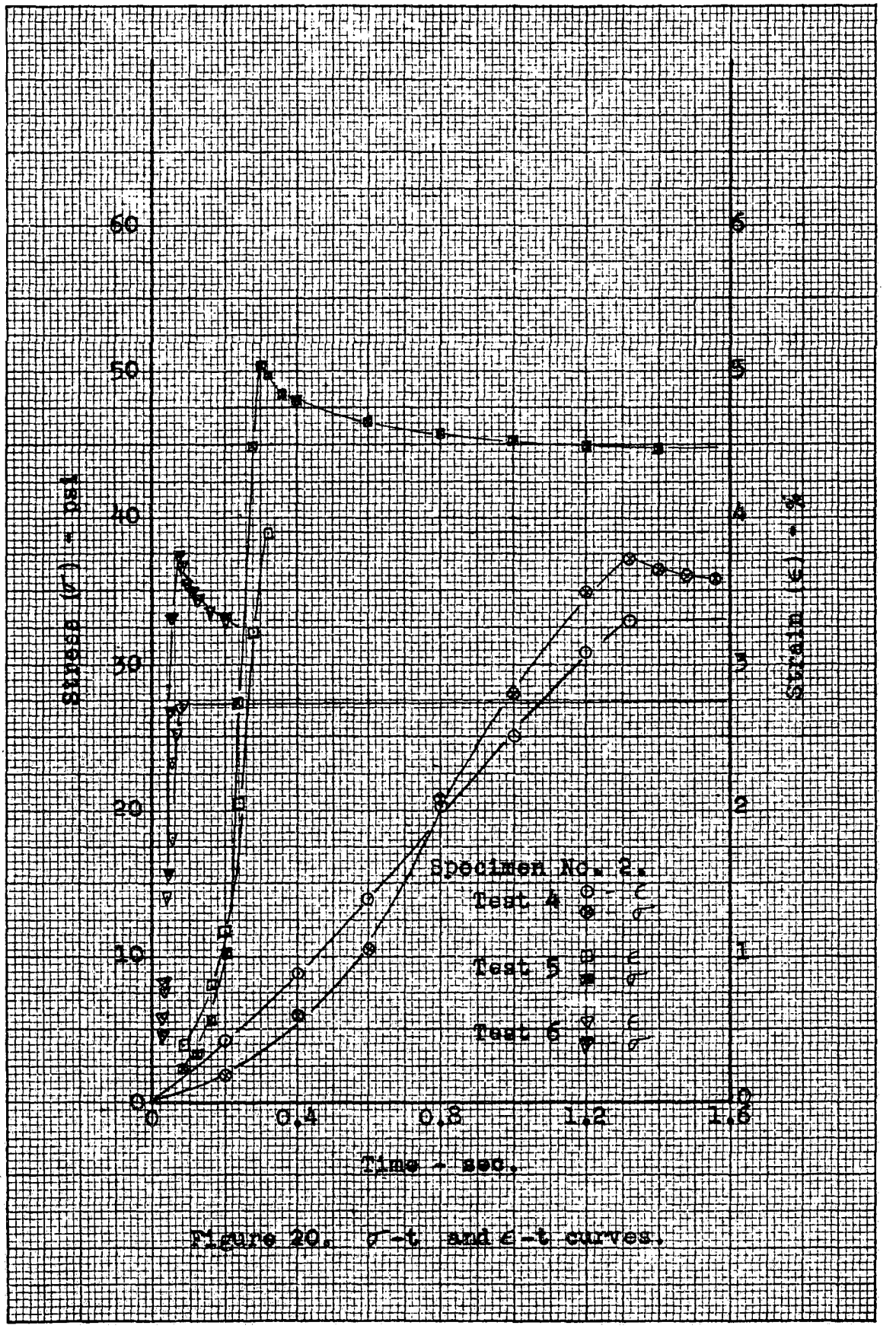

Figure 20. σ-t and ϵ-t curves.

observed maximum stress which has already been referred to is apparent in this figure also.

To predict the shape of the $\sigma - \epsilon$ curve produced by straining at a constant rate and then unstraining at the same rate equations (23) and (26a) are used: With 'T' set equal to zero equation (23) is used during the period of increasing strain and equation (26a) is used for the period during which strain is decreasing. Using the values for τ , $f_u(\epsilon)$, and $f_r(\epsilon)$ given previously, and with T = 0, equation (23) reduces to

$$\sigma = 4.76\,\epsilon^{1.455} + 8.77\,\epsilon^{1.455} \quad \left[\epsilon, \text{ Series}\right] . \qquad (35a)$$

Equation (26a) is written as

$$\sigma = \frac{M\,\epsilon^{p+1}}{p+1} + RN\,\epsilon^{p+1} \quad \left[\epsilon, \text{ Series}\right]$$

$$\times \left[e^{-\frac{2}{b\tau}(\epsilon_m - \dot{\epsilon})} - 2\,e^{-\frac{1}{b\tau}(\epsilon_m - \epsilon)} \right]$$

$$- \frac{2\,RN(\epsilon_m^{p+1} - \epsilon^{p+1})}{p+1} + 2\,RN\,\epsilon_m^{p+1} \quad \left[\epsilon_m, \text{ Series}\right]$$

in which

$$\frac{2\ RN}{p+1} = \frac{(2)(8.77)}{1.455} = 12.1$$

$$2\ RN = (2)(8.77) = 17.5$$

and $\left[\epsilon_m, \text{Series}\right]$ is the $\left[\epsilon, \text{Series}\right]$ evaluated for $\epsilon = \epsilon_m$. $\frac{M\epsilon^{p+1}}{p+1}$ and RN have the same values as when these terms were substituted in equation (23) above. Substituting these numerical values, equation (26a) reduces to

$$\sigma = 4.76\,\epsilon^{1.455} + 8.77\,\epsilon^{1.455}\left[\epsilon, \text{Series}\right]$$

$$x\left[e^{-\frac{2}{0.69b}(\epsilon_m - \epsilon)} - 2\,e^{-\frac{1}{0.69b}(\epsilon_m - \epsilon)}\right]$$

$$- 12.1\,(\epsilon_m^{1.455} - \epsilon^{1.455})$$

$$+ 17.5\,\epsilon_m^{1.455}\left[\epsilon_m, \text{Series}\right]. \qquad (36)$$

This expression has been solved for selected values of b, ϵ, and ϵ_m using the tabular form presented in Appendix D.

The stress-strain loop predicted for the chosen values of b and ϵ_m is shown on Figure 21. The points superimposed on the same figure are values which were determined experimentally in test 7. The stress-time and strain-time diagrams for this test are shown on Figure 22.

The predicted stress-strain loop in Figure 21 has been constructed for a constant rate of strain cycle; the value of the strain rate being equal to the average value obtained during the straining period in test 7. Figure 22 indicated that test 7 was not a true constant rate of strain cycle, and this fact again accounts for some of the difference between the predicted and experimentally determined stress-strain curves during the period of increasing strain. Figure 22 also indicates that in test 7 values of strain near the maximum value are held for a period of approximately 0.2 seconds rather than the strain being instantaniously reversed. This apparently affects the width of the stress-strain cycle at its upper end. The most striking difference between the predicted and the experimentally determined stress-strain loops occurs at the bottom of the loop. The assumption that relaxation acts continously to reduce the value of stress gives a value of residual strain (stress = 0) which is apparently too large. As was pointed out in the section titled "Theoretical Investigation" the relaxed stress-strain curve represents the lowest value of

Form E-5

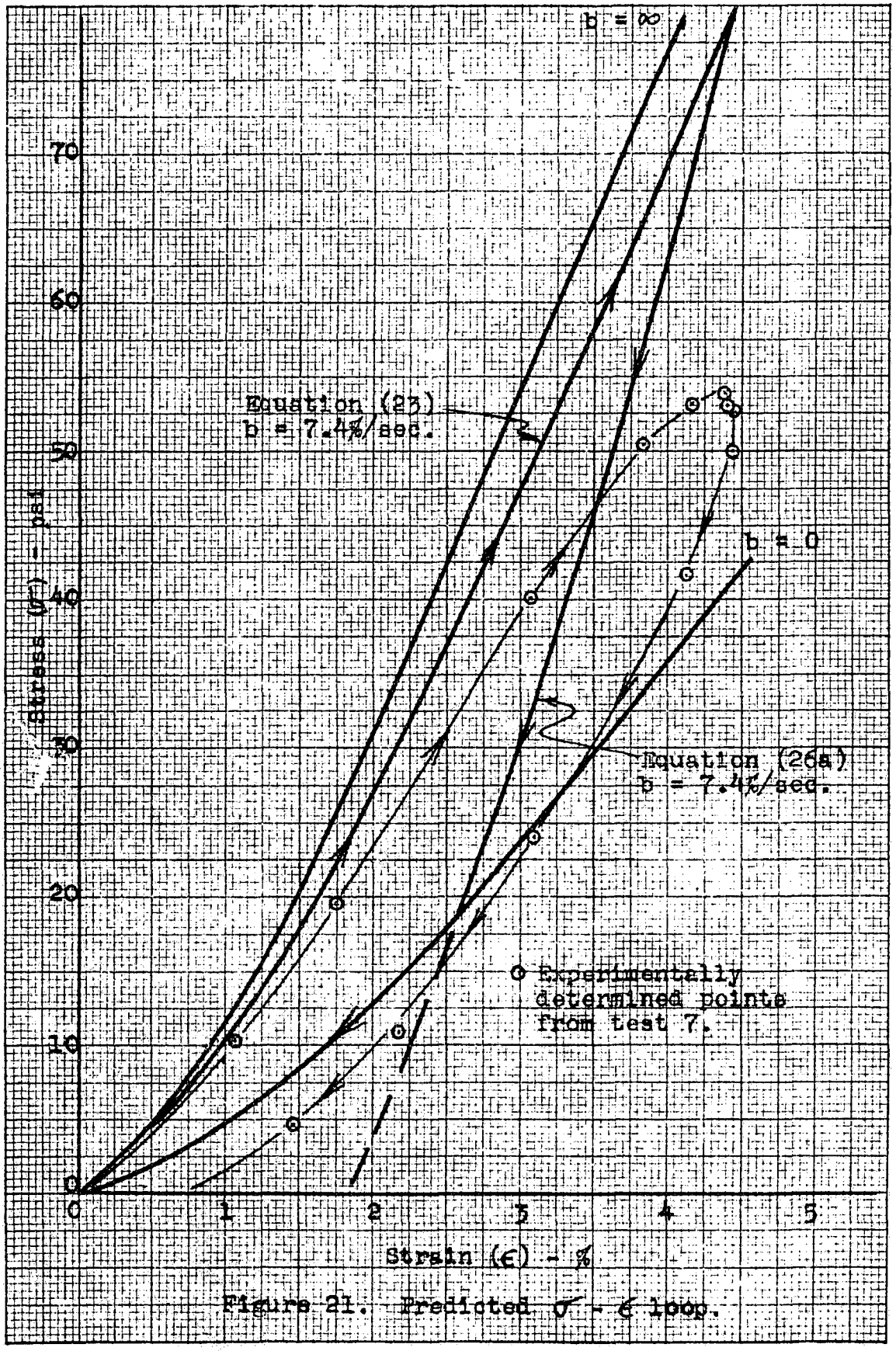

Figure 21. Predicted σ - ϵ loop.

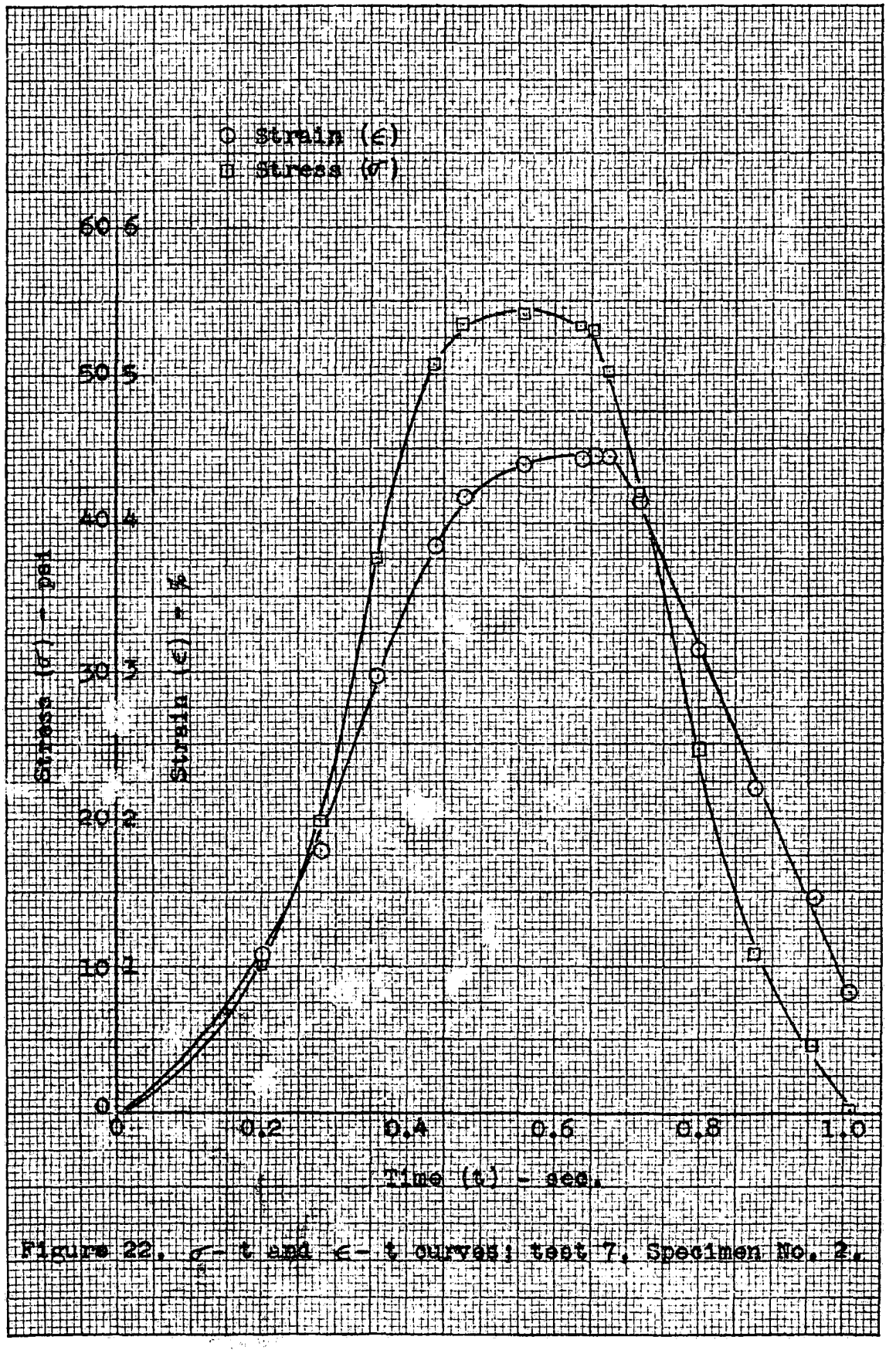

Figure 22. σ - t and ϵ - t curves; test 7, Specimen No. 2.

stress that can co-exist with a given value of strain, and hence a more logical assumption appears to be that relaxation acts to reduce the value of stress associated with a given value of strain only until the relaxed stress-strain curve is reached. When strain is further reduced at any finite rate, relaxation acts to increase the value of stress; this results in an unstraining curve which tends to follow the relaxed stress-strain curve after the relaxed stress-strain curve is crossed. With a low unstraining rate the unstraining curve will follow the relaxed stress-strain curve closely, and the residual strain will be small. With high unstraining rates the unstraining curves depart by greater amounts from the relaxed stress-strain curve and the residual strains will then be greater.

To further test the assumption that relaxation acts to make the true stress approach the relaxed stress-strain curve whether from above or below, test numbers 8 and 9 were conducted. In test 8 the strain was increased rapidly and then decreased in a series of steps. The stress-time and strain-time curves from test 8 are shown on Figure 23. In test 9 the strain was increased very slowly, then after a period of time long enough to allow nearly complete relaxation, the strain was again decreased in a series of steps. The stress-time and strain-time curves from test 9 are shown on Figure 24. The stress-strain curves for these two tests

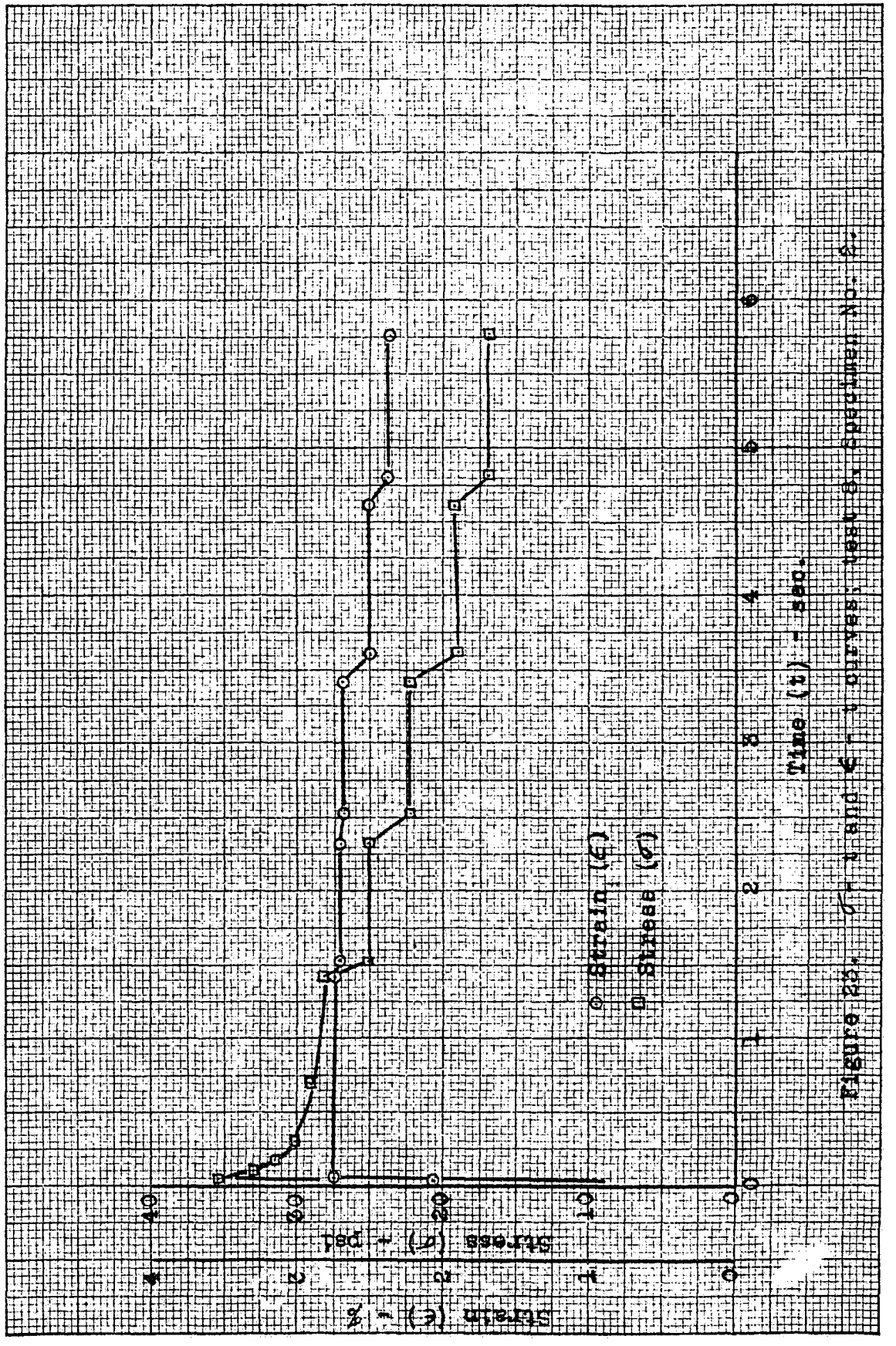

Figure 23. Stress-strain-time curves for test no. 2.

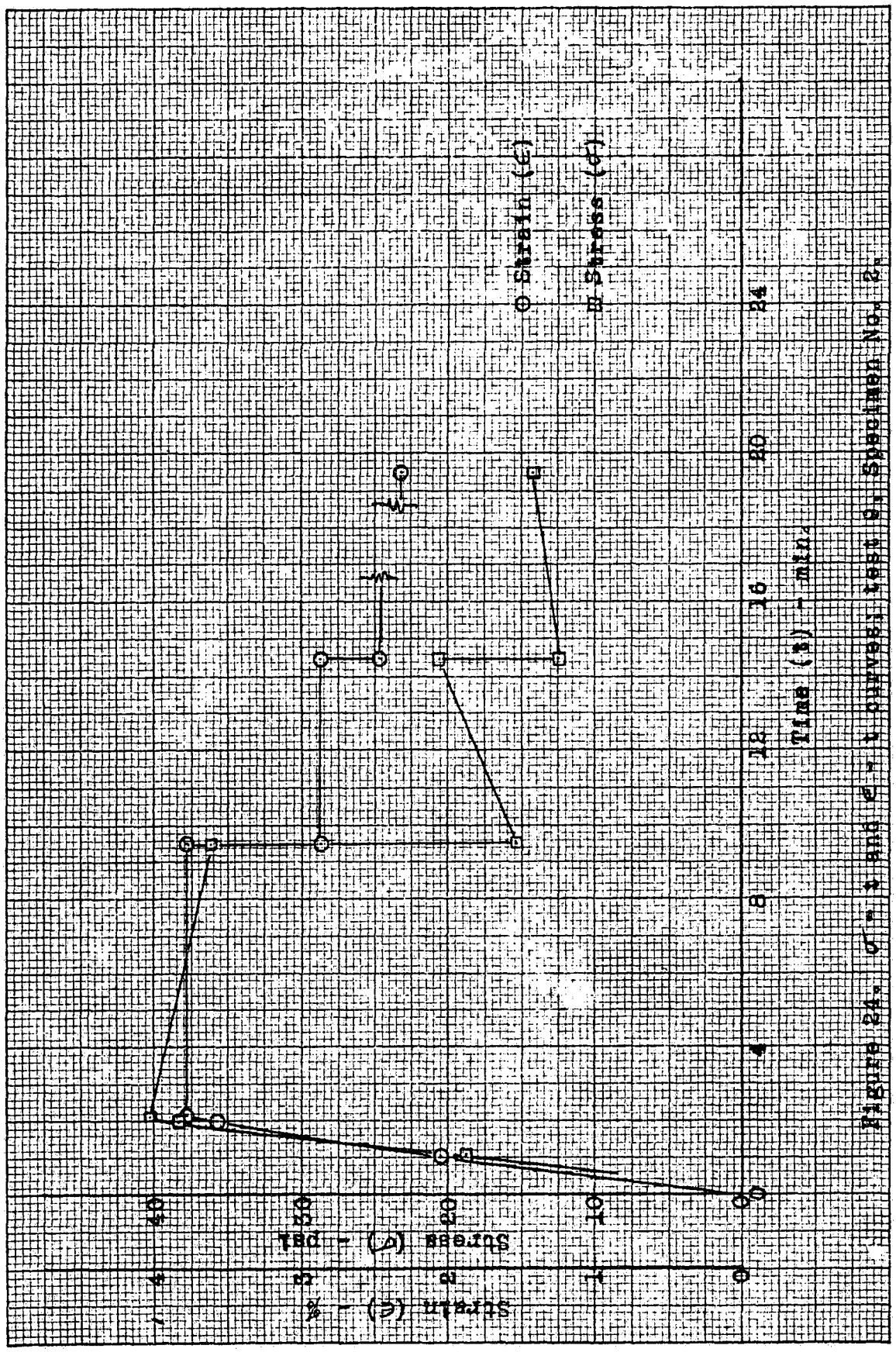

Figure 24. σ - ε and ε - t curves, test 9, Specimen No. 2.

are shown on Figure 25. These curves indicate that relaxation does cause the stress to approach the relaxed stress-strain curve whether this requires and increase or decrease in stress with time.

From the foregoing it appears that the use of equation (26a) for predicting values of stress during periods of decreasing strain must be limited to values of stress equal to or greater than the relaxed value of stress associated with a given strain. That is, equation (26a) may be applied provided that

$$RN\epsilon^{p+1}\left[\epsilon, \text{ Series}\right]\left[e^{-\frac{2}{b\gamma}(\epsilon_m-\epsilon)} - 2\,e^{-\frac{1}{b\gamma}(\epsilon_m-\epsilon)}\right] - \frac{2\,RN(\epsilon_m^{p+1}-\epsilon^{p+1})}{p+1} + 2RN\epsilon_m^{p+1}\left[\epsilon_m, \text{ Series}\right] \geq 0. \qquad (37)$$

What modification of equation (26a) is necessary to predict values of stress less than the relaxed value will depend upon the form of this "reversed" relaxation process. Until the nature of this reversed relaxation process is determined the stress-strain loop can best be predicted using equations (23), (26a) and the relaxed stress-strain curve. This approximation for the stress-strain cycle should approach the true cycle as the rate of straining is increased, since

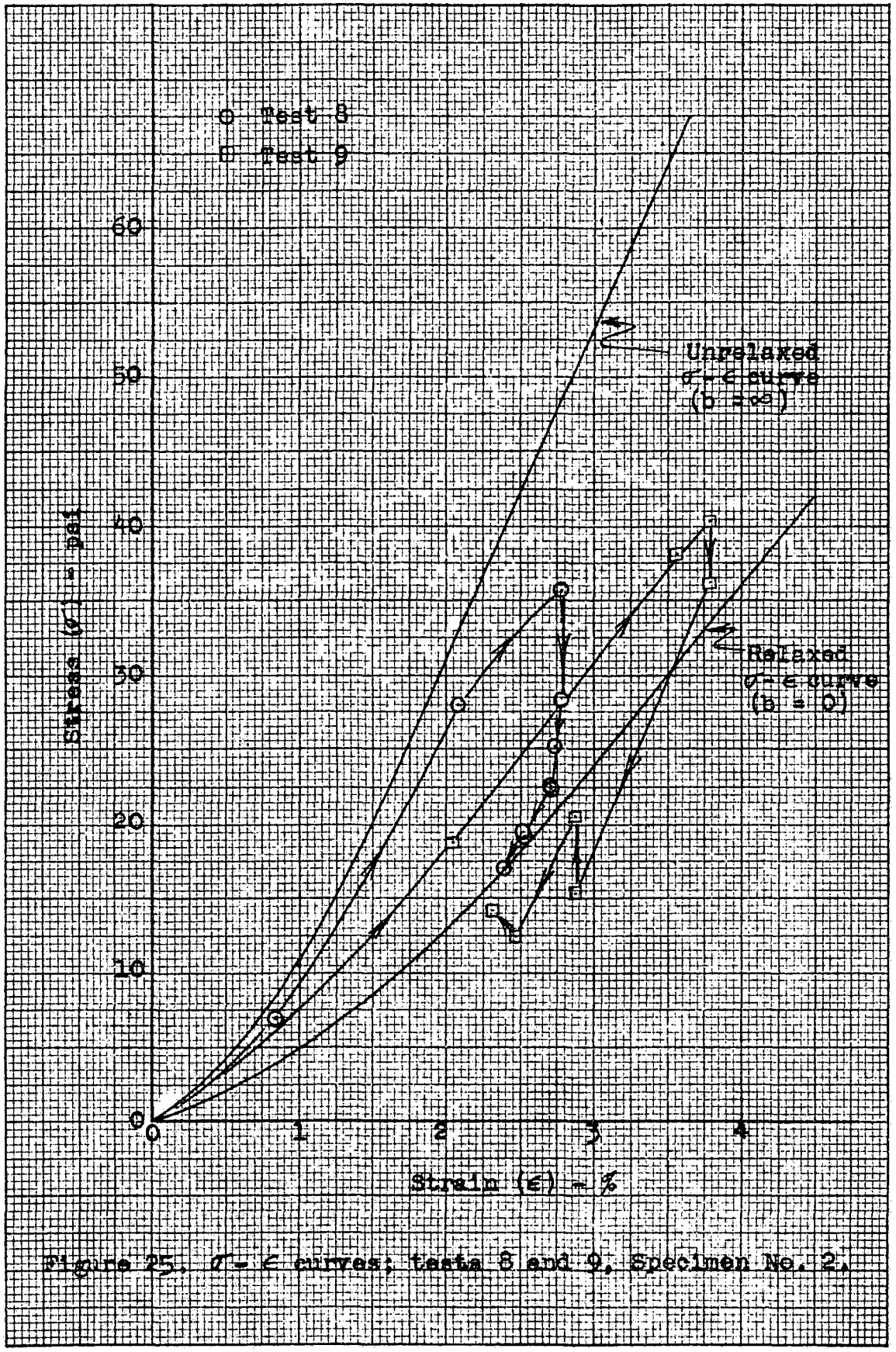

Figure 25. σ - ∈ curves; tests 8 and 9, Specimen No. 2.

with high rates of straining and unstraining the true value of stress will fall below the relaxed value of stress only when the strain has returned very nearly to zero.

Wave propagation tests

As yet, the theoretical expression for the velocity of propagation of a longitudinal strain wave in terms of $f_u(\epsilon)$, $f_r(\epsilon)$ and τ has not been developed. Therefore, the observed results of wave propagation tests can not be used to check the theory in the way in which the observed results of constant rate of strain and constant rate strain cycling tests were used. However, from the preceding discussion on strain cycling it appears that for a very high rate of straining and unstraining both stress-strain curves (one for increasing strain and one for decreasing strain) will follow the unrelaxed stress-strain curve very closely. For the material used in these tests the relaxation constant (τ) was found to be 0.69 seconds. Strain waves having a frequency of 100 cycles per second or more might therefore be considered to be practically unaffected by relaxation. In this case the velocity of propagation would be controlled by the unrelaxed elastic modulus.

Tests were made using the wave propagation test equipment in which sinusoidal strain waves of various frequencies were used. Reproductions of the photographs from which the

velocities of wave propagation were computed are included as Figures 26, 27, 28, and 29. Figure 26 is the reproduction of the oscilloscope photograph taken during the test in which the frequency of the strain waves was 100 cps. The lower trace in this figure shows the signal received from the gage point B (i.e., the gage point nearest the loudspeaker where the strain waves were originated). The upper trace shows the signal received from the gage point T. The circuit was arranged so that a signal that produces an upward deflection of one trace will produce a downward deflection of the other trace. Both traces begin at the left. In Figure 26 when the first strain pulse reaches gage point B the lower trace is deflected downward to the peak marked B_1, this pulse if followed by a strain of opposite sense and the trace is deflected upward to the peak marked B_2, etc. When the first strain pulse reaches gage point T the top trace is deflected upward to the peak marked T_1, etc. The speed with which the trace travels from left to right (i.e., the sweep rate) was determined for each test by using a wave of known frequency. The time required for a strain pulse to travel from the gage point B to the gage point T was obtained from the spacing between any two corresponding peaks (B_1 to T_1) on the upper and lower traces. The velocity of wave propagation was then computed by dividing the distance between the gage points

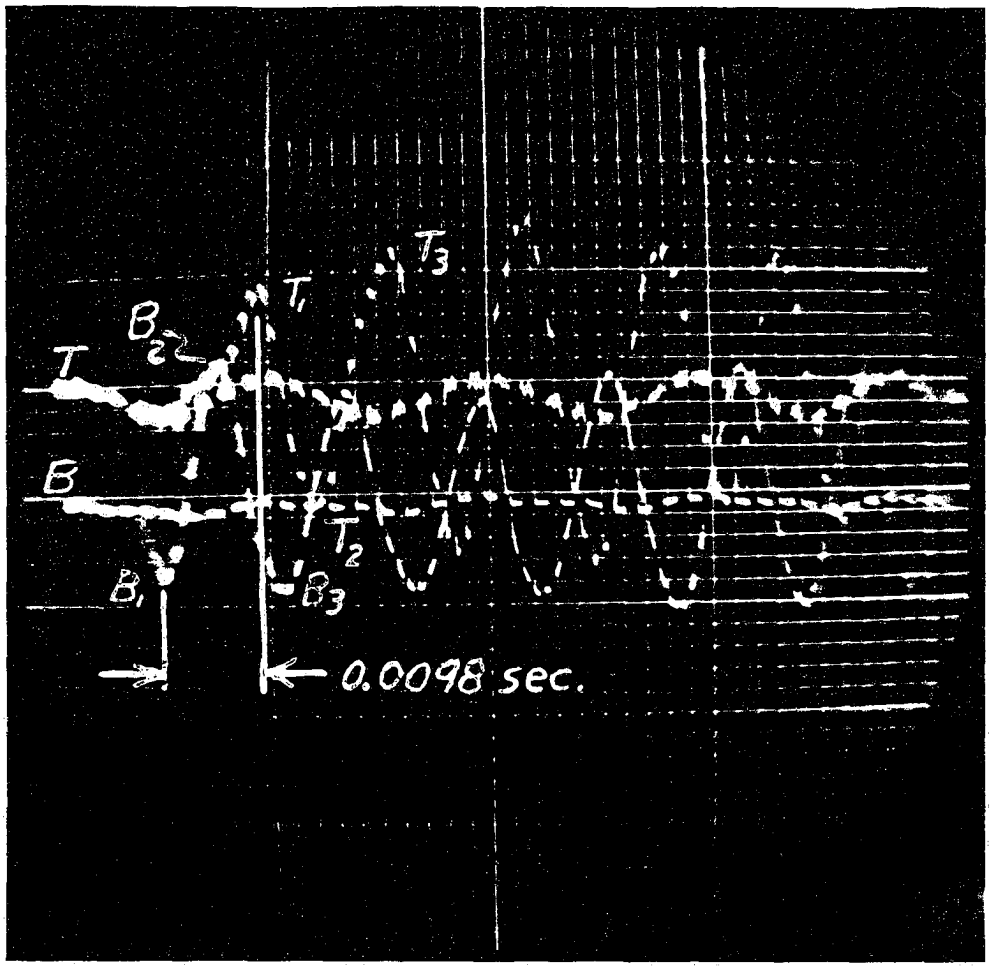

T - Strain wave as it passes gage point "T", Figure 9.

B - Strain wave as it passes gage point "B", Figure 9.

Base line of each trace is sinusoidal due to noise in circuit.

Figure 26. 100 cps strain waves.

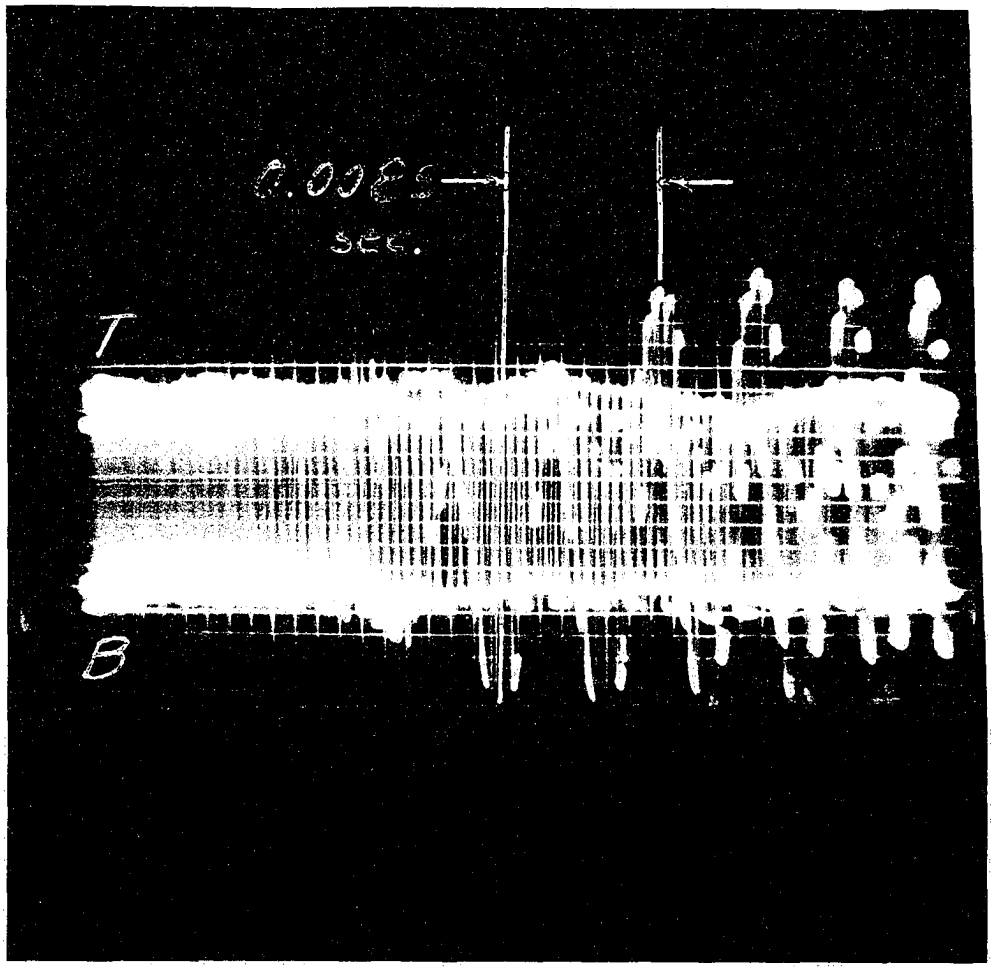

T - Strain wave as it passes gage point "T", Figure 9.

B - Strain wave as it passes gage point "B", Figure 9.

Base line of each trace is sinusoidal due to noise in circuit.

Figure 27. 200 cps strain waves.

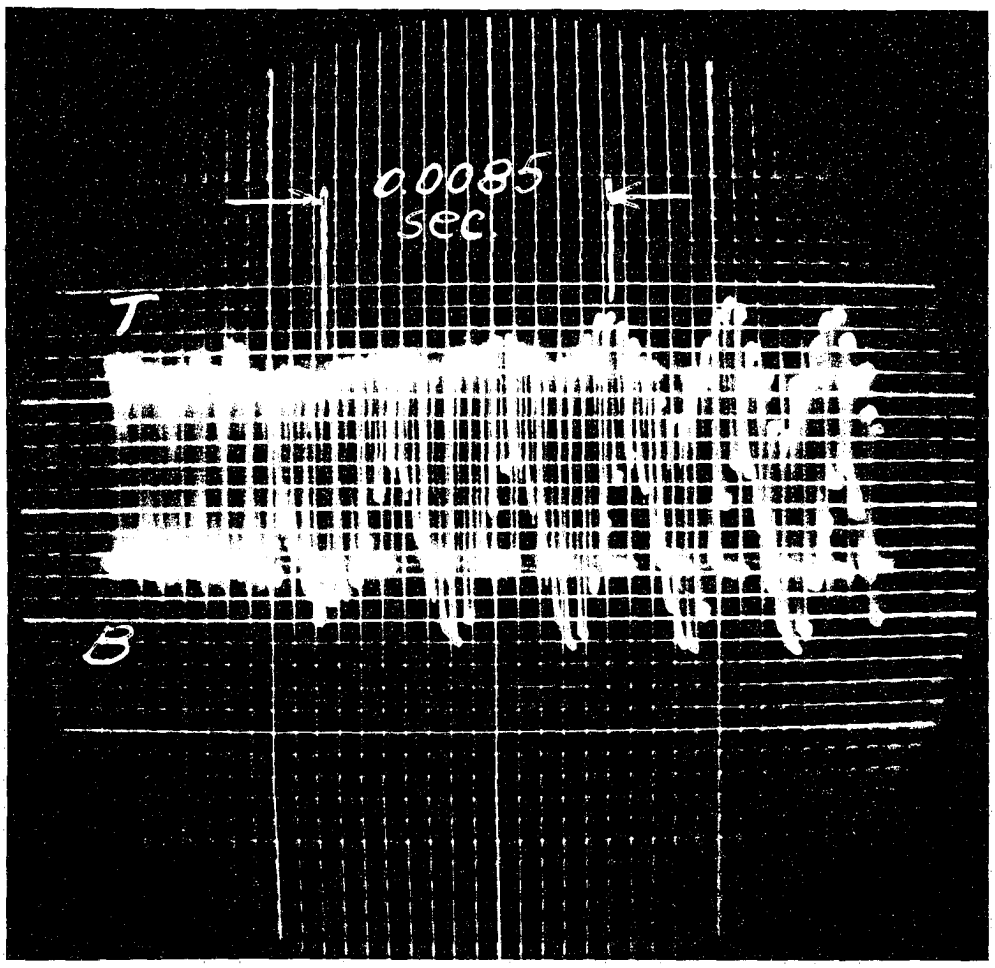

T - Strain wave as it passes gage point "T", Figure 9.

B - Strain wave as it passes gage point "B", Figure 9.

Base line of each trace is sinusoidal due to noise in circuit.

Figure 28. 300 cps strain waves.

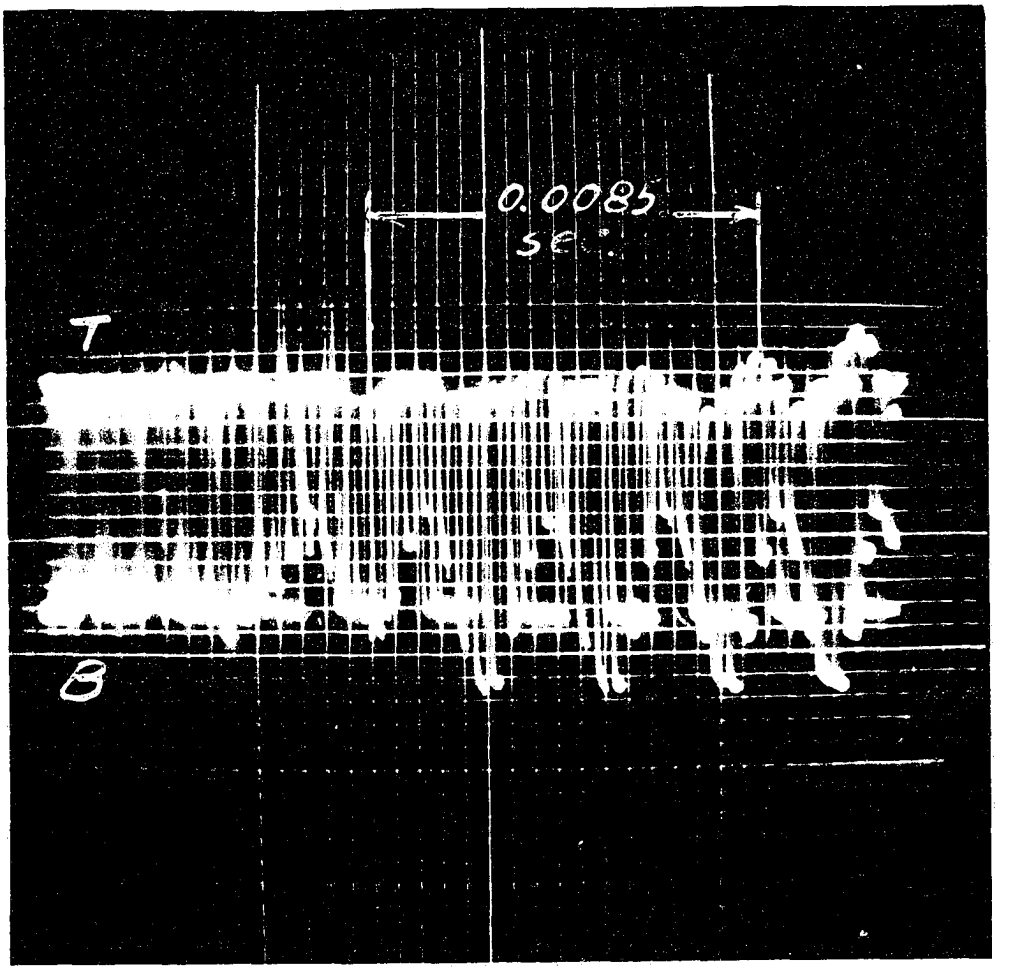

T - Strain wave as it passes gage point "T", Figure 9.

B - Strain wave as it passes gage point "B", Figure 9.

Base line of each trace is sinusoidal due to noise in circuit.

Figure 29. 400 cps strain waves.

(50 inches) by the time required by the strain pulse to travel from B to T. The photographs taken during the tests in which 200, 300 and 400 cps strain waves were used were analyzed in the manner just described for the test using 100 cps strain waves (Figure 26).

The values of c obtained from these tests are tabulated in Table 1. The values of E given in Table 1 were obtained by solving equation (1)[1] for E, using these measured values of c

$$c = \sqrt{\frac{E}{\rho}} \qquad (1)$$

or

$$E = \rho c^2 .$$

For the material used in these tests

$$\rho = \frac{72.9}{1728 \times 386} \qquad \frac{lb - sec^2}{in^4} .$$

[1] With the large wave lengths involved here the ratio of $\frac{d}{h}$ is so small that the Pochhammer-Chree correction is negligible.

Table 1. Results of wave propagation tests.

Frequency of Strain Waves (cps)	Velocity of Wave Propagation (in/sec)	Value of E from Equ.(1) (psi)	% Reduction in Wave Amplitude between B & T (% of Value at B)
100	5100	2840	10
200	5890	3790	27
300	5850	3740	28
400	5890	3790	50

The effect of the strain wave frequency on the velocity of propagation and effective modulus of elasticity is not clearly defined by this limited number of values. However, it appears that the velocity of propagation and the effective modulus of elasticity remain nearly constant for strain wave frequencies between 200 and 400 cps. The slope of the straight line portion of the experimentally determined unrelaxed $\sigma - \epsilon$ curve (Figure 15) corresponds to a value of E of 2400 psi. The slope of the straight line portion of the relaxed $\sigma - \epsilon$ curve (Figure 15) corresponds to a value of E of 1300 psi. No direct comparison is possible since the $\sigma - \epsilon$ curves on Figure 15 are compression curves whereas during the wave propagation tests the rod was in tension, due to some initial loading, and also due to its own weight. However, values of E even greater than the value associated with the experimentally

determined unrelaxed $\sigma - \epsilon$ curve would be expected at very high strain rates.

It is apparent that, at least for the material used in these tests, the usual static modulus of elasticity (given as 1800 psi by the manufacturer for this material) can not be determined by measuring the velocity of longitudinal wave propagation and then solving equation (1) for E. However, this method of establishing E is widely used for all types of materials, including rubber and rubber-like materials.

SUMMARY AND CONCLUSIONS

In this thesis a method for predicting the stress-strain diagram for a material subjected to a dynamic load has been developed. This method involves the concept of unrelaxed and relaxed stresses within the material as well as the concept of a material property which determines how the relaxation of stress progresses with time. Theoretical background for these concepts may be found in the theory of anelasticity. Equations for evaluating the stress (σ) associated with a given strain (ϵ) at a given time (t) have been developed for selected ϵ - t curves (Figures 1, 2, 3). The general differential equation used in obtaining the σ - ϵ - t relationships for these selected ϵ - t curves is discussed in detail (equation 20). This general differential equation may be used to develop the σ - ϵ - t relationship for any ϵ - t curve; numerical methods may have to be resorted to, however.

An experimental technique for evaluating the material properties ($f_u(\epsilon)$, $f_r(\epsilon)$, γ) involved in the σ - ϵ - t relationships was developed and applied using rubber as the test material. Using the material properties determined by this experimental technique the theoretical σ - ϵ - t relationships were used to predict the σ - ϵ curves

associated with various constant strain rates and with a constant rate strain cycle. These predicted σ - ϵ curves were compared to experimentally determined curves. The velocity of strain wave propagation was studied experimentally to establish what, if any, relationship exists between the unrelaxed elastic modulus (E_u) and the velocity of wave propagation.

The agreement between the theoretical σ - ϵ curves and the experimental curves (Figures 18 and 21) justifies the conclusion that, at least for the material used in these tests and within the range of strains and strain rates investigated, the proposed method is suitable for predicting in advance how the rate of straining will affect σ - ϵ characteristics. In the author's opinion the results obtained in applying the proposed method to rubber are adequate to justify additional study in which the possibility of applying the proposed method to other materials would be investigated. A method similar to the one proposed in this thesis has been applied to the study of metals in Russia (44).

RECOMMENDATIONS FOR FURTHER INVESTIGATIONS

The reversed relaxation process which was discussed briefly in the section titled RESULTS and which is apparent on Figure 25 appears to present an area worthy of further study.

Development of equations for the velocity of strain wave propagation in terms of $f_u(\epsilon)$, $f_r(\epsilon)$, and τ so that wave propagation tests can be used to establish the values of $f_r(\epsilon)$, $f_r(\epsilon)$, and τ offers another area to which the present work might be extended.

In the wave propagation test it was observed that the attenuation of the traveling strain waves was greatly affected by the frequency of the strain waves. The values given in Table 1 indicate that with a wave frequency of 100 cps the wave amplitude is decreased by ten percent while traveling from point B to point T (Figure 9), a distance of 50 inches, and that the amount of attenuation increased with increasing wave frequency. With a wave frequency of 500 cps the attenuation of the strain pulse was so great that the signal at the second gage point (T) was difficult to read and with a wave frequency of 750 cps the strain pulse appeared to be completely absorbed before reaching the second gage point. The severe attenuation

can not easily be explained in terms of the relaxation coefficient previously established for this material (0.69 seconds), since at all of these frequencies the relaxation associated with this relaxation coefficient would be expected to be almost negligible. This raises the question of just how the effects of a series of completely reversed strain pulses may differ from the effects produced by a single straining-unstraining cycle.

LITERATURE CITED

(1) Thomson, W. T. Mechanical vibrations. p. 179-183. New York, Prentice-Hall, Inc. 1948.

(2) Den Hartog, J. P. Mechanical vibrations. 2d. ed. p. 164-172. New York, McGraw-Hill Book Co. Inc. 1940.

(3) Timoshenko, S. Vibration problems in engineering. 2d. ed. p. 307 & 397. New York, D. Van Nostrand Co. Inc. 1937.

(4) Timoshenko, S. and Young, D. H. Advanced dynamics. p. 110-111. New York, McGraw-Hill Book Co. Inc. 1948.

(5) Lord Rayleigh (Strutt, J. W.) The theory of sound. 2d. ed. vol. 1 & 2. vol. 1, p. 242-254. & vol. 2, p. 415-431. New York, Dover Publications. 1945.

(6) Timoshenko, S. and Goodier, J. N. Theory of elasticity. 2d. ed. p. 438-459. New York, McGraw-Hill Book Co. Inc. 1951.

(7) Love, A. E. H. A treatise on the mathematical theory of elasticity. 4 ed. p. 378, 293, & 427. New York, Dover Publications. 1944.

(8) Pochhammer, L. Schwingungen eines isotropen kreiscylinders. J. Reine und Angewandte Mathematik (Crelles J.) 81, 324-336, 1876.

(9) Chree, C. Two or more distinct elastic solid media in contact separated by parallel planes. Quart. J. of Pure and Appl. Math. 21, 107-129, 1886.

(10) Bancroft, D. The velocity of longitudinal waves in cylindrical bars. Phys. Rev. 59, 588-593, 1941.

(11) Davies, R. M. A critical study of the Hopkinson pressure bar. Roy. Soc. of London, Philosophical Trans. Series A, 240, 375-457, 1948.

(12) Donnell, L. H. Longitudinal wave transmission and impact. A.S.M.E. Trans. 52, APM 153-167, 1930.

(13) De Juhasz, K. J. Graphical analysis of impact of bars stressed above the elastic range. Franklin Inst. J. 248, 15-48, 1949 (Part I). 248, 113-42, 1949 (Part II).

(14) Cole, B. N. Impact stresses in systems of bars. Engineer 189, 264-6, 1950 (Part I). 189, 288-290, 1950 (Part II).

(15) von Kármán, T. and Duwez, P. The propagation of plastic deformation in solids. J. Appl. Phys. 21, 987-94, 1950.

(16) Taylor, G. I. The testing of materials at high rates of loading. Inst. of Civ. Engr. London J. 26, 486-519, 1946.

(17) White, M. P. On the impact behavior of a material with a yield point. A.S.M.E. Trans. (J. of Appl. Mech.) 16, 39-52, 1949.

(18) White, M. P. and Griffis, L. Permanent strain in uniform bar due to longitudinal impact. A.S.M.E. Trans. (J. of Appl. Mech.) 14, A337-43, 1947.

(19) Wood, D. S. On longitudinal plane waves of elastic-plastic strain in solids. A.S.M.E. Trans. (J. of Appl. Mech.) 19, 521-35, 1952.

(20) Weibull, W. Waves in compressible media. Trans. of the Roy. Inst. of Tech. Stockholm, Sweden, 18, 1-37, 1948.

(21) Sternglass, E. J. and Stuart, D. A. An experimental study of the propagation of transient longitudinal deformations in elastoplastic media. J. of Appl. Mech. 20, 427-434, 1953.

(22) Malvern, L. E. The propagation of longitudinal waves of plastic deformation in a bar of material exhibiting a strain-rate effect. A.S.M.E. Trans. (J. of Appl. Mech.) 18, 203-8, 1951.

(23) Kolsky, H. Stress waves in solids. p. 116-122. London, England, Oxford Uni. Press. 1953.

(24) Hillier, K. W. A method of measuring some dynamic elastic constants and its application to the study of high polymers. Proc. of Phys. Soc. 62, 701-712, 1949.

(25) Glauz, R. D. Transient wave analysis in linear time dependent material. Unpublished Technical Report No. 2. Picatinny Arsenal, Naval Ordinance Dept. 1952.

(26) Morrison, J. A. Wave propagation in a rod of Voigt material. Unpublished Technical Report No. 5. Picatinny Arsenal, Naval Ordinance Dept. 1953.

(27) _____ Wave propagation in rods of visco-elastic materials with three parameter models. Unpublished Technical Report No. 6. Picatinny Arsenal, Naval Ordinance Dept. 1953.

(28) Lethersich, W. and Pelzer, H. The measurement of the coefficient of internal friction of solid rods by a resonance method. Brit. J. Appl. Phys. 1, 18-22, 1950.

(29) Nolle, A. W. Acoustical determination of the physical constants of rubber-like materials. Acoustical Soc. Am. J. 19, 194-201, 1947.

(30) Kolsky, H. An investigation of the mechanical properties of materials at very high rates of loading. Phys. Soc. Proc. 62, 676-700, 1949.

(31) Clark, D. S. and Duwez, P. E. The influence of strain rate on some tensile properties of steel. A.S.T.M. Proc. 50, 560-76, 1950.

(32) Johnson, J. E., Wood, D. S. and Clark, D. S. Dynamic stress-strain relations for annealed 2 S aluminum under compression impact. J. of Appl. Mech. 20, 523-29, 1953.

(33) Hsiao, C. C. and Sauer, J. A. Effect of strain rate on the tensile and compressive stress-strain properties of polystyrene. A.S.T.M. Bul. 172, 29-35, 1951.

(34) Fine, M. E. Dynamic methods for determining the elastic constants and their temperature variation in metals. A.S.T.M. Symposium on determination of elastic constants. Special Technical Publ. No. 129, 1952.

(35) Campbell, W. R. Determination of dynamic stress-strain curves from strain waves in long bars. Soc. for Exp. Stress Analysis. Exp. Stress Analysis. 10, 113-124, 1952.

(36) Fredrickson, J. W. and Eyring, H. Statistical rate theory of metals -I Am. Inst. of Mining and Metal. Engrs. Metals Tech. 15, Pt. 2, Technical Publ. No. 2423, 1948.

(37) Hogan, M. B. The engineering application of the absolute rate theory to plastics. I, II, and III. Uni. of Utah, Engr. Exp. Station Bul. 56, 58, 59, 1951, 1952, 1952.

(38) Zener, C. Dynamics of slip bands. In A.S. for Metals. Cold Working of Metals. p. 180-196. Cleveland, Ohio. the Society. 1949.

(39) Brush Development Company. Universal analyzer -model BL-320, operating instructions. 3405 Perkins Ave., Cleveland 14, Ohio. Brush Development Co. 1950.

(40) Timoshenko, S. and Goodier, J. N. Theory of elasticity. 2d. ed. p. 442. New York, McGraw-Hill Book Co. Inc. 1951.

(41) Dohrenwend, C. O. and Mehaffey, W. R. Electrical-resistance gages and circuit theory. In Hetenyi, M., ed. Handbook of Experimental Stress Analysis. p. 180-182. New York, John Wiley and Sons, Inc. 1950.

(42) Dobie, W. B. and Isaac, P. C. G. Electric resistance strain gauges. p. 78-79. London, the English Uni. Press Limited. 1948.

(43) Baldwin Locomotive Works. Bulletin 279-A. Philadelphia 42, Pa. Baldwin Locomotive Works. 1949.

(44) Oding. I. A., Sorokin, O. V., and Sazanova, N. D. Relation between creep and relaxation of stresses in metals (in Russian). Doklady Akademii Nauk SSSR, 92, 565-68, 1953. English translation in National Science Foundation Trans. No. 152, 1953. Office of Tech. Ser., Dept. Commerce, Wash. 25, D. C.

ACKNOWLEDGMENTS

The author is especially grateful for the advice and encouragement given by Dr. Glenn Murphy, Professor of Theoretical and Applied Mechanics. He also takes this opportunity to express his gratitude to Mrs. Lois L. Dove, who typed the manuscript.

The author is also indebted to Mr. C. W. Gamerdinger and Mr. J. W. Liska, both of whom are associated with The Firestone Tire and Rubber Company, for their aid in procuring the test specimen.

Acknowledgment is made to the National Science Foundation, who made it possible for the author to continue his graduate study.

APPENDICES

Appendix A: Records and Data from Evaluation and Calibration Tests

Creep which might occur in the relaxation test equipment pull bar and/or strain gage bond would produce an apparent value of stress relaxation greater than the true value. Evaluation tests were conducted to determine how this creep might affect the results of tests made using this equipment. In these evaluation tests the usual rubber specimen was replaced by a specimen made of steel. Under this condition any apparent stress relaxation may be attributed to creep in the pull bar or in the strain gage bond. Figure 30a shows a reproduction of an oscillograph record taken during one of these tests. The return of the applied load curve to its original zero upon removal of the load indicates that creep of the strain gage bond is effectively zero. The gradual decrease in the applied load signal indicates that the pull bar does creep to some extent under the action of this applied load.

Evaluation tests were also conducted to determine the magnitude of the accelerating forces which are included in the total resistive forces measured by the gages on the relaxation test equipment pull bar. With no test specimen

in place the loading nut was turned to produce a magnitude of acceleration at least as great as those that would be produced in later tests. Under this condition any force measured by the gages on the pull bar may be considered to be accelerating forces. Figure 30b shows a reproduction of an oscillograph record taken during one of these tests. This record shows that the accelerating forces are so small as to be immeasurable with this recording equipment.

The effect of inertia on the pen of the recording oscillograph was evaluated by making additional tests in which the usual rubber specimen was replaced by the steel specimen. In these tests the rate of straining was progressively increased until pen overshoot produced a measurable effect. Figure 31a is a reproduction of an oscillograph record taken during one of these tests. This record shows that for a straining time of 0.11 sec. there is no measurable pen overshoot. Figure 31b is a reproduction of a record which shows considerable pen overshoot when the straining time is approximately 0.01 sec.

The applied force measuring circuit of the relaxation test equipment was calibrated by making an oscillograph record of the pen displacements produced by various dead weights. Before making this calibration test and prior to each subsequent test the recording system amplification was adjusted to produce 15 mm of pen displacement, at an

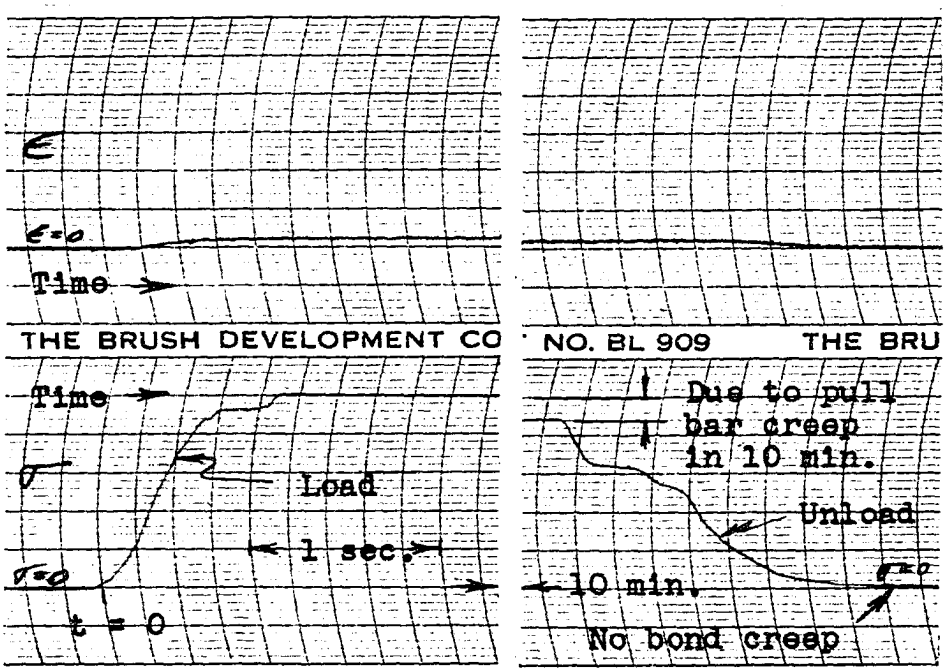

30a. Effect of creep

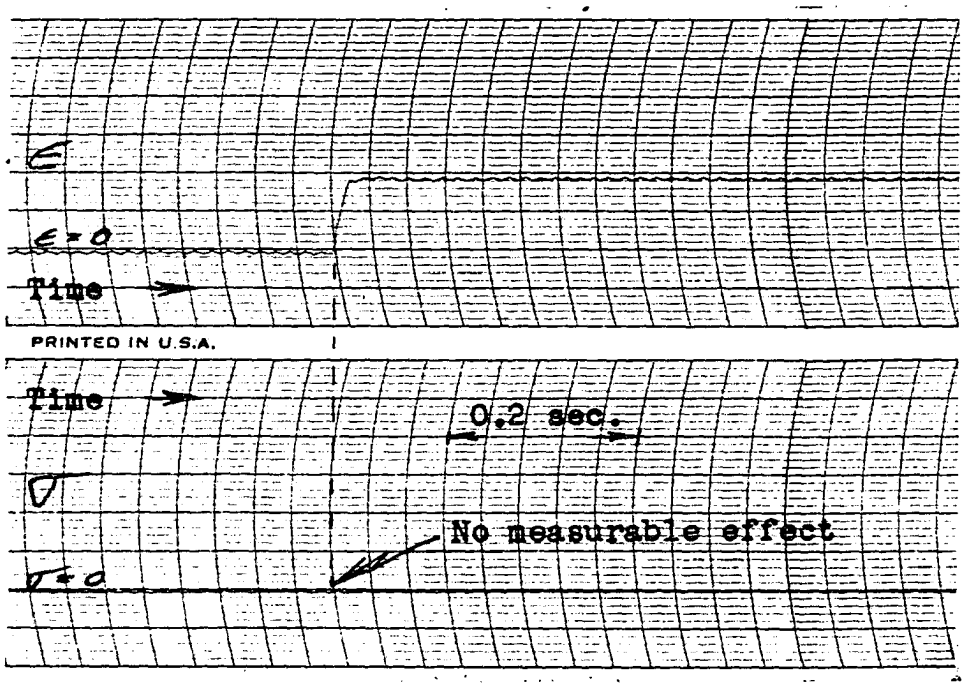

30b. Effect of inertia forces

Figure 30. Evaluation test records.

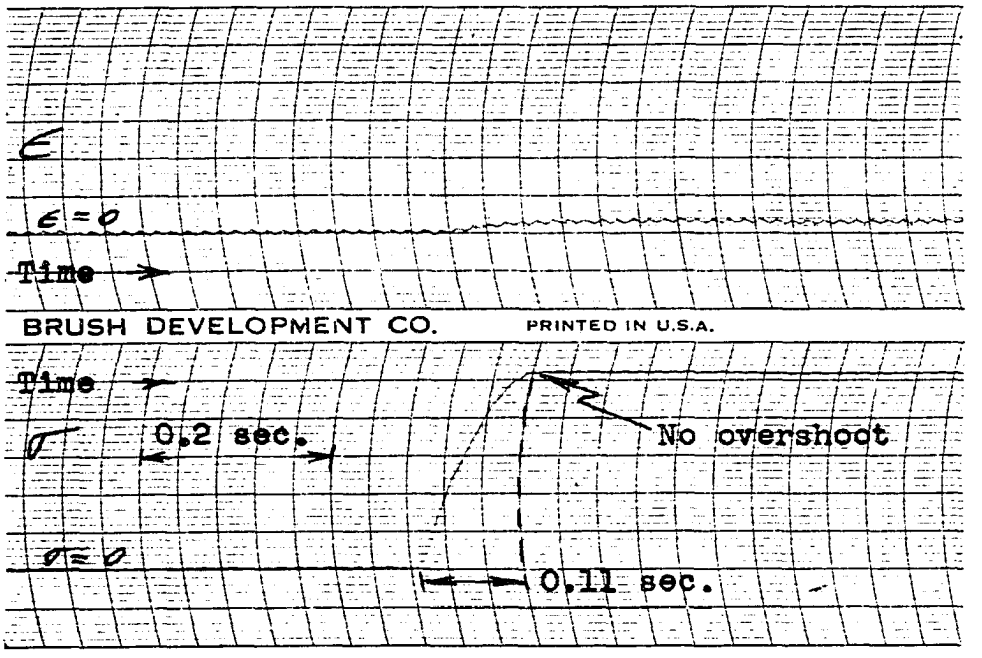

31a. Effect of pen inertia

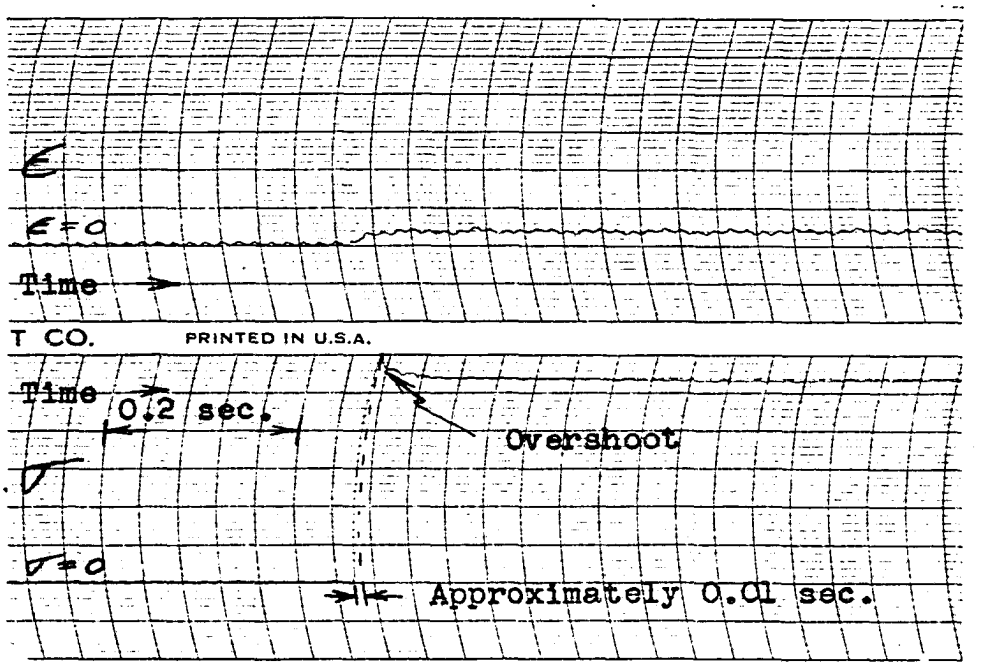

31b. Effect of pen inertia

Figure 31. Evaluation test records.

attenuation setting of one to one, when a standard 390,000 ohm resistance was connected in parallel with gage A. During the calibration test and all subsequent tests the attenuation setting was five to one. The data taken from this calibration test are tabulated in Table 2. These data were used to construct the applied force calibration curve, Figure 8a.

The pull bar displacement measuring circuit of the relaxation test equipment was calibrated by recording oscillograph pen displacement versus the pull bar displacement as measured by the depth micrometer. Before making this calibration test and prior to each subsequent test the recording system amplification was adjusted to produce three mm of pen displacement, at an attenuation setting of ten to one, when a standard 390,000 ohm resistance was connected in parallel with coil A. During this calibration and in all subsequent tests the attenuation setting was ten to one. The data taken from this calibration test are tabulated in Table 2. These data were used to construct the pull bar displacement calibration curve, Figure 8b.

Table 2. Applied force and pull bar displacement calibration data.

Applied Load (lbs)	Pen Displacement Produced by Applied Load (mm)	Pull Bar Displacement (in x 10^{-3})	Pen Displacement Produced by Pull Bar Displacement (mm)
0.0	0.0	0.0	0.0
5.0	7.0	2.0	2.5
7.0	9.8	4.0	5.0
9.0	12.5	12.0	15.0
11.0	15.1	15.5	20.0
13.0	18.0	11.5	15.0
15.0	20.8	7.2	10.0
13.0	18.0	3.7	5.0
11.0	15.5	0.0	0.0
9.0	13.0		
7.0	10.0		
5.0	7.1		
0.0	0.0		

Appendix B: Data from Preliminary Tests

The first set of preliminary tests consisted of three tests made on Specimen No. 1. The dimension of Specimen No. 1 were: thickness = 0.226 in.

outside dia. = 0.925 in.

inside dia. = 0.500 in.

which gives an original cross sectional area of

$A = 0.476 \text{ in.}^2$.

With this value of A and using the applied force - pen displacement calibration from Figure 8a the stress may be expressed as

$$\sigma_{psi} = \frac{F}{A} = \frac{1}{(1.40)(0.476)} \times \text{mm pen displacement}$$

$$= 1.50 \times \text{mm pen displacement.}$$

With the value of original thickness given above using the pull bar displacement - pen displacement calibration from Figure 8b the compressive strain may be expressed as

$$\epsilon_{\%} = \frac{\text{compression}}{\text{thickness}} = \frac{0.769 \times 10^{-3}}{0.226} \times 100 \times \text{mm pen displacement}$$

$$= 0.34 \times \text{mm pen displacement.}$$

The time is obtained by running the oscillograph record at a constant speed. In test numbers 1 and 2 of this first set the record speed used was 25 mm/sec., hence one mm on the record equals a time interval of 0.04 sec. In test number 3 the record speed used was 125 mm/sec., hence one mm on the record equals a time interval of 0.008 sec.

Data from the records taken during these three tests are tabulated in Table 3 together with values of time, stress, and strain computed from these data. These values were used to construct the stress-time and strain-time curves shown on Figure 10.

Table 3. Data taken during the first set of preliminary tests (Specimen No. 1.).

Time (t)		Strain (ϵ)		Stress (σ)	
(mm)	(sec)	(mm)	(%)	(mm)	(psi)
Test No. 1, Specimen No. 1.					
0	0.0	0.0	0.00	0.0	0.0
10	0.4	1.8	0.61	1.8	2.7
20	0.8	4.5	1.53	4.2	6.3
30	1.2	7.0	2.38	7.2	10.8
40	1.6	8.9	3.02	10.1	15.2
50	2.0	10.4	3.54	13.0	19.5
60	2.4	12.3	4.18	16.8	25.2
70	2.8	13.7	4.55	19.2	28.8
80	3.2	15.0	5.10	22.0	33.0
84	3.4	15.5	5.27	22.9	34.3
90	3.6	15.6	5.30	22.4	33.6
100	4.0	15.6	5.30	22.0	33.0
110	4.4	15.6	5.30	21.8	32.7
120	4.8	15.6	5.30	21.3	31.9
130	5.2	15.6	5.30	21.2	31.8
140	5.6	15.6	5.30	21.1	31.6
160	6.4	15.6	5.30	21.0	31.5
180	7.2	15.6	5.30	20.9	31.4
200	8.0	15.6	5.30	20.8	31.2
Test No. 2, Specimen No. 1.					
0.0	0.00	0.0	0.00	0.0	0.0
3.0	0.12	0.4	0.14	0.3	0.5
5.5	0.22	1.0	0.34	0.8	1.2
8.0	0.32	1.7	0.58	1.1	1.7
10.5	0.42	2.2	0.75	1.7	2.6
13.0	0.52	3.0	1.02	2.2	3.3
15.5	0.62	4.6	1.56	4.1	6.2
18.0	0.72	6.2	2.11	6.2	9.3
20.5	0.82	7.8	2.65	9.1	13.6
23.0	0.92	8.9	3.02	11.2	16.8
25.5	1.02	10.2	3.47	14.1	21.1
28.0	1.12	11.7	3.98	17.0	25.5
30.5	1.22	12.8	4.35	19.5	29.2
33.0	1.32	14.0	4.76	21.8	32.7
35.5	1.42	15.1	5.14	24.1	36.2
38.0	1.52	15.2	5.17	24.0	36.0

Table 3. (Continued)

Time (t)		Strain (ϵ)		Stress (σ)	
(mm)	(sec)	(mm)	(%)	(mm)	(psi)
Test No. 2, Specimen No. 1 (Continued)					
40.5	1.62	15.2	5.17	23.6	35.4
43.0	1.72	15.4	5.24	23.3	35.0
48.0	1.92	15.4	5.24	23.0	34.5
53.0	2.12	15.4	5.24	22.8	34.2
58.0	2.32	15.4	5.24	22.5	33.7
63.0	2.52	15.4	5.24	22.3	33.4
88.0	3.52	15.4	5.24	21.5	32.2
113.0	4.52	15.4	5.24	21.2	31.8
138.0	5.52	15.4	5.24	21.1	31.6
Test No. 3, Specimen No. 1.					
0	0.00	0.0	0.00	0.0	0.0
5	0.04	0.1	0.03	0.5	0.8
10	0.08	1.0	0.34	1.0	1.5
15	0.12	1.8	0.61	1.9	2.9
20	0.16	2.4	0.82	2.2	3.3
25	0.20	4.0	1.36	4.0	6.0
30	0.24	7.2	2.45	8.4	12.6
35	0.28	9.5	3.23	13.7	20.6
40	0.32	12.1	4.12	20.0	30.0
45	0.36	14.9	5.07	26.0	39.0
50	0.40	16.3	5.55	29.2	43.8
55	0.44	17.2	5.85	30.1	45.2
60	0.48	17.2	5.85	29.8	44.7
65	0.52	17.2	5.85	29.2	43.8
70	0.56	17.2	5.85	28.9	43.4
75	0.60	17.2	5.85	28.8	43.2
80	0.64	17.2	5.85	28.5	42.7
90	0.72	17.2	5.85	28.1	42.2
100	0.80	17.2	5.85	28.0	42.0
110	0.88	17.2	5.85	27.8	41.7
130	1.04	17.2	5.85	27.3	40.9
150	1.20	17.2	5.85	27.2	40.8
200	1.60	17.2	5.85	26.9	40.4
250	2.00	17.2	5.85	26.2	39.3
300	2.40	17.2	5.85	26.1	39.1

The second set of preliminary tests consisted of two tests made on Specimen No. 2. The dimensions of Specimen No. 2 were: thickness = 0.283 in.

outside dia. = 0.911 in.

inside dia. = 0.500 in.

which gives an original cross sectional area of

$A = 0.455 \text{ in.}^2$.

Using this value of A and the applied force - pen displacement calibration from Figure 8a the stress may be expressed as

$$\sigma_{psi} = \frac{F}{A} = \frac{1}{(1.40)(0.455)} \times \text{mm pen displacement}$$

$$= 1.575 \times \text{mm pen displacement.}$$

Using the value of thickness given above and the pull bar displacement - pen displacement calibration from Figure 8b the strain may be expressed as

$$\epsilon_{\%} = \frac{\text{compression}}{\text{thickness}} = \frac{0.769 \times 10^{-3}}{0.283} \times 100 \times \text{mm pen displacement}$$

$$= 0.272 \times \text{mm pen displacement.}$$

The time base is obtained, as before, by running the oscillograph record at a constant speed. In the first test on Specimen No. 2 the total strain was applied in six nearly equal increments. After each increment of strain was applied, sufficient time was allowed for a large part of

the stress relaxation to occur.

Data from the record taken during the first test on Specimen No. 2 are tabulated in Table 4 together with values of time, stress, strain, increment of strain added ($\Delta\epsilon$), and increment of stress ($\Delta\sigma$) computed from these data. These values were used to construct the unrelaxed stress-strain curve shown on Figure 12 and the stress relaxation curves shown on Figure 14.

Table 4. Data taken during the first test on Specimen No. 2.

Time[a]			Strain				Stress			
	Δt	t	ϵ		$\Delta\epsilon$		σ		$\Delta\sigma$	
(mm)	(sec)	(sec)	(mm)	(%)	(mm)	(%)	(mm)	(psi)	(mm)	(psi)
$\Delta\epsilon_1$ - First Strain Increment.										
0	0.0	0.0	0.0	0.00	0.0	0.00	0.0	0.00	0.0	0.00
25	0.2	0.0	2.1	0.57	2.1	0.57	2.9	4.57	2.9	4.57
50		0.2	2.1	0.57	2.1	0.57	2.7	4.25	2.7	4.25
75		0.4	2.1	0.57	2.1	0.57	2.5	3.94	2.5	3.94
100		0.6	2.1	0.57	2.1	0.57	2.4	3.78	2.4	3.78
125		0.8	2.1	0.57	2.1	0.57	2.4	3.78	2.4	3.78
150		1.0	2.1	0.57	2.1	0.57	2.3	3.62	2.3	3.62
175		1.2	2.1	0.57	2.1	0.57	2.2	3.46	2.2	3.46
200		1.4	2.1	0.57	2.1	0.57	2.1	3.31	2.1	3.31
225		1.6	2.1	0.57	2.1	0.57	2.1	3.31	2.1	3.31
250		1.8	2.1	0.57	2.1	0.57	2.1	3.31	2.1	3.31
275		2.0	2.1	0.57	2.1	0.57	2.1	3.31	2.1	3.31
	5 min.		2.1	0.57	2.1	0.57	2.0	3.15	2.0	3.15

[a] Δt represents the time required to apply a given $\Delta\epsilon$. In this case t is the time during which $\Delta\epsilon$ is held constant. The record speed was 125 mm/sec., hence one mm = 0.008 sec.

Table 4. (Continued)

Time Δt (mm)	Time Δt (sec)	Time t (sec)	Strain ε (mm)	Strain ε (%)	Strain Δε (mm)	Strain Δε (%)	Stress σ (mm)	Stress σ (psi)	Stress Δσ (mm)	Stress Δσ (psi)
$\Delta\epsilon_2$ - Second Strain Increment.										
0	0.0		2.1	0.57	0.0	0.00	2.0	3.15	0.0	0.00
25	0.2	0.0	4.7	1.28	2.6	0.71	7.0	11.02	5.0	7.87
50		0.2	4.7	1.28	2.6	0.71	6.5	10.24	4.5	7.09
75		0.4	4.7	1.28	2.6	0.71	6.4	10.08	4.4	6.94
100		0.6	4.7	1.28	2.6	0.71	6.2	9.76	4.2	6.61
125		0.8	4.7	1.28	2.6	0.71	6.2	9.76	4.2	6.61
150		1.0	4.7	1.28	2.6	0.71	6.1	9.60	4.1	6.46
175		1.2	4.7	1.28	2.6	0.71	6.1	9.60	4.1	6.46
200		1.4	4.7	1.28	2.6	0.71	6.1	9.60	4.1	6.46
225		1.6	4.7	1.28	2.6	0.71	6.1	9.60	4.1	6.46
250		1.8	4.7	1.28	2.6	0.71	6.1	9.60	4.1	6.46
275		2.0	4.7	1.28	2.6	0.71	6.1	9.60	4.1	6.46
	5 min.		5.0[b]	1.36[b]	2.9[b]	0.79[b]	5.2	8.20	3.2	5.04
$\Delta\epsilon_3$ - Third Strain Increment.										
0	0.00		5.0	1.36	0.0	0.00	5.2	8.20	0.0	0.00
17	0.14	0.0	7.5	2.04	2.5	0.68	12.8	20.18	7.6	11.96
42		0.2	7.5	2.04	2.5	0.68	12.1		6.9	10.86
67		0.4	7.5	2.04	2.5	0.68	11.9		6.7	10.54
92		0.6	7.5	2.04	2.5	0.68	11.8		6.6	10.39
117		0.8	7.5	2.04	2.5	0.68	11.6		6.4	10.08
142		1.0	7.5	2.04	2.5	0.68	11.5		6.3	9.91
167		1.2	7.5	2.04	2.5	0.68	11.5		6.3	9.91
192		1.4	7.5	2.04	2.5	0.68	11.5		6.3	9.91
217		1.6	7.5	2.04	2.5	0.68	11.4		6.2	9.76
242		1.8	7.5	2.04	2.5	0.68	11.3		6.1	9.60
267		2.0	7.5	2.04	2.5	0.68	11.2		6.0	9.45
	5 min.		7.5	2.04	2.5	0.68	9.9	15.60	4.7	7.40

[b]Increase in strain due to recording pen shift.

Table 4. (Continued)

Time			Strain				Stress			
	Δt	t	ϵ		$\Delta\epsilon$		σ		$\Delta\sigma$	
(mm)	(sec)	(sec)	(mm)	(%)	(mm)	(%)	(mm)	(psi)	(mm)	(psi)
$\Delta\epsilon_4$ - Fourth Strain Increment.										
0	0.00		7.5	2.04	0.0	0.00	9.9	15.60	0.0	0.00
15	0.12	0.0	10.2	2.78	2.7	0.74	20.1	31.65	10.2	16.05
40		0.2	10.2	2.78	2.7	0.74	19.1		9.2	14.50
65		0.4	10.2	2.78	2.7	0.74	18.9		9.0	14.18
90		0.6	10.2	2.78	2.7	0.74	18.5		8.6	13.53
115		0.8	10.2	2.78	2.7	0.74	18.2		8.3	13.08
140		1.0	10.2	2.78	2.7	0.74	18.1		8.2	12.90
165		1.2	10.2	2.78	2.7	0.74	18.1		8.2	12.90
190		1.4	10.2	2.78	2.7	0.74	18.0		8.1	12.75
215		1.6	10.2	2.78	2.7	0.74	18.0		8.1	12.75
240		1.8	10.2	2.78	2.7	0.74	18.0		8.1	12.75
265		2.0	10.2	2.78	2.7	0.74	17.9		8.0	12.60
		5 min.	10.2	2.78	2.7	0.74	15.8	24.90	5.9	9.29
$\Delta\epsilon_5$ - Fifth Strain Increment.										
0	0.00		10.2	2.78	0.0	0.00	15.8	24.90	0.0	0.00
17	0.14	0.0	13.3	3.62	3.1	0.84	26.0	41.00	10.2	16.05
42		0.2	13.3	3.62	3.1	0.84	24.9		9.1	14.31
67		0.4	13.3	3.62	3.1	0.84	24.5		8.7	13.70
92		0.6	13.3	3.62	3.1	0.84	24.3		8.5	13.38
117		0.8	13.3	3.62	3.1	0.84	24.2		8.4	13.21
142		1.0	13.3	3.62	3.1	0.84	24.0		8.2	12.90
167		1.2	13.3	3.62	3.1	0.84	23.9		8.1	12.75
192		1.4	13.3	3.62	3.1	0.84	23.9		8.1	12.75
217		1.6	13.3	3.62	3.1	0.84	23.9		8.1	12.75
242		1.8	13.3	3.62	3.1	0.84	23.9		8.1	12.75
267		2.0	13.3	3.62	3.1	0.84	23.6		7.8	12.28
		5 min.	13.3	3.62	3.1	0.84	21.0	33.10	5.2	8.19

Table 4. (Continued)

Time			Strain				Stress			
Δt (mm)	Δt (sec)	t (sec)	ϵ (mm)	ϵ (%)	$\Delta\epsilon$ (mm)	$\Delta\epsilon$ (%)	σ (mm)	σ (psi)	$\Delta\sigma$ (mm)	$\Delta\sigma$ (psi)
$\Delta\epsilon_6$ - Sixth Strain Increment.										
0	0.00		13.3	3.62	0.0	0.00	21.0	33.10	0.0	0.00
—	——	0.0	14.1	3.84	0.8	0.22	24.9	39.20	3.9	6.15
	5 min.		14.1	3.84	0.8	0.22	23.0	36.20	2.0	3.15

[c]The exact time required for the maximum strain to be obtained was difficult to determine because the point at which ϵ reaches its maximum value is not well defined on the test record.

In the second test on Specimen No. 2 the strain was applied as slowly as possible with intermediate stops of sufficient length to allow nearly complete relaxation of stress. Data from the record taken during this test are tabulated in Table 5 together with values of stress and strain computed from these data. These values were used to construct the relaxed stress-strain curve shown on Figure 12.

Table 5. Data taken during the second test on Specimen No. 2.

Time[a] (min)	Strain (ϵ) (mm)	(psi)	Stress (σ) (mm)	(%)
0	0.0	0.00	0.0	0.0
3	3.0	0.82	2.0	3.2
7	6.0	1.63	5.5	8.7
12	9.0	2.45	13.0	20.5
22	12.0	3.26	18.1	28.5
37	15.0	4.18	23.5	37.0

[a]The oscillograph record speed used was 5 mm/sec. but the times were obtained, in this test only, by means of a stop watch.

Appendix C: Records and Data from Tests Made to Evaluate Material Constants

Data obtained from the third test on Specimen No. 2 were used to determine the numerical value of N, p, and τ. Figure 32 is a reproduction of the record taken during this test. Data taken during this test are tabulated in Table 6 together with values of time, stress, strain, increment of strain added ($\Delta\epsilon$), and increment of stress ($\Delta\sigma$) computed from these data. These values were used to construct the unrelaxed stress-strain curve shown in Figure 15 and the stress relaxation curves shown on Figure 17.

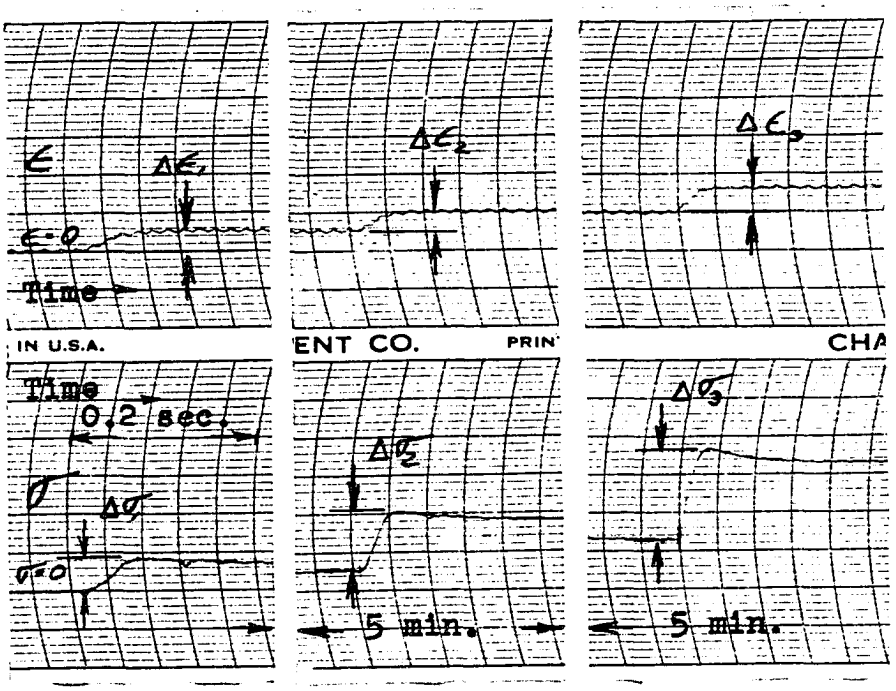

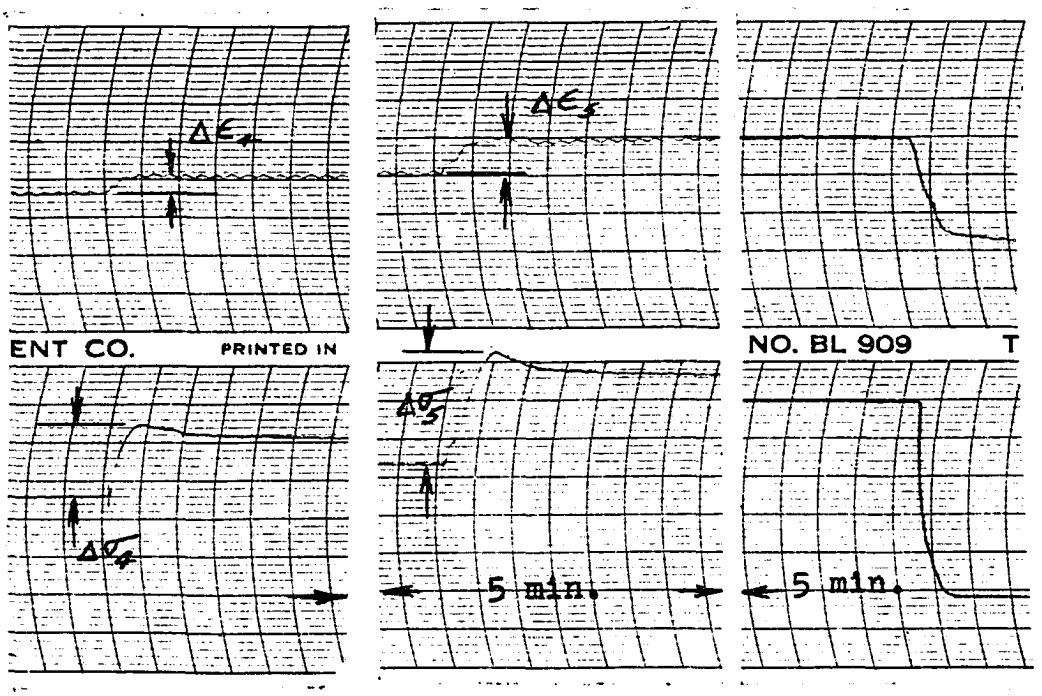

Figure 32. Test 3, Specimen No. 2.

Table 6. Data taken during the third test on Specimen No. 2.

Time[a] Δt (mm)	(sec)	T (mm)	(sec)	Strain ε (mm)	(%)	Δε (mm)	(%)	Stress σ (mm)	(psi)	Δσ (mm)	(psi)
$\Delta\epsilon_1$ - First Strain Increment.											
0	0.000			0.0	0.00	0.0	0.00	0.0	0.00	0.0	0.00
7	0.056	0	0.000	2.7	0.74	2.7	0.74	4.1	6.45	4.1	6.45
		11	0.088	2.7	0.74	2.7	0.74	3.9	6.14	3.9	6.14
		21	0.168	2.7	0.74	2.7	0.74	3.5	5.51	3.5	5.51
		5 min.		2.7	0.74	2.7	0.74	2.7	4.25	2.7	4.25
$\Delta\epsilon_2$ - Second Strain Increment.											
0	0.000			2.7	0.74	0.0	0.00	2.7	4.25	0.0	0.00
6	0.048	0	0.000	5.0	1.36	2.3	0.62	10.1	15.89	7.4	11.64
		3	0.024	5.0	1.36	2.3	0.62	9.7	15.30		
		8	0.064	5.0	1.36	2.3	0.62	9.4	14.80		
		13	0.104	5.0	1.36	2.3	0.62	9.2	14.50		
		18	0.144	5.0	1.36	2.3	0.62	9.1	14.30		
		5 min.		5.0	1.36	2.3	0.62	6.5	10.24		
$\Delta\epsilon_3$ - Third Strain Increment.											
0	0.000			5.0	1.36	0.0	0.00	6.5	10.24	0.0	0.00
3	0.024	0	0.000	8.1	2.20	3.1	0.84	18.2	28.70	11.7	18.46
		2	0.016	8.1	2.20	3.1	0.84	18.0	28.40		
		7	0.056	8.1	2.20	3.1	0.84	17.0	26.80		
		12	0.096	8.1	2.20	3.1	0.84	16.6	26.20		
		17	0.136	8.1	2.20	3.1	0.84	16.5	26.00		
		5 min.		8.1	2.20	3.1	0.84	13.0	20.58		

[a] Δt is the time required to apply a given $\Delta\epsilon$, and T is the time during which $\Delta\epsilon$ is held constant. The record speed was 125 mm/sec.

Table 6. (Continued)

Time Δt (mm)	Time Δt (sec)	Time T (mm)	Time T (sec)	Strain ε (mm)	Strain ε (%)	Strain Δε (mm)	Strain Δε (%)	Stress σ (mm)	Stress σ (psi)	Stress Δσ (mm)	Stress Δσ (psi)
$\Delta\epsilon_4$ - Fourth Strain Increment.											
0	0.000			8.1	2.20	0.0	0.00	13.0	20.58	0.0	0.00
3	0.024	0	0.000	10.5	2.86	2.4	0.65	22.3	35.20	9.3	14.62
		6	0.048	10.5	2.86	2.4	0.65	21.2	33.40		
		11	0.088	10.5	2.86	2.4	0.65	20.9	32.90		
		16	0.128	10.5	2.86	2.4	0.65	20.7	32.60		
		5	min.	10.5	2.86	2.4	0.65	16.7	26.40		
$\Delta\epsilon_5$ - Fifth Strain Increment.											
0	0.000			10.5	2.86	0.0	0.00	16.7	26.40	0.0	0.00
4	0.032	0	0.000	14.5	3.94	4.0	1.09	31.3	49.40	14.6	23.00
		5	0.040	14.5	3.94	4.0	1.09	29.5	46.50		
		10	0.080	14.5	3.94	4.0	1.09	28.9	45.50		
		15	0.120	14.5	3.94	4.0	1.09	28.5	44.90		

Appendix D: Tabular Forms Used for the Computation of Results

Table 7. Tabular form for solving equation (35).

(1) ϵ %	(2) T Sec	(3) $\epsilon^{1.455}$	(4) $4.76\epsilon^{1.455}$	(5) $8.77\epsilon^{1.455}$	(6) $\epsilon/0.69b$
I. b = 2.5 %/sec.					
1.00	0.00	1.00	4.8	8.8	0.58
2.00	0.00	2.74	13.0	24.0	1.16
3.00	0.00	4.94	23.5	43.4	1.74
3.29	0.00	5.65	26.9	49.5	1.91
3.29	0.10	5.65	26.9	49.5	1.91
3.29	0.20	5.65	26.9	49.5	1.91
3.29	0.30	5.65	26.9	49.5	1.91
3.29	0.40	5.65	26.9	49.5	1.91
II. b = 12.2 %/sec.					
1.00	0.00	1.00	4.8	8.8	0.119
2.00	0.00	2.74	13.0	24.0	0.238
3.00	0.00	4.94	23.5	43.4	0.356
3.89	0.00	7.21	34.4	63.3	0.462
3.89	0.10	7.21	34.4	63.3	0.462
3.89	0.20	7.21	34.4	63.3	0.462
3.89	0.30	7.21	34.4	63.3	0.462
3.89	0.50	7.21	34.4	63.3	0.462
3.89	0.75	7.21	34.4	63.3	0.462
3.89	1.25	7.21	34.4	63.3	0.462
III. b = 34.0 %/sec.					
1.00	0.00	1.00	4.8	8.8	0.043
2.00	0.00	2.74	13.0	24.0	0.085
2.72	0.00	4.29	20.4	37.6	0.116
2.72	0.02	4.29	20.4	37.6	0.116
2.72	0.07	4.29	20.4	37.6	0.116
2.72	0.12	4.29	20.4	37.6	0.116

Table 7. (Continued)

ϵ	T	(7)[a] $[\epsilon, \text{Series}]$	(8) (5)x(7)	(9) (4)+(8) $\sigma_{T=0}$	(10) $e^{-\frac{T}{\tau}}$
I. b = 2.5 %/sec.					
1.00	0.00	0.548	4.8	9.6	
2.00	0.00	0.448	10.8	23.8	
3.00	0.00	0.375	16.2	39.7	
3.29	0.00	0.355	17.6	44.5	1.000
3.29	0.10	0.355	17.6		0.865
3.29	0.20	0.355	17.6		0.749
3.29	0.30	0.355	17.6		0.647
3.29	0.40	0.355	17.6		0.560
II. b = 12.2 %/sec.					
1.00	0.00	0.656	5.8	10.6	
2.00	0.00	0.626	15.0	28.0	
3.00	0.00	0.597	25.9	49.4	
3.89	0.00	0.573	36.2	70.6	1.000
3.89	0.10	0.573	36.2		0.865
3.89	0.20	0.573	36.2		0.749
3.89	0.30	0.573	36.2		0.647
3.89	0.50	0.573	36.2		0.484
3.89	0.75	0.573	36.2		0.336
3.89	1.25	0.573	36.2		0.164
III. b = 34.0 %/sec.					
1.00	0.00	0.676	5.9	10.7	
2.00	0.00	0.664	15.9	28.9	
2.72	0.00	0.657	24.7	45.1	1.000
2.72	0.02	0.657	24.7		0.974
2.72	0.07	0.657	24.7		0.905
2.72	0.12	0.657	24.7		0.840

[a]In all cases this computation has been carried to a point such that the error involved in neglecting the remainder is less than 0.01 of the value obtained.

Table 7. (Continued)

ϵ	T	(11) (8)x(10)	(12) (4)÷(11) $\sigma_{T=T}$	(13) $\frac{\epsilon}{b}$ + T
I. b = 2.5 %/sec.				
1.00	0.00			0.40
2.00	0.00			0.80
3.00	0.00			1.20
3.29	0.00	17.6	44.5	1.32
3.29	0.10	15.2	42.1	1.42
3.29	0.20	13.2	40.1	1.52
3.29	0.30	11.4	38.3	1.62
3.29	0.40	9.9	36.8	1.72
II. b = 12.2 %/sec.				
1.00	0.00			0.08
2.00	0.00			0.16
3.00	0.00			0.25
3.89	0.00	36.2	70.6	0.32
3.89	0.10	31.3	65.7	0.42
3.89	0.20	27.1	61.5	0.52
3.89	0.30	23.4	57.8	0.62
3.89	0.50	17.5	51.9	0.82
3.89	0.75	12.2	46.6	1.07
3.89	1.25	5.9	40.3	1.57
III. b = 34.0 %/sec.				
1.00	0.00			0.029
2.00	0.00			0.059
2.72	0.00	24.7	45.1	0.080
2.72	0.02	24.0	44.4	0.100
2.72	0.07	22.3	42.7	0.150
2.72	0.12	20.7	41.1	0.200

Table 8. Tabular form for solving equations (35a) and (36).

(1)[a]	(2)	(3)	(4)	(5)
ϵ %	$\epsilon^{1.455}$	$4.76\epsilon^{1.455}$	$8.77\epsilon^{1.455}$	$\epsilon/0.69b$
b = 7.4 %/sec.				
1.00	1.00	4.8	8.8	0.196
2.00	2.74	13.0	24.0	0.392
3.00	4.94	23.5	43.4	0.588
4.00	7.51	35.8	65.9	0.784
4.45_m	8.79_m	41.9_m	77.1_m	0.873_m

	(6)	(7)	(8)	(9)
ϵ	$\epsilon_m-\epsilon$	$e^{-\frac{2(\epsilon_m-\epsilon)}{0.69b}}$	$e^{-\frac{(\epsilon_m-\epsilon)}{0.69b}}$	(7)-2(8)
b = 7.4 %/sec.				
1.00	3.45	0.258	0.508	-0.758
2.00	2.45	0.383	0.619	-0.855
3.00	1.45	0.568	0.754	-0.940
4.00	0.45	0.837	0.915	-0.993
4.45_m	0.00	1.000	1.000	-1.000

	(10)	(11)	(12)	(13)
ϵ	$\epsilon_m^{1.455}-\epsilon^{1.455}$ $(2)_m - (2)$	$[\epsilon$, Series]	(4)x(11)	(3)+(12) σ inc.ϵ
b = 7.4 %/sec.				
1.00	7.79	0.636	5.6	10.4
2.00	6.05	0.590	14.2	27.2
3.00	3.85	0.548	23.8	47.3
4.00	1.28	0.510	33.6	69.4
4.45_m	0.00	0.495_m	38.1	80.0

[a]Subscript m indicates ϵ_m and values computed from ϵ_m.

Table 8. (Continued)

ϵ	(14) (12)x(9)	(15) (12.1(10)	(16) 17.5$(2)_m$x$(11)_m$	(17) $\sigma_{dec.}$ (3)+(14)-(15)+(16)
b = 7.4 %/sec.				
1.00	- 4.2	94.1		-17.4
2.00	-12.1	73.2		3.8
3.00	-22.4	46.5		30.7
4.00	-33.4	15.5		63.0
4.45_m	-38.2	0.0	76.1	79.8